DEFINING THE DEVELOPMENTAL SIGNALS OF THE
CARDIAC FIBROBLAST

APPROVED BY SUPERVISORY COMMITTEE

Michelle D. Tallquist, Ph.D.

Thomas J. Carroll, Ph.D.

Jane E. Johnson, Ph.D.

Raymond J. MacDonald, Ph.D.

DEDICATION

To my wife, Eunjin Yun, accompanying me on our journey of life and science

# DEFINING THE DEVELOPMENTAL SIGNALS OF THE CARDIAC FIBROBLAST

by

SEUNG TAE BAEK

DISSERTATION

Presented to the Faculty of the Graduate School of Biomedical Sciences

The University of Texas Southwestern Medical Center at Dallas

In Partial Fulfillment of the Requirements

For the Degree of

DOCTOR OF PHILOSOPHY

The University of Texas Southwestern Medical Center at Dallas

Dallas, Texas

August, 2012

DEFINING THE DEVELOPMENTAL SIGNALS OF THE
CARDIAC FIBROBLAST

SEUNG TAE BAEK, Ph.D.

The University of Texas Southwestern Medical Center at Dallas, 2012

MICHELLE D. TALLQUIST, Ph.D.

Cardiac fibroblasts play a central role as a mediator of inflammatory and fibrotic response and also secrete extracellular matrix components that provide structural support for regeneration and remodeling of the wound. Despite the importance of the cardiac fibroblast in heart disease, very little is known about factors that are essential for differentiation along the cardiac fibroblast lineage. Using a combination of gene knockout and cardiac fibroblast-detecting methods, we have identified genes that are involved in the formation of cardiac fibroblasts. Our results demonstrate that in the absence of Tcf21, a basic helix-loop-helix transcription factor, cardiac fibroblast progenitors fail to migrate into the myocardium resulting in a specific loss of the cardiac

fibroblast population. Loss of the receptor tyrosine kinase Pdgfrα also results in loss of the cardiac fibroblast population. Interestingly, *Tcf21* and *Pdgfra* are involved in the epithelial to mesenchymal transition (EMT) of epicardial cells.

The epicardium (outer surface of the heart) functions as a pool of progenitor cells for the coronary vasculature and interstitial connective tissue during embryonic development. Although several signaling pathways have been identified that disrupt EMT, no component has been reported that negatively regulates EMT, which may also involved in the cardiac fibroblast development. Using a conditional knockout of neurofibromin 1 (*Nf1*) in the epicardium, we identified Nf1 as a key mediator of epicardial EMT. We found that the process of EMT occurred earlier in *Nf1* mutant hearts, with an increase in epicardial cells entering the compact myocardium. Moreover, loss of *Nf1* caused increased epicardial-derived cell proliferation and resulted in the expansion of cardiac fibroblasts and coronary vascular smooth muscle cells. In addition to revealing the function of *Nf1*, *Tcf21* and *Pdgfra* in epicardial EMT and cardiac fibroblast development, we generated and established mouse models to study the role of cardiac fibroblasts and the function of these genes during heart pathogenesis. Because developmental processes are often recapitulated in normal and pathological conditions, a better understanding of the epicardium and cardiac fibroblast development may help identify targets for therapeutics to treat heart disease.

TABLE OF CONTENTS

## PRIOR PUBLICATIONS

Acharya A, **Baek ST**, Huang G, Eskiocak B, Goetsch S, Sung CY, Banfi S, Sauer MF, Olsen GS, Duffield JS, Olson EN, Tallquist MD. The bhlh transcription factor Tcf21, is required for lineage-specific EMT of cardiac fibroblast progenitors. *Development.* 2012 Jun;139(12):2139-2149.

**Baek ST** and Tallquist MD. Nf1 limits epicardial derivative expansion by regulating epithelial to mesenchymal transition and proliferation. *Development.* 2012 Jun;139(11):2040-2049.

Acharya A, **Baek ST**, Banfi S, Eskiocak B, Tallquist MD. Efficient inducible Cre-mediated recombination in Tcf21 cell lineages in the heart and kidney. *Genesis.* 2011 Nov;49(11):870-722.

Smith CL, **Baek ST**, Sung CY, Tallquist MD. Epicardial-derived cell epithelial to mesenchymal transition and fate specification require PDGF receptor signaling. *Circulation Research.* 2011 Jun 10;108(12):e15-26.

LIST OF FIGURES

LIST OF TABLE

## LIST OF DEFINITIONS

atRA – all-trans retinoic acid

bHLH – basic helix-loop-helix

DAPI – 4,6-diamidino-2-phenylindol

EMT – epithelial to mesenchymal transition

EPDC – epicardial derived cell

FGF – fibroblast growth factor

GAP – GTPase activating protein

IHC – immunohistochemistry

ISH – in situ hybridization

MAPK – mitogen-activated protein kinase

MMP – matrix metalloproteinases

MTC – Masson Trichrome

Nf1 – neurofibromin 1

PDGF – platelet derived growth factor

TAB – Thoracic aortic banding

TGF – transforming growth factor

TIMP – tissue inhibitors of metalloproteinase

VSD – ventricular septal defect

cVSMC – coronary vascular smooth muscle cell

# CHAPTER ONE

# INTRODUCTION TO EPICARDIUM DEVELOPMENT

During development, the epicardium provides cells that populate the coronary vasculature and interstitial connective tissue. By providing soluble factors, it also coordinates cardiac muscle and vascular development (Smith and Bader, 2007). In the adult heart the epicardium provides a protective outer layer to the heart and facilitates heart movement during contraction and relaxation. More recent studies have shown that the epicardium is a signaling center for heart regeneration (Kikuchi et al.). Because developmental processes are often recapitulated in normal and pathological conditions, a better understanding of the epicardium during development may help identify targets for therapeutics to treat heart disease.

## Epithelial to mesenchymal transition and epicardial-derived cells

### *Overview of epicardial development*

As summarized in Figure 1-1, the epicardium originates from the proepicardium which is a transient organ that arises from the mesothelium of the septum transversum (Komiyama et al., 1987). Starting at embryonic day (E) 9.5 to 12.5, proepicardial cells (Figure 1-1A,B) migrate and spread over the developing heart tube to form the epicardium (Olivey et al., 2004). As the epicardium wraps around the heart, a subset of epicardial cells loses their epithelial nature and acquire mesenchymal characteristics through the process known as epithelial to mesenchymal transition (EMT) (Figure 1-

1A,C) (Mikawa and Gourdie, 1996). As EMT occurs, a subset of epicardial cells loses contact with adjacent cells and invades the underlying basement membrane. They then migrate into the myocardium. These migrated epicardial cells are referred to as epicardial-derived cells (EPDCs), which become differentiated coronary vascular smooth muscle cells (cVSMCs) and cardiac fibroblasts (Figure 1-1A,D) (Dettman et al., 1998; Manner et al., 2001; Mikawa and Gourdie, 1996).

*Epithelial to mesenchymal transition*

Epithelial and mesenchymal cells are different in various characteristics. Epithelial cells are associated with a basement membrane and are connected by abundant cellular junctions. Mesenchymal cells are typically neither associated with basement membrane and are motile. Early studies showed that the conversion of epithelial cells into mesenchymal cells by a process known as EMT (Greenburg and Hay, 1982; Greenburg and Hay, 1986). For several decades, many studies have shown that EMT is an essential component of embryonic development, including mesoderm formation, neural crest development, and heart valve and epicardial development. There is now very compelling evidence that EMT plays crucial roles in cancer progression. (Thiery et al., 2009; Yang and Weinberg, 2008).

Signaling from growth factors, such as transforming growth factor β (TGFβ), fibroblast growth factors (FGFs), platelet-derived growth factors (PDGFs) and wingless-related MMTV integration sites (Wnt) are major inductive signals of EMT. The TGFβ superfamily has been shown to induce EMT of endothelial cells during cardiac valve development and palate fusion (Ahmed et al., 2007; Boyer et al., 1999; Mercado-

Pimentel and Runyan, 2007). Signals by BMP, another TGFβ superfamily member, and FGF induce EMT of neural crest cell (Liem et al., 1995). Signals by the Wnt family of growth factors, mediated by β-catenin and *Snai2*, also activate neural crest EMT (Vallin et al., 2001). PDGF signaling during TGFβ-induced EMT is required to complete EMT in instances of cancer progression (Fischer et al., 2007; Jechlinger et al., 2003).

Studies have shown that some common machinery exists for EMT, yet each tissue has a unique set of EMT signals which crosstalk to result in the final mesenchymal cell populations. For example signals mediated by *Snai1* (Snail), *Snai2* (Slug) and *Cdh1* (E-cadherin) have been implicated in many EMT processes including mesoderm formation (Carver et al., 2001), neural crest cell development (Nieto, 2002) and cardiac valve development (Kokudo et al., 2008). Growth factor signals activate phosphoinositide-3-kinase (PI3K) and Ras. Subsequent activation of mitogen-activated protein kinase (MAPK) results in upregulation of *Snai1* and *Snai2* which in turn can repress E-cadherin expression, a key adherens junctional component, leading to EMT. Although some pathways are common for the EMT process in different cell types, each EMT is regulated by a unique subset of growth factors and downstream signaling pathways.

*EMT and epicardial development*

Several signaling pathways including TGFβ (Austin et al., 2008; Sridurongrit et al., 2008), FGF (Pennisi and Mikawa, 2009) and PDGF (Lu et al., 2001; Mellgren et al., 2008; Van Den Akker et al., 2005) also have been implicated in the process of epicardial EMT during development. However, relatively little is known about the signaling

pathways that are involved in epicardial EMT. Some specific questions regarding EMT are: 1) What signaling components initiate epicardial EMT? 2) What is the source of the signals that initiates epicardial EMT in such a regional specific manner? 3) How is EMT restricted temporally?

Disruption of epicardial EMT often results in severe heart defects. Because the epicardium is a source of noncardiomyocyte progenitor cells of the heart, failure in epicardial EMT often results in disruption of heart architecture and vasculature. Inhibition of epicardial outgrowth results in disruption of both the myocardium, and endocardial cushion, ventricle septation, and coronary vessel formation (Eralp et al., 2005; Gittenberger-de Groot et al., 2000). Studies with avian hearts have shown that the inhibition of α4-integrin stimulate the epicardial cells to undergo EMT but altering its differentiation in VSMC (Dettman et al., 2003). VCAM-1, a ligand of α4β1-integrin, could inhibit TGFβ-induced EMT by modulating Rho activity in chick epicardial cells (Dokic and Dettman, 2006). Growth factor signals are also involved in epicardial EMT. Knock-down of FGFR-1 inhibit epicardial EMT and differentiation into VSMC (Pennisi and Mikawa, 2009). In mouse, ablation of Alk5, TGFβ type I receptor, results in failure of EMT in vitro and also defective VSMC formation (Sridurongrit et al., 2008). Epicardial loss of Pdgfrβ results in the failure of epicardial migration and subsequent loss of cVSMCs (Mellgren et al., 2008). Wt1 transcriptionally regulates Snail and E-cadherin in epicardial cells. Wt1 is also crucial for the repression of epithelial phenotype (Martinez-Estrada et al., 2010). Wnt/β-catenin signaling pathway also has shown to function during epicardial EMT as β-catenin is required for epicardial migration and

differentiation into cVSMC (Zamora et al., 2007).

Amazingly, epicardial gene expression reverts to an embryonic profile during zebrafish cardiac regeneration and repair. The epicardial genes, *Tbx18* and *Raldh2*, are activated in the epicardium which is reminiscent of embryonic development of the epicardium. During cardiac regeneration, a subset of epicardial cells undergoes EMT and contributes to new vasculature which supplies blood to newly formed cardiac muscle (Lepilina et al., 2006). Another study has shown that activation of *Raldh2* in both the epicardium and endocardium is required for cardiomyocyte proliferation during cardiac regeneration in zebrafish but not in mouse (Kikuchi et al., 2011). Several studies propose that the adult epicardium is also a source of cardiomyocyte progenitors (Di Meglio et al., ; Limana et al., 2007) and a signaling source during the heart regeneration (Winter et al., 2007; Zhou et al.). It has been proposed that the human epicardium may be a good source of progenitor cells which can be expanded for therapeutic purposes (van Tuyn et al., 2007; van Tuyn et al., 2005).

*Epicardial-derived cells*

After epicardial cells migrate into the heart, they then differentiate predominantly into cVSMCs and cardiac fibroblasts. The suggestion that these are the cells that arise from the epicardium was demonstrated using viral tracing (Dettman et al., 1998; Mikawa and Gourdie, 1996), quail-chick chimeras (Lie-Venema et al., 2005; Poelmann et al., 1993) and reporter gene tracing (Merki et al., 2005). Other reports also suggest cell types other than cardiac fibroblasts and cVSMCs are derived from epicardium such as the outer leaflets of the atrioventricular valves (del Monte et al., 2011; Grieskamp et al., 2011;

Mellgren et al., 2008; Merki et al., 2005; Sridurongrit et al., 2008). The contribution of epicardial cell to the vascular endothelium and cardiomyocytes is controversial, and often different results are obtained depending on the model organism and method of analysis. This is, in part, due to the limitation of methods available for unambiguously labeling and detecting epicardial cells. More recent studies suggest that these cells have a different origin other than the epicardium (Cai et al., 2008; Christoffels et al., 2009; Katz et al., ; Red-Horse et al., ; Zhou et al., 2008).

The signals between EPDCs and other cell types within the heart, such as cardiomyocytes and endocardium, are multidirectional (Ieda et al., 2009; Smith and Bader, 2007), and paracrine signals by EPDCs play roles during the formation of coronary vasculatures. Conversely, local environmental cues also determine further differentiation or survival of EPDCs as endothelial cells are important regulators of VSMC migration and proliferation (Tomanek, 2005).

**Genes involved in epicardial EMT**

Both in vivo and in vitro studies revealed genes involved in epicardial EMT including growth factors, downstream mediators, and transcription factors as described above. This section focuses on two newly discovered genes in epicardial EMT: neurofibromin 1 (Nf1), a negative regulator of Ras and Tcf21, a basic helix-loop-helix transcription factor.

*Neurofibromin 1*

Neurofibromin 1 (Nf1) which contains a Ras-GTPase activating protein (GAP) domain is a well-known tumor suppressor. Nf1 can accelerate the intrinsic activity of Ras-GTPase which results in the conversion of active Ras-GTP to inactive RAS-GDP (Martin et al., 1990; Xu et al., 1990). Mutation in *Nf1* causes neurofibromatosis type 1 (NF1), one of the most common autosomal dominant diseases, characterized by benign and malignant tumors (Lynch and Gutmann, 2002). Cardiovascular disease is a frequent cause of death in persons with neurofibromatosis 1 less than 30 years old (Rasmussen et al., 2001). The frequency of heart defects is about two times higher in people with NF1, suggesting a role for *Nf1* during heart development (Lin et al., 2000). Studies in mice revealed that inactivation of *Nf1* causes lethality at mid-gestation with severe heart defects including malformation of the outflow tract, a thinned myocardium, a ventricular septal defect (VSD), and enlarged endocardial cushions (Brannan et al., 1994; Jacks et al., 1994). Furthermore, endothelial-specific deletion of *Nf1* recapitulates most of these early heart defects suggesting an essential role for Nf1 in this cell type (Gitler et al., 2003). During EMT of the cardiac valves, a subset of endothelial cells delaminates from the surface layer, migrates into the cardiac jelly, and becomes mesenchymal. Interestingly, endocardial cushion cells from *Nf1* null mice exhibit abnormal EMT (Lakkis and Epstein, 1998). These studies demonstrated that Nf1 modulates EMT and proliferation in developing endocardial cushions by regulating Ras activity (Lakkis and Epstein, 1998). Vascular defects are often reported in people with neurofibromatosis 1, and some defects are attributed to congenital abnormalities in outflow track (Friedman et al., 2002; Lin et al., 2000). Interestingly, increased neointima formation in *Nf1* heterozygote mice is

observed and can be mitigated by Imatinib treatment suggesting a possible role for PDGF signaling on exaggerated vascular injury responses associated with the loss of *Nf1* (Lasater et al., 2008). Neural crest cells contribute to outflow track septum and pulmonary artery during heart development (Boot et al., 2003), and neural crest defects have also been reported in Nf1-deficient mice (Gitler et al., 2003). Since EMT is an essential process during development of neural crest cells (Acloque et al., 2009), defective EMT in neural crest cells may be the underlying cause of outflow track abnormalities and pathogies in people with neurofibromatosis 1.

Recent studies suggest a broader involvement of EPDCs in several cardiac diseases such as interstitial fibrosis, valve abnormalities, vascular remodeling and myocardial disarray (Olivotto et al., 2009) which are also higher in people with neurofibromatosis type 1 (Lin et al., 2000; Rasmussen et al., 2001). Moreover, EMT also occurs as pathological responses to cardiac injury or stress, and these processes share common signaling pathways with developmental EMT (Thiery et al., 2009). Understanding Nf1 function during heart development as well as in adult hearts will give us insight about the underlying cause of cardiac abnormalities and cardiovascular diseases in people with Nf1.

*Tcf21*

Tcf21 is a basic helix loop helix (bHLH) transcription factor that is expressed in and required for the proper development of multiple cell types (Cui et al., 2004; Cui et al., 2003; Hong et al., 2005; Lu et al., 2000; Lu et al., 2002; von Scheven et al., 2006). *Tcf21*-null mice have hypoplastic lung resulting postnatal lethality and also do not form spleen

(Lu et al., 2000; Quaggin et al., 1999). Loss of *Tcf21* also leading to developmental defects in the gonad and kidney (Cui et al., 2004; Cui et al., 2003). Analysis of Tcf21 function suggests that it can function in cranial muscle as both a transcriptional activator as well as a repressor (Lu et al., 2002). It works cooperatively with other factors, such as E2A or MyoR to regulate genes that mediate lineage-specific differentiation in various cell types (Funato et al., 2003; Plotkin and Mudunuri, 2008). Although *Tcf21* is widely utilized to detect epicardium, its function has not been investigated thoroughly in the epicardium and EPDCs development.

**Development and function of cardiac fibroblasts**

During development, the majority of cardiac fibroblasts are believed to be derived from the epicardium by epicardial EMT (Dettman et al., 1998; Mikawa and Gourdie, 1996; Poelmann et al., 1993). Several studies also proposed some contribution of endocardial cells by endocardial cushion EMT, endothelial cells, and hematopoietic cells by postnatal recruitment of circulating bone marrow cells (Norris et al., 2008) suggesting a heterogeneous origin of cardiac fibroblast.

Cardiac fibroblasts provide structural support and enhance mechanical signaling in the heart (Nag, 1980). They play a central role in synthesizing and secreting most of the components of the extracellular matrix (ECM) including collagens, laminins, fibronectins and tenascins. Cardiac fibroblasts also regulate the degradation of ECM by producing matrix metalloproteinases (MMP) and tissue inhibitors of metalloproteinase (TIMP) enabling homeostatic maintenance of ECM (Brown et al., 2005; Souders et al.,

2009).

Cardiac fibroblasts also play a central role as mediators of the inflammatory and fibrotic response. Following injury, cardiac fibroblasts and other fibrotic cells are recruited to the site of the wound and secrete ECM to provide structural support for regeneration and remodeling. At the final stage of wound healing, MMPs and TIMPs by cardiac fibroblasts remove excessive ECM. Dysregulation of the injury repair response may lead to ineffective or over exuberant pathological wound healing (Martin, 1997; Pardo and Selman, 2006; Tomasek et al., 2002).

Fibrosis is caused by excess deposition of ECM by cardiac fibroblast-like cells (Takeda et al., 2010). Although, fibrosis is initiated to protect damaged tissue, it becomes pathogenic if it goes unchecked. Current treatments target the inflammatory response which does not directly targeting the mechanism of fibrosis (Wynn, 2004). This leads to a general lack of efficacy. Despite the importance of the cardiac fibroblast in heart disease, very little is known about the transcriptional pathways that direct the embryonic development of these cells. Understanding the components required for the development of cardiac fibroblasts will provide us with information regarding the derivation and the function of these cells and may implicate better strategies for treating fibrosis.

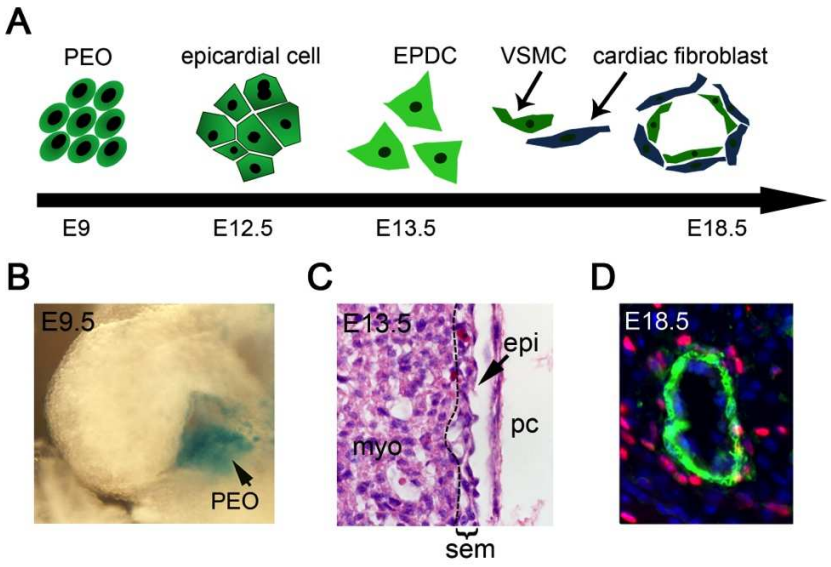


Figure 1-1. Epicardial development

(A) Schematic diagram of the epicardial development. Epicardial progenitor cells in the proepicardium (PEO) move toward and wrap around heart tube to form the epicardium. Epicardial cells undergo epithelial to mesenchymal transition, migrate into heart and form epicardial-derived cells (EPDCs). EPDCs differentiate into vascular smooth muscle cells (VSMCs) or cardiac fibroblasts. (B[1]) Whole mount image for developing heart from *Tcf21*$^{lacZ/+}$ embryo at E9.5 showing PEO (arrow). Embryos are stained for β-galactosidase activity. (C) H&E-stained image of heart section at E13.5 showing formation of EPDCs in subepicardial region. myo, myocardium; sem, subepicardial mesenchyme; pc, pericardium; epi, epicardium. (D) Fluorescence image of heart section at E18.5. Sections were stained for SM22α (green) and Sox9 (red). Nuclei (blue) were visualized by DAPI.

[1] The image in Figure 1-1B was adopted from Acharya et al., 2012.

# CHAPTER TWO

# DEVELOPMENT AND FUNCTION OF CARDIAC FIBROBLASTS: AN EPICARDIAL CONTRIBUTION

## Introduction

Chapter 2 summarizes my contribution to three published reports (Acharya et al., 2011; Acharya et al., 2012; Smith et al., 2011). The major focus of this chapter is to investigate the function of two epicardially-expressed genes, *Tcf21* and *Pdgfra*, during embryonic heart development. Work done by Christopher Smith showed that loss of *Pdgfra* resulted in a disruption in epicardial EMT in a subset of epicardial cells. Also, two previous lab members, Gregory Olsen and Banu Eskiocak, initially characterized the *Tcf21*-null heart phenotypes showing defective epicardial migration of cells that have *Tcf21* promoter activity in *Tcf21*-null embryos. From those results, two hypotheses were set to be tested: 1) How does loss of *Pdgfra* in epicardial cells affect epicardial-derived cell (EPDC) formation? 2) How does loss of *Tcf21* affect epicardial EMT and EPDC formation? To test these hypotheses, especially the investigation of EPDC formation, methods were needed that could detect cardiac fibroblasts.

Early studies characterized cardiac fibroblasts based on their morphological features. Cardiac fibroblasts are defined as flat, spindle-shaped cells displaying an extensive Golgi apparatus and rough endoplasmic reticulum which do not have basement membrane (Nag, 1980; Zak, 1974). In vitro isolation methods are frequently used to collect and culture cardiac fibroblasts. The methods are not specific and are more

permissive to cardiac fibroblast growth than cardiomyocyte or endothelial growth. Some groups have proposed that certain genes are cardiac fibroblast- or fibroblast-specific, such as discoidin domain receptor 2 (DDR2) (Goldsmith et al., 2004), fibroblast-specific protein 1 (FSP-1) (Strutz et al., 1995) and Thy1.1 (Hudon-David et al., 2007). Other markers that are enriched in fibroblasts, such as vimentin, fibronectin, connexins, prolyl 4-hydroxylase and periostin, have been used for the detection of cardiac fibroblasts (Goldsmith et al., 2004; Kivirikko et al., 1989; Snider et al., 2009). However, expression of these genes in other cell types often makes them less definitive as markers (Souders et al., 2009). Detection by multiple markers and exclusion by other cell type-specific markers are often used to increase specificity. A more effective and reproducible method for detection of cardiac fibroblasts was required to help understand this dynamic cell type and to investigate the function of genes that are important for cardiac fibroblast development.

My contribution to the paper Smith et al., 2011 was in the investigation of the development of epicardial cells and the generation of adenovirus for Sox9 overexpression to rescue the loss of *Pdgfra*. In the papers Acharya et al., 2011 and Acharya et al., 2012, I was involved in the characterization of Tcf21-lineages in various organs using $Tcf21^{iCre}$ mice, investigation of epicardial cell formation and spreading, and defining the function of Tcf21 during epicardial EMT. Importantly, one of the major contributions to these studies was to establish an effective and reproducible method for the identification of cardiac fibroblasts by in situ hybridization, immunohistochemistry and fluorescence-activated cell sorting. With the methods that I will describe in the results sections, we were able to detect cardiac fibroblast deficits in $PDGFR\alpha^{EKO}$ and *Tcf21* mutant mice.

Conversely, *Pdgfra* and *Tcf21* can now be used for the detection of cardiac fibroblasts as we characterize their specific function and expression during cardiac fibroblast development.

## Materials and Methods[2]

### *Mice*

Mice were maintained on a mixed C57/Bl6 X 129SV background. The strains in these experiments included *PDGFRα*$^{fl}$ (Tallquist et al., 2003), *PDGFRβ*$^{fl}$ (Richarte et al., 2007; Schmahl et al., 2008) and *R26R*$^{lacZ}$ (Soriano, 1999). *Tcf21*$^{LacZ/+}$ (Lu et al., 2000) *Tcf21*$^{iCre/+}$ and *Gata5Cre*$^{Tg/0}$ (Merki et al., 2005) mice have been previously described. Reporter strains used in the study include: *R26R*$^{YFP}$ (Srinivas et al., 2001), *R26R*$^{tdT}$ (Madisen et al., 2010) and *XlacZ4* mice (Tidhar et al., 2001). All animal protocols and experiments were approved by the UTSW IACUC and conformed to National Institutes of Health guidelines for care and use of laboratory animals. All procedures described in this study were approved by the Institutional Animal Care and Use Committees of UT Southwestern Medical Center and conformed to NIH guidelines for care and use of laboratory animals. Mice were maintained on a mixed C57BL6/129SV background and data for each experiment was deduced from a minimum of three nulls and three littermate controls.

---

[2] The text in Materials and Methods section was adopted, in part, from three articles: Acharya et al., 2011; Acharya et al., 2012; Smith et al., 2011.

*In situ Hybridization*

Digoxigenin labeled probes: *Tbx18* (from Sylvia Evans, UCSD), *Col1a1, Col3a1* (from Benoit Crombrugghe, MD Anderson Cancer Center), *Tcf21* (from Anthony Firulli, IUPUI), *Pdgfra* (from Christer Betsholtz, Karolinska Institute) and *Raldh2*, which was synthesized using the sequence information from accession number BC075704, were used. Whole mount in situ hybridization was done as described previously (Piette et al., 2008). Briefly, embryos were isolated, fixed in 4% PFA and processed for in situ hybridization or dehydrated through ethanol series and stored -20ºC for later use. Embryos were bleached with 6% hydrogen peroxide/PBT to remove color from blood and digested with proteinase K (10μg/ml) for 3 min and washed with glycine (2ml/ml). After fixation with 4% PFA, embryos were equilibrated with prehybridization solution before hybridized with the RNA probes. Section in situ hybridization was performed as described previously (Schaeren-Wiemers and Gerfin-Moser, 1993; Smith et al., 2011). Briefly, embryonic hearts were isolated, fixed in 4% PFA, frozen embedded and sectioned 16 μm. Sections were digested with proteinase K (15 μg/ml, Fisher Scientific, BP1700-100) followed by brief fixation with 4% PFA and acetylated with acetic anhydride before hybridizing with digoxigenin-labeled RNA probes.

*Tamoxifen induction and immunohistochemistry*

Pregnant mice were administered tamoxifen (MP Biomedicals 156708, 0.1mg/gm body weight) by oral gavage. Cre activity was detected by the expression of $R26R^{YFP}$ or $R26R^{lacZ}$ reporter allele. No reporter activity was detected at anytime in the absence of tamoxifen. For immunohistochemistry, hearts were isolated in PBS, fixed in 4%

PFA for 1h, frozen embedded, and sectioned. Immunostaining of tissue was performed using the following antibodies: anti-GFP, Molecular probes Invitrogen (A11122, 1:250). Immunohistochemistry on paraffin sections was performed for the following antibodies: anti-periostin, Santa-cruz (Sc-49480, 1:50) and anti-cardiac troponin T, Abcam (ab9937, 1:500).

*Western blotting*

Whole cell extracts from E18.5 hearts (atria and conotruncal regions removed) were immunoblotted with the following antibodies: anti-periostin (1:500, Santa Cruz SC-49480); anti goat HRP (1:1000, Sigma)**;** anti-b-tubulin (1:1000, BD 556321); anti-mouse IgM (1:3000, Zymed); anti-SM22a (1:200, abcam).

*Adenoviral production and ex vivo migration assay*

AdGFP and Adbgal were kindly provided by Robert Gerrard (UTSW). AdSox9 was generated from a full-length cDNA (Open Biosystems, 5320371) and cloned into pAd/CMV/V5-DEST (Invitrogen). Ex vivo migration assay was performed as described previously (Mellgren et al., 2008) with a few modifications. Pregnant female mice resulting from a cross with *Tcf21*$^{iCre}$ knock-in mice carrying the *R26R*$^{tdTomato}$ reporter were induced with tamoxifen at E10.5. A day later (E11.5), hearts positive for reporter activity were isolated and cultured in 10% FBS 1:1 DMEM:M199 supplemented with basic fibroblast growth factor (2 ng/ml, Sigma) in presence of green fluorescent protein expressing adenovirus (AdGFP) for 12 h. Hearts were then stimulated with TGFβ1 (10 ng/ml, otherwise indicated) and PDGF-BB (20 ng/ml) to promote epithelial to

mesenchymal transition of the epicardium. After 48 h, hearts were fixed in 4% PFA for 2 h, frozen embedded, sectioned, and visualized for fluorescence.

*Imaging and Statistical Analysis*

The following equipment was used for imaging: Fluorescent imaging (Zeis Axiovert 200 with a Hamamatsu ORCA-ER camera), color imaging (Zeiss Axiovert 200 with an Olympus DP71 camera), and whole mount imaging (Zeiss Stemi SV 11 Apo with an Olympus DP71 camera). All images and figures were edited and created in Photoshop CS4. All statistical calculations were performed using Prism 5 (Graph Pad). *P* values for statistical significance were obtained using Student t-test for single variables between control and test samples.

*Flow Cytometry*

Hearts from E18.5 embryos were dissected and conotruncal/valves were removed. The tissue was subsequently minced with forceps and incubated with 0.2U/ml of Blendzyme 3 (Roche) in Earl's buffer (140mM NaCl, 8mM KCl, 1.8mM $CaCl_2$, 0.9mM $MgCl_2$, 25mM HEPES, pH 7.4) for 30min at 37°C. Cells were washed in PBS and were incubated with 1:100 dilution of Thy1-PE (Invitrogen, MCD9004) and 1:100 CD31-APC (eBioscience, 17-0311-80). All samples were analyzed on a BD FACS Calibur.

*Cell culture and isolation*

Primary epicardial cells were cultured from E12.5 hearts as published previously (Mellgren et al., 2008). To assay for EMT following *Tcf21* overexpression in primary

epicardial cultures, wild-type E12.5 hearts (atria and cushions removed) were cultured in 10% FBS 1:1 DMEM: M199 supplemented with basic fibroblast growth factor (2ng/ml). After 2 days, the hearts were removed and cells were allowed to grow for an additional 3 days. Cultures were then transduced with either the control virus (Adbgal) or AdTcf21 for 2 days followed by immunostaining for cell-cell junctional marker (β-catenin, BD Transduction laboratories, 610153, 1:200) and cytoskeletal actin (Phalloidin, Invitrogen, A12379, 1:500). Primary cardiac fibroblasts were isolated from E18.5 hearts after removing the atria, outflow tract, and the cardiac valves. The tissue was carefully minced with forceps and incubated in Dulbecco's Modified Eagle Medium (DMEM) containing 0.05% bovine serum albumin (BSA), 500U/ml Collagenase 2 (Worthington biomedical Corporation), and 0.003% trypsin at 37$^{o}$C with continuous shaking for an hour. Dissociated cells were filtered through a cell strainer (70mm) and pelleted by centrifuging at 1000g for 3 min. Cells were then resuspended in fresh media and plated for 1hr to allow fibroblasts to adhere. *Tcf21*$^{lacZ}$ allele carrying control and null cultures were fixed in 0.2% glutaraldehyde for 5 min, and stained for β-galactosidase activity.

**Results**

*Defective EMT in Tcf21-null epicardium*

Tcf21 expression has been documented using the *Tcf21*$^{lacZ}$ allele (Lu et al., 2000). *Tcf21* locus in the heart was first detectable in the proepicardium and was evident subsequently in the growing epicardium, atrioventricular canal and an interstitial cell population within the heart (Lu et al., 1998). In effort to study the function of Tcf21 in

epicardium during heart development, the expression of *Tcf21* in embryonic heart was examined more closely. Notably, a decrease in expression was detected at E12.5 and E13.5 relative to E11.5 by in situ hybridization studies (Figure 2-1).

Because Tcf21 is predominantly expressed by the epicardium within the heart, we investigated initial formation and spreading of the epicardium in the *Tcf21*-null hearts using in situ hybridization for epicardial genes, including *Tbx18* and *Raldh2* (Figure 2-2). Although regions of epicardial detachment were detected in null hearts, in situ hybridization demonstrated normal expression of epicardial markers suggesting epicardium can be formed in the absence of Tcf21.

Next, we examined epicardial cell migration into the myocardium using $R26R^{YFP}$ expression driven by the $Gata5Cre^{Tg}$ allele (Figure 2-3). At E14.5 in controls, $YFP^{+}$ cells were detected both in epicardium and within myocardial walls which were negative for the cardiomyocyte marker (cardiac troponin T, Tnnt2). However in *Tcf21*-null hearts, the number of $YFP^{+}$; $Tnnt2^{-}$ in myocardial walls was decreased suggesting the defective migration of epicardial cells (Figure 2-3). Because *Tcf21*-null hearts have no alteration in apoptosis or epicardial cell proliferation (Figure 2-4), loss of EPDCs inside the heart was probably caused by a failure of epicardial cell migration.

A $Tcf21^{iCre}$ allele (Acharya et al., 2011)was utilized to document Tcf21-lineage cells in various tissues. In this allele, a Cre recombinase protein fused to two mutant estrogen-receptor ligand-binding domains (Zhang et al., 1996) under the control of the endogenous *Tcf21* locus by homologous recombination. Tamoxifen induction resulted in Cre recombination, and Tcf21-expressing cells and all of their progeny were detected by reporter gene expression such as $R26R^{YFP}$ or $R26R^{lacZ}$. As shown in Figure 2-5, $Tcf21^{iCre}$-

labeled cells ($YFP^+$) are present within the myocardium of the hearts. *Tcf21*$^{iCre}$-labeled cells are also founded in other organs including the kidney, spleen, aderenal gland and testis. To demonstrate that a Tcf21-expressing cell population migrates into the subepicardial space, an ex vivo migration assay was performed. In this assay, adenovirus specifically transduces only the surface epicardial cells. Figure 2-6 demonstrates a significant overlap of the adeno-GFP tagged cells with *Tcf21*$^{iCre}$ lineage traced cells. Taken together, these data suggest that Tcf21 is required for epicardial migration, at least in a subset of epicardial cells.

*Selective loss of cardiac fibroblasts in Tcf21-null and Pdgfra mutant hearts*

*Guided by multiple growth factor signaling cues, the epicardium gives rise primarily to two cell fates: cVSMCs and cardiac fibroblasts (Winter and Gittenberger-de Groot, 2007). To determine how the defect in epicardial migration affects the development of these two EPDC fates, formation of cVSMCs in Tcf21-nulls was examined using mice possessing an XlacZ4 transgene that drives nuclear β-galactosidase expression in populations of smooth muscle cells (Tidhar et al., 2001). Figure 2-7 shows that cVSMCs were detectable in both null and control hearts. Thus, despite defective epicardial EMT of Tcf21 reporter-tagged cells, Tcf21-null hearts develop cVSMCs.*[3]

For the detection of cardiac fibroblasts, we examined the expression of ECM gene (*Col1a1*) which is predominantly synthesized by cardiac fibroblasts along with *Pdgfra*. First, the expression of *Col1a1* and *Pdgfra* were examined at various time points

[3] The italicized text was adopted from the article Acharya et al., 2012.

to establish the optimal stage to quantify developing fibroblasts (Figure 2-8). Cells expressing these two genes were evident from E18.5 to P7, but after P7, in situ detection of gene expression appeared to be decreased (Figure 2-9). These data suggested that *Col1a1* and *Pdgfra* expression fell within a very discrete time window. In the epicardial specific knockout of both *Pdgfra* and *Pdgfrb* (*PDGFR*$^{EKO}$) hearts, a reduction of greater than 50% for cells expressing *Col1a1* at P7, and a reduction in fibroblast markers was also observed in a *Pdgfra* epicardial mutant (*PDGFR*$\alpha^{EKO}$) at E18.5 (Figure 2-9). These calculations were over estimations of the remaining fibroblasts as VSMCs surrounding the coronary vasculature also produce collagen (Figure 2-9). These results suggested that cardiac fibroblast development was disrupted in *PDGFR*$^{EKO}$ and *PDGFR*$\alpha^{EKO}$ hearts and that epicardial-derived fibroblasts are required for matrix production in the developing heart. The results also have shown that disruption of cardiac fibroblasts can be effectively examined by detecting the expression of ECM component genes.

Compared to control hearts, interstitial *Col1a1* or *Col3a1* expression was also reduced in *Tcf21*$^{-/-}$ hearts at E18.5 although some residual expression was maintained around the vessels, most likely by the VSMC population (Figure 2-10) (Ponticos et al., 2004). Results described above and in previous studies (Mellgren et al., 2008; Smith et al., 2011) suggest a specific function for and expression of *Pdgfra* in cardiac fibroblasts. Thus, we utilized *Pdgfra* expression for the detection of cardiac fibroblasts in developing hearts. Consistent with *Col1a1* and *Col3a1* expression, the number of cells that expresses *Pdgfra* was also reduced in *Tcf21*-null hearts (Figure 2-10).

We further detected cardiac fibroblasts using additional methods. First, expression of periostin (Postn), a TGFβ-inducible protein secreted by cardiac fibroblasts,

within the wall of the ventricles was also reduced in *Tcf21*-null hearts compared with wild-type controls (Figure 2-11). Similar results were obtained with immunoblotting of whole-cell extracts for selective cell type markers (Figure 2-11). Importantly, *Tcf21*-null hearts maintained expression of fibroblast markers in the cardiac valves and septum suggesting that the fibroblast defects may be specific to epicardially-derived cardiac fibroblasts (Figure 2-10, Figure 2-11).

Next, utilizing *Gata5Cre* transgenic mice (Merki et al., 2005) and a $R26R^{YFP}$ reporter (Srinivas et al., 2001), epicardial-derived cells were tagged and their numbers examined in the presence or absence of Tcf21. Single cell suspensions from E18.5 hearts were generated. We utilized Thy1.1, a membrane glycoprotein expressed on the surface of cardiac fibroblasts and endothelial cells (Rege and Hagood, 2006). Endothelial cells were excluded from the sorting for cells that were $CD31^-$ cells. Cells with an epicardial origin were sorted by YFP detection. Cells that were double-positive for Thy1.1 and YFP but negative for CD31 population were classified as epicardial-derived cardiac fibroblasts. The proportion of $Thy1^+$; $YFP^+$; $CD31^-$ cells were compared with the total number of $Thy1^+$ cells in the heart. As shown in Figure 2-12, $Tcf21^{-/-}$ had far fewer epicardial-derived cardiac fibroblasts compared to wild-type and heterozygotes. Finally, we also isolated and cultured cardiac fibroblasts from control and null hearts at E18.5 (Figure 2-13). Far fewer cardiac fibroblasts were obtained from null hearts. In summary, our data support a specific loss of cardiac fibroblasts in *Tcf21*-null hearts.

*Function of Tcf21 and in epicardial EMT*

To examine the ability of Tcf21 to induce cell migration, wild-type E12.5 hearts

were transduced with adenovirus expressing GFP (AdGFP) in the presence or absence of AdTcf21. As shown in Figure 2-14, adenoviral transduction of GFP efficiently labels >98% of epicardial cells but not the cells within myocardium. However, overexpression of Tcf21 in cultured wild-type hearts induced epicardial cell migration. We then detected the cells that were undergoing EMT in vivo by Sox9. Recent data have suggested a potential role for Sox9 in epicardial EMT (Smith et al., 2011). Sox9 expression is significantly reduced in epicardial cells that fail to undergo EMT, suggesting that Sox9 expression correlates with epicardial EMT. In addition, Sox9 is involved in neural crest cell and endocardial cushion EMT (Akiyama et al., 2004; Sakai et al., 2006) and also has been shown to be a downstream mediator of Nf1-dependent metastasis (Powers et al., 2007). Thus, we examined Sox9 expression at E14.5. At E14.5, the number of $Sox9^{+}$ cells in myocardium were decreased both in left and right ventricles of *Tcf21*-null hearts compared to controls (Figure 2-15). Notably, in the mutant hearts, the number of $Sox9^{+}$ cells in epicardium was increased compared to controls.

To investigate possible migration defects of *Tcf21*-null epicardial cells, we cultured primary epicardial cells. The epicardial nature of the cultured cells was monitored over time by tracing promoter activity of epicardial genes using $Tcf21^{lacZ}$ or $Pdgfra^{GFP}$ allele (Figure 2-16). Further characterization was done by quantifying gene expression over a 14 day period where the percentage of gene expression by these cells gradually decreased over time (Figure 2-17). The decrease in epicardial gene expression was also noted after inducing cultures with TGFβ1. Expression of *Dermo* (*Twist2*), a potential marker for EMT, was noted at around day 7. Epicardial cells initially spread out from the heart explants without a noticeable difference in morphology between mutants

and controls. However, after removing the cardiomyocyte containing portion of the heart explants, *Tcf21*-null epicardial cells (and to some extent heterozygotes) became rounded in shape and lost cellular junctions as detected by α-Catenin (Figure 2-18). To examine the possibility of a cell autonomous defect, we co-cultured mutant epicardial cells with controls in the same well. After removing heart explants, morphological defects were still present in mutant epicardial cells while control epicardial cells appeared normal (Figure 2-18). These results suggest a cell autonomous requirement for Tcf21 in maintaining epicardial cell morphology. To investigate these cells response to EMT inductions, we treated cultures with TGFβ1. In control cultures, treatment of TGFβ1 induced morphological changes reminiscent of EMT, but *Tcf21*-null epicardial cells reverted to an epithelial morphology upon TGFβ1 treatment (Figure 2-19).

To understand the molecular mechanism of the epithelial morphology defects, previous members Christopher Smith and Banu Eskiocak performed microarray to identify differentially expressed genes in *Tcf21*-null epicardial cultures. Among the ~50 genes that were down-regulated in mutant cultures (Table 2-1), we further screened and selected the candidate genes that are known to be expressed in the epicardium and EPDCs or whose function is involved in EMT or migration. Two genes, *Snail* (*Snai1*) and *Nedd9* (*Hef1*), met the criteria and were further investigated their relationship with Tcf21. Consistent with the microarray data, the expression of *Snail* and *Nedd9* was down regulated in *Tcf21*-null cultures, and treatment of TGFβ1 resulted in increased expression of both genes (Figure 2-19). To test how Nedd9 interacts with the *Tcf21*-null phenotype, we generated adenovirus for Nedd9 expression (Figure 2-19). Nedd9 has a reported function in cell adhesion and migration (Aquino et al., 2009) and adenoviral transduction

of Nedd9 caused control epicardial cells to be spread, similar to TGFβ1-induced epicardial cells. In *Tcf21*-null cultures, the morphological defects were partially rescued by Nedd9 expression (Figure 2-19). We then measured the *Nedd9* expression with the presence of known inducers of its transcription such as TGFβ1 or all-trans retinoic acid (atRA). In the mouse epicardial cell (MEC) cultures, *Nedd9* expression was increased dose-dependently by the treatment of TGFβ1 or atRA (Figure 2-20). However, no increase in *Nedd9* expression was detected by the overexpression of Tcf21. Consistent with previous ex vivo migration results (Figure 2-14), Tcf21 overexpression resulted in the increase of *Snail*, a transcription factor involved in the EMT process (Figure 2-20). Because Tcf21-null epicardial cells have a migration defect, we decided to test whether Tcf21 overexpression could induce actin cytoskeleton rearrangements and focal adhesions formation. We stained epicardial cultures for phospho-focal adhesion kinase (pFAK), paxillin and vinculin. As shown in Figure 2-21, adenoviral transduction of Tcf21 in the primary epicardial cultures induced the formation of focal adhesions especially in the protrusion of cell bodies.

**Discussion**

Cardiac fibroblasts are often defined as a major source of ECM including collagen 1 and collagen 3. However, expression of these genes was not often used to detect cardiac fibroblasts. In situ hybridization results show that the expression of *col1a1* and *col3a1* was dramatically decreased after P7, suggesting that they may not be good readouts for the presence of cardiac fibroblasts in adult hearts. Nonetheless, the detection

of *col1a1* and *col3a1* expression was enough to visualize and quantify cardiac fibroblasts in embryonic stages and enabled us to characterize heart defects that are specific to cardiac fibroblast development in several mutant mice, including *PDGFRα*$^{EKO}$ and *Tcf21*$^{-/-}$. Importantly, further characterizations of *Pdgfra* and *Tcf21* expression during cardiac fibroblast development have shown that these genes can be used for the detection of cardiac fibroblasts. Expression of *Pdgfra* and *Col1a1* was similar during development. Specific labeling of cardiac fibroblasts by the inducible mouse line expressing *Tcf21*$^{iCre}$ will allow us to study its physiological role during the pathogenesis of adult hearts, which will be discussed in Chapter 4. Tcf21-expressing cells also can be detected in multiple organs including heart, kidney, spleen, liver and adrenal glands (Figure 2-22) at various ages. The characterization of Tcf21-expressing cells and specific function of Tcf21 in these cells remain to be investigated.

The body of work described in this chapter also showed a specific function for Tcf21 in epicardial EMT and cardiac fibroblast development. In the absence of Tcf21, epicardial cells do not migrate into the heart. Interestingly, both treatment with TGFβ1 and overexpression of Nedd9 partially rescued the morphological defects of *Tcf21*-null epicardial cells. These results may indicate that a complex signaling network exists for epicardial EMT. This signaling can be defined by: 1) expression of EMT transcription factors including Twist, Snail and Slug; 2) expression of cytoskeletal elements such as vimentin, αSMA and filamentous actin; 3) morphological and functional changes, such as the loss of epithelial shape and cell-cell junctions, and 4) functional changes, such as the acquisition of migratory or invasive properties. It appears that the best way to examine EMT is by using a combination of these readouts to assess the process. Finally, it is worth

noting that the individual characteristics of EMT may depend on the cell-type-of-interest. For example, epicardial cells are of mesothelial origin and often have both epithelial and mesenchymal characteristics during development. The unique mode of epicardial EMT often makes it difficult to define and this issue will be briefly discussed in the Chapter 3.

Results described above have shown defects in cardiac fibroblast formation at the time of epicardial EMT when *Pdgfra* or *Tcf2 1*were disrupted. However, one question still remains: is *Pdgfra* or *Tcf21* involved in cardiac fibroblast specification? Testing this interesting question will be challenging, in part, due to the limitation of techniques and complexity of the processes. Acharya et al., 2012 suggests that the Tcf21 expressing epicardial cells gradually lose their ability to form VSMC as early as E10.5, a time point concomitant with epicardial EMT. Thus, it will be challenging to distinguish processes controlling EMT from those directing cell fate specification. To distinguish these, techniques to label and to trace EPDCs might be useful. $Wt1^{CreERT2}$ allele was tested for this purpose; however, it labels both epicardium and EPDCs and labeling efficiency was markedly decreased after E15.5. These limitations make it less useful to address the question. Inducible Cre that is expressed in epicardial cells even after the E15.5 will allow us to address the question properly. As an alternative, in vitro detection of EMT and cardiac fibroblast differentiation could be done. However, there are major limitations in distinguishing cardiac fibroblasts from undifferentiated epicardial cells or VSMCs in vitro. The current culture conditions for primary epicardial cells seem to direct epicardial cells to differentiate into VSMCs. Thus, identification of an inductive condition for cardiac fibroblast differentiation might be useful to test the differentiation of epicardial cell in vitro.

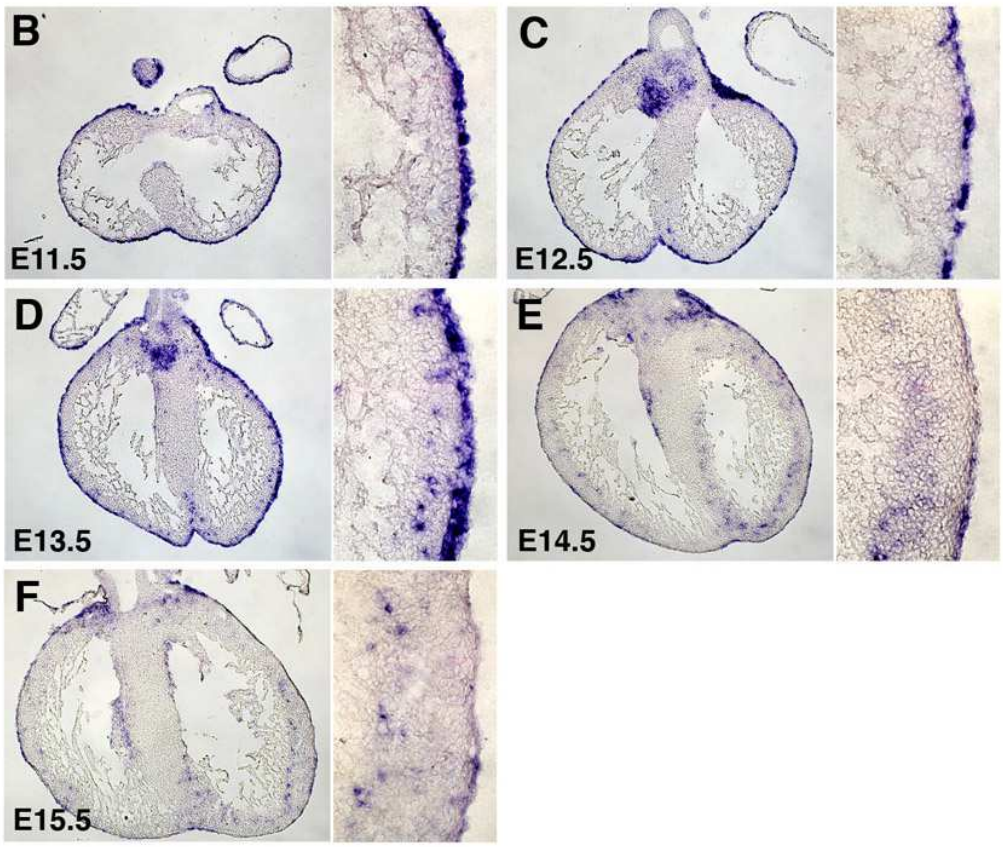


Figure 2-1. *Tcf21* expression in developing hearts

In situ hybridization showing *Tcf21* expression in wild-type hearts between E11.5 and E15.5.

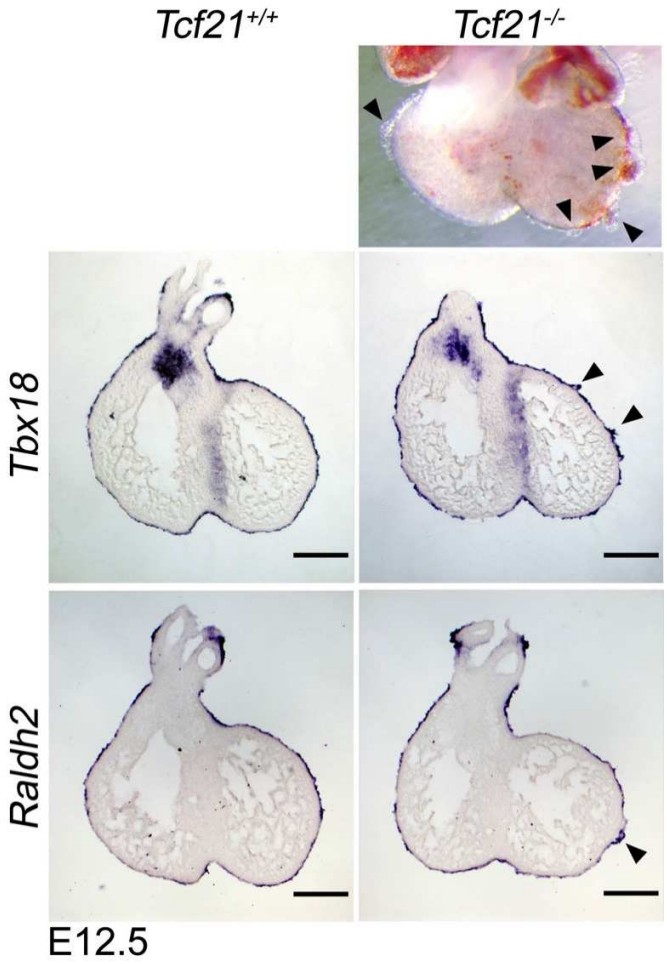


Figure 2-2. Epicardial development in *Tcf21*-null hearts

Whole-mount images of E12.5 wild-type and *Tcf21*-null hearts. Expression of epicardial genes (*Tbx18* or *Raldh2*) was examined by in situ hybridization on E12.5 embryonic heart sections. Arrowheads indicate regions of epicardial detachment in null hearts. Scale bars, 400 μm.

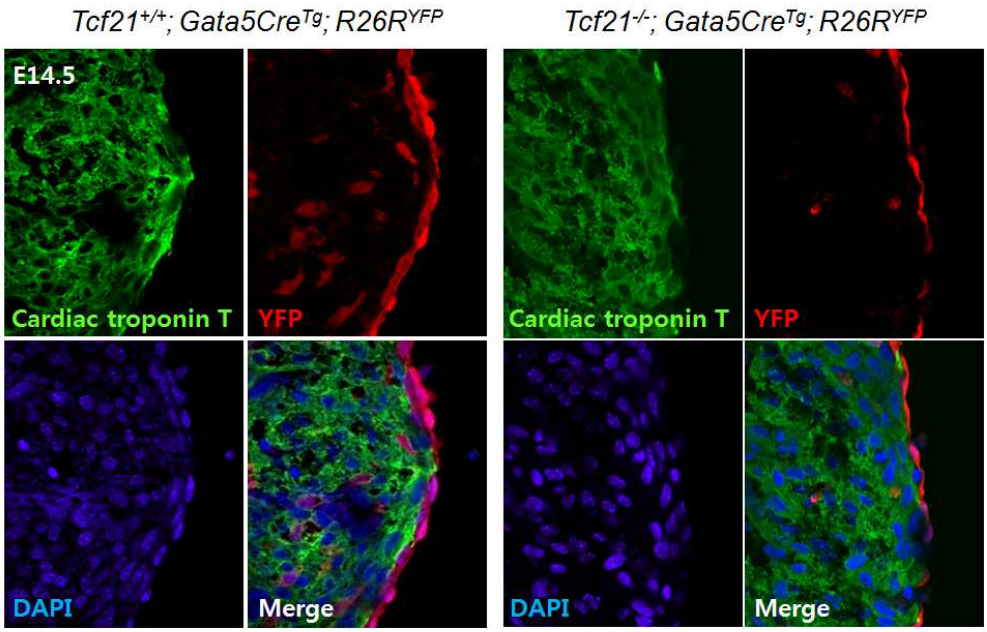


Figure 2-3. Defective migration of epicardial cells in *Tcf21*-null hearts

Migration of epicardial cells was traced in control and *Tcf21*-null hearts at E14.5. Epicardium and epicardial cells were identified by YFP expression. Cardiomyocytes were detected by antibody staining against cardiac troponin T. Nuclei were visualized by DAPI.

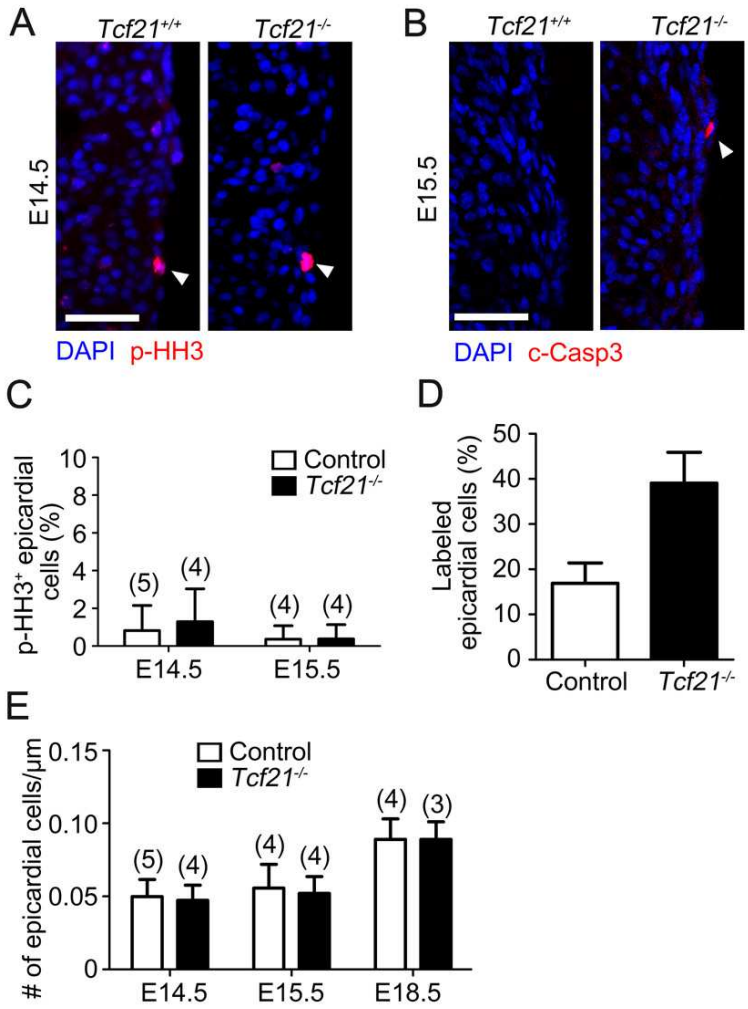


Figure 2-4. No obvious differences in epicardial proliferation or survival

(**A**,**B**) Representative heart sections immunostained for phospho-histone H3 (p-HH3; A) or cleaved-caspase 3 (c-Casp3; B) are shown. B indicates a rare apoptotic epicardial cell at E15.5 in the null, whereas at E14.5, no apoptotic cells were observed in the epicardium, c-Casp3$^{+}$ cells in endocardial cushion region of the same heart sections served as the positive control. Scale bars represent 50 µm. (**C**) Quantification of A. Percentage of p-

HH3$^{+}$ epicardial cells in LV normalized to the total number of epicardial cells in a 20× field of view. (**D**) Quantification of *Tcf21*$^{iCre}$*;R26R*$^{tdT}$-labeled epicardial cell retained in E18.5 hearts that were induced at E14.5. Percentage of tomato$^{+}$;DAPI$^{+}$ epicardial cells relative to the total number of DAPI+ epicardial cells is shown. (**E**) Quantification of overall epicardial cell number between wild-type and *Tcf21*-null hearts[4]. Error bars represent s.d. *n* is indicated in parentheses.

[4] The number of epicardial cells in epicardium at E14.5 and E15.5 was examined by Asha Acharya.

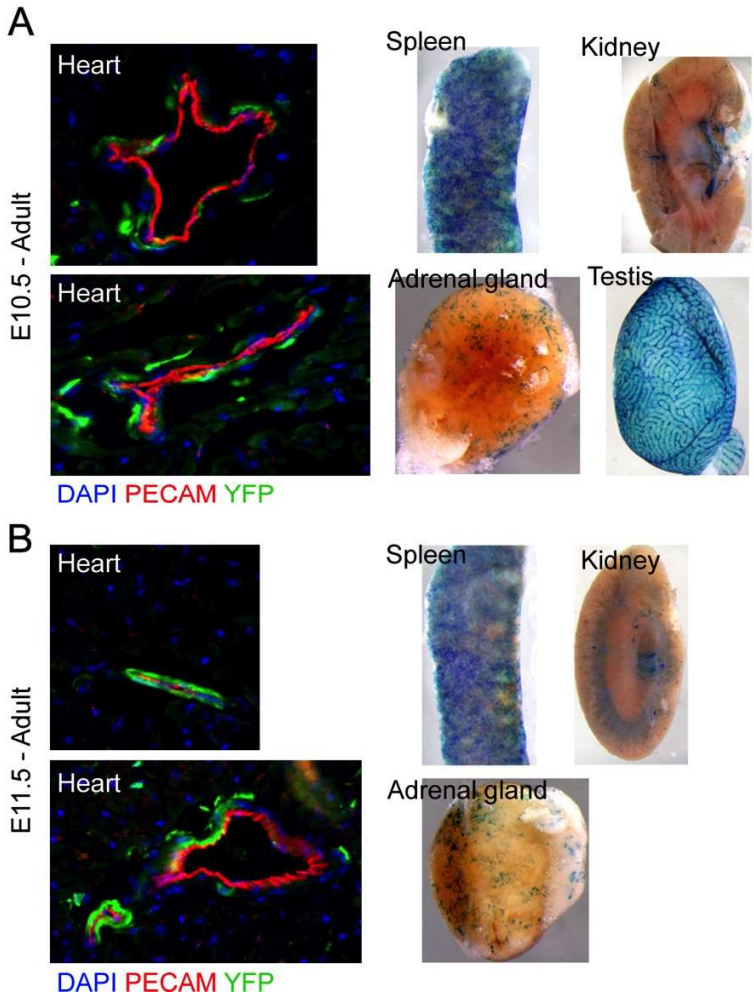


Figure 2-5. Tracing of *Tcf21*-expressing cells by $Tcf21^{iCre}$

(**A, B**) Cre was induced embryonically in $Tcf21^{iCre/0}$; $R26R^{YFP/lacZ}$ animals by oral gavage of tamoxifen to pregnant females at (A) E10.5 or (B) E11.5. *Tcf21*-expressing cells were traced postnatally by detecting the cells expressing $R26R^{YFP}$ or $R26R^{lacZ}$ in heart, spleen, kidney, adrenal gland and testis. Endothelial cells were detected by antibody staining against PECAM. Nuclei were visualized by DAPI

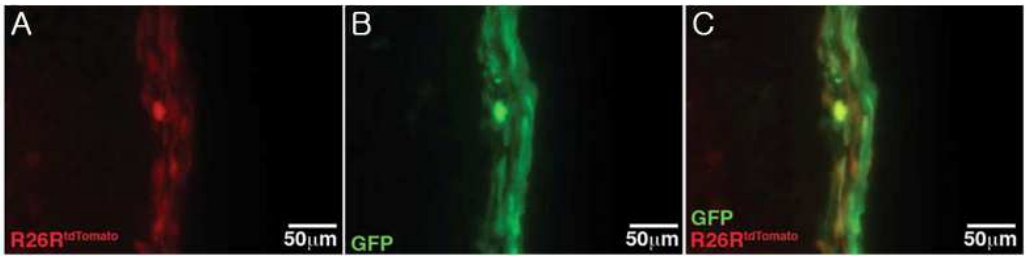


Figure 2-6. Migration of *Tcf21*$^{iCre}$ lineage epicardium

(A-C) Ex vivo migration assay showing *Tcf21*$^{iCre}$ labeled cells in the myocardium (red) are derived from AdGFP transduced (green) epicardial cells. E11-5 hearts induced a day before were analyzed following AdGFP transduction and culture in vitro. Scale bars represent the indicated magnifications.

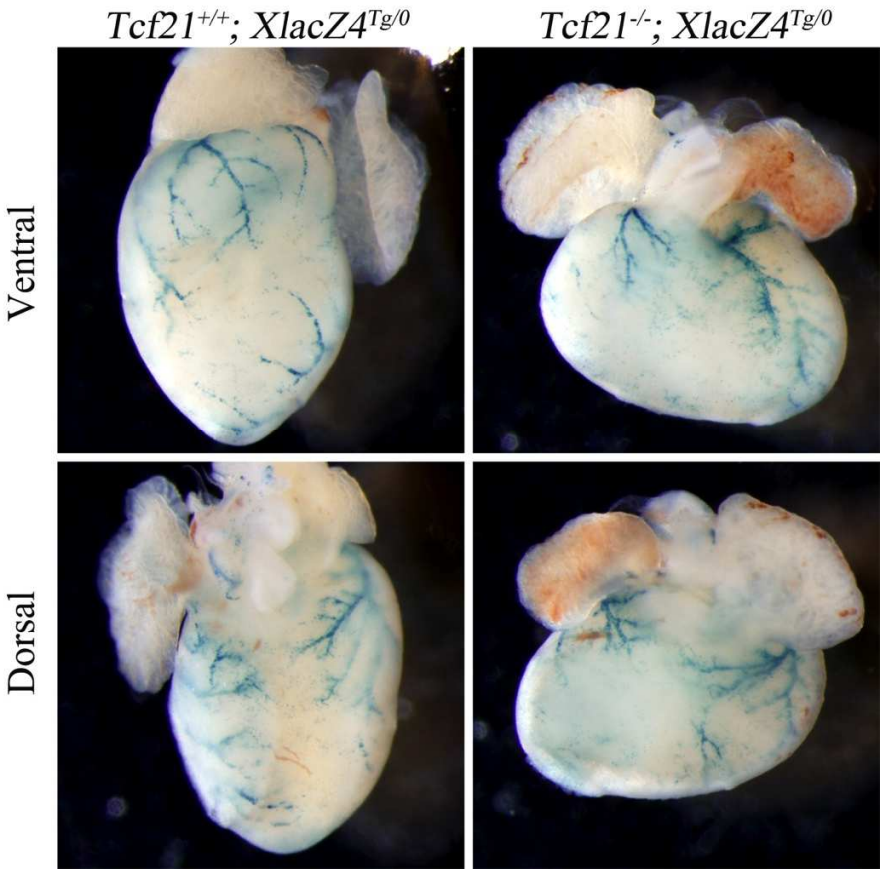


Figure 2-7. *Tcf21*-null hearts form cVSMCs

Development of coronary vasculature detected using whole-mount β-galactosidase staining of control and *Tcf21*-null E18.5 hearts carrying the *XlacZ4* transgene.

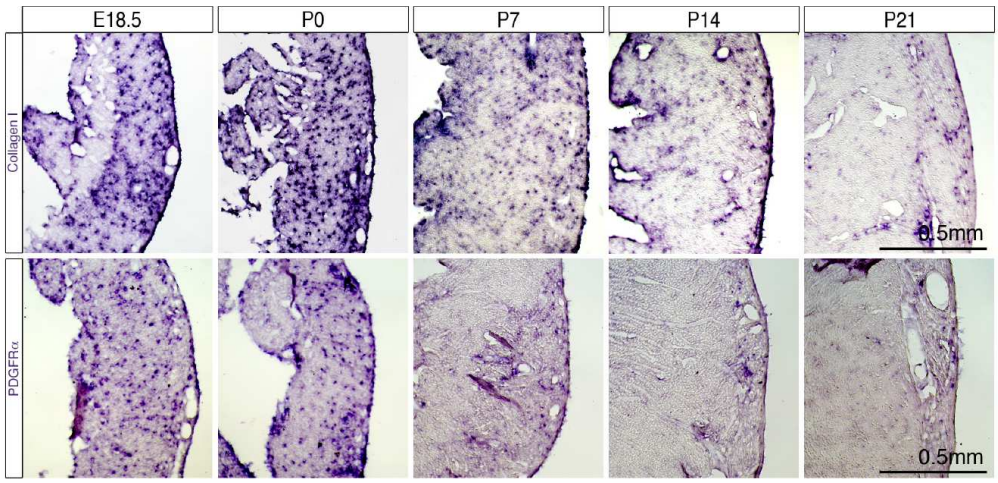


Figure 2-8. *Col1a1* and *Pdgfra* expression during postnatal development

*Col1a1* and *Pdgfra* in situ hybridization of left ventricles at the indicated ages. Time course was completed using wild-type animals of a mixed background.

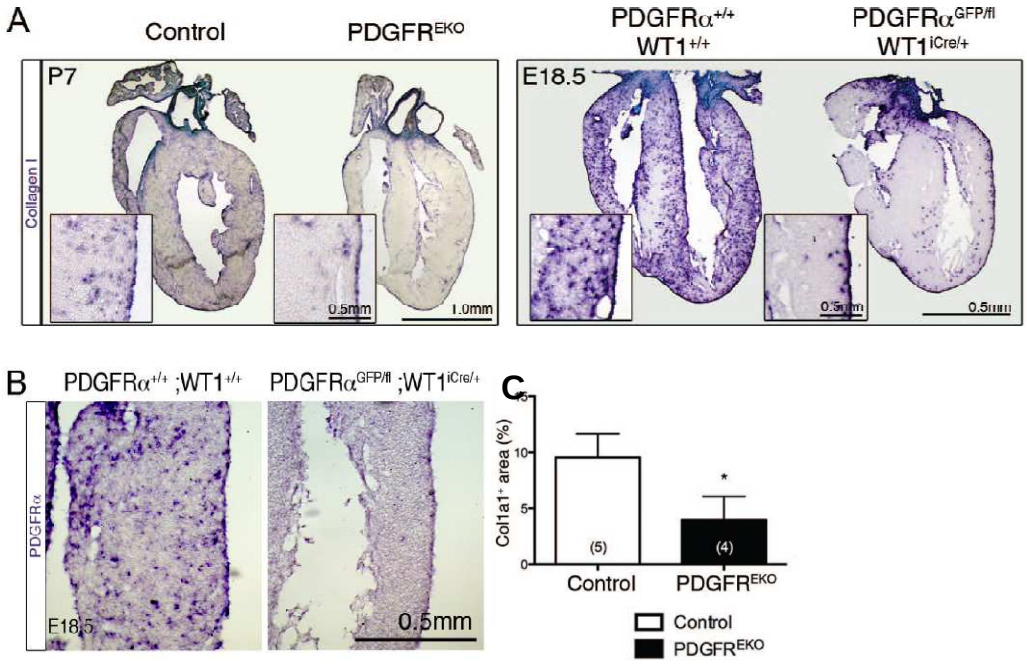


Figure 2-9. *Pdgfra* is required for cardiac fibroblast development

A, *Col1a1* in situ hybridization of the indicated genotypes and ages. Insets represent higher magnifications of left ventricle. B, *Pdgfra* in situ hybridization of control and *Pdgfra* mutant hearts. C, Quantification of interstitial *Col1a1* expression in A. **p*<0.005. *n* values are indicated in parentheses.

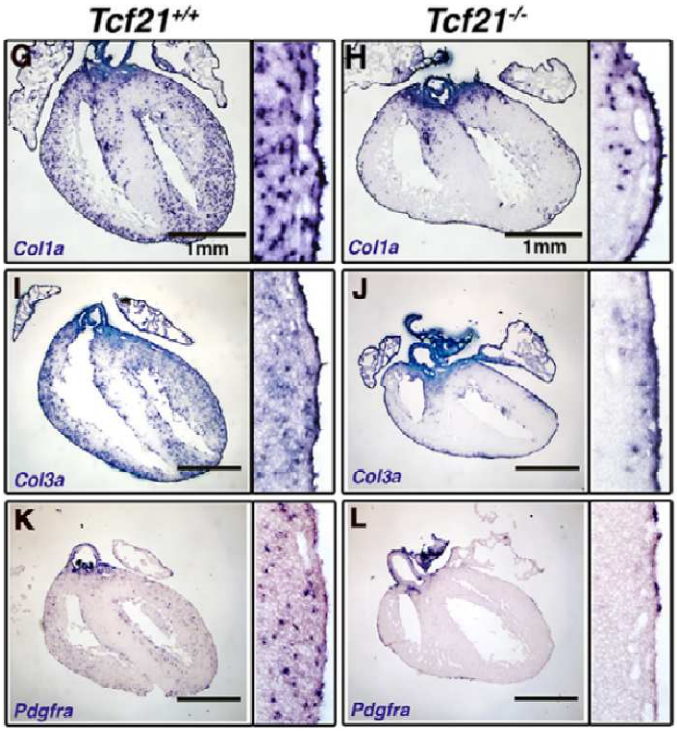


Figure 2-10. Loss of cardiac fibroblast in *Tcf21*-null hearts

(G-L) In situ hybridization of wild-type (G,I,K) and *Tcf21*-null (H,J,L) hearts. Expression of cardiac fibroblast specific genes *Col1a1* (G,H), *Col3a1* (I,J) and *Pdgfra* (K,L) is shown. Corresponding higher magnification images of the LV are shown to the right.

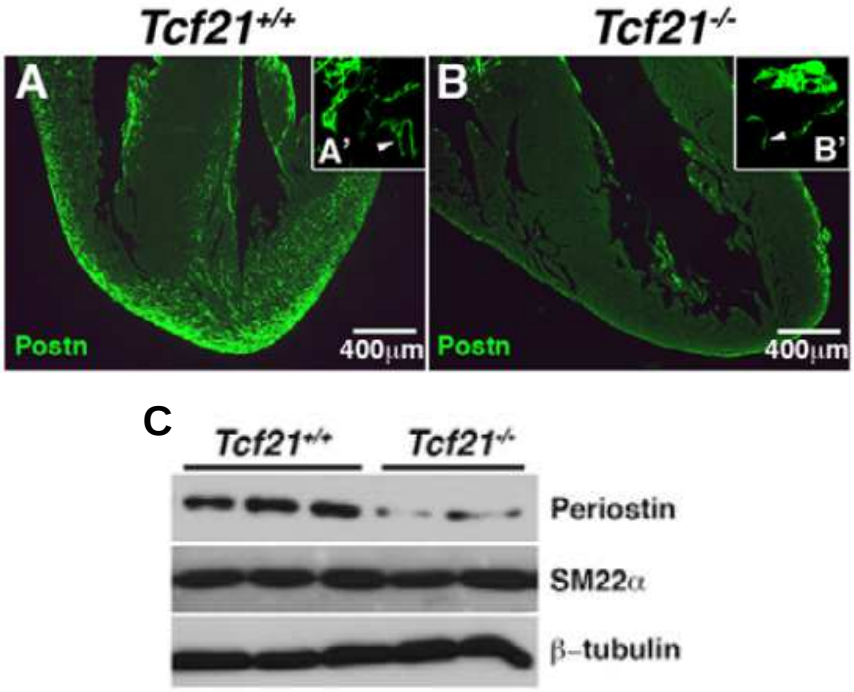


Figure 2-11. Periostin expression in *Tcf21*-null hearts

(**A-B'**) Periostin immunohistochemistry on wild-type (A) and *Tcf21*$^{-/-}$ (B) hearts. Inset images (A', B') show staining of the atrioventricular valve region. Arrowheads indicate valves. (**C**) Immunoblots comparing cardiac fibroblast (periostin) and VSMC (SM22α) protein expression in control versus *Tcf21*$^{-/-}$ hearts. Protein amounts were normalized using β-tubulin. All experiments were performed using E18.5 hearts.

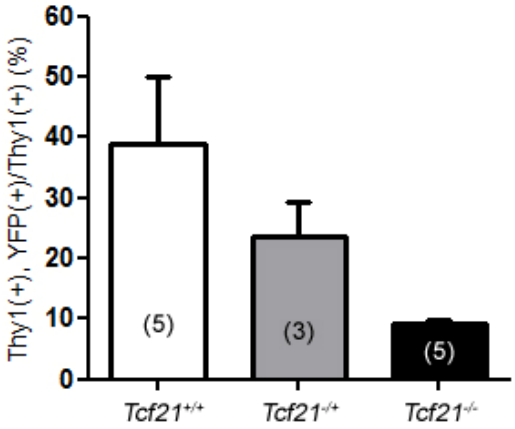


Figure 2-12. *Tcf21*-null hearts lack epicardial-derived cardiac fibroblasts

Percentage of epicardial-derived cardiac fibroblasts ($Thy1^+;YFP^+/Thy1^+$) from wild-type, $Tcf21^{+/-}$ and $Tcf21^{-/-}$ hearts. $CD31^+$ endothelial cells were excluded from the analysis. *n* values are indicated in parentheses.

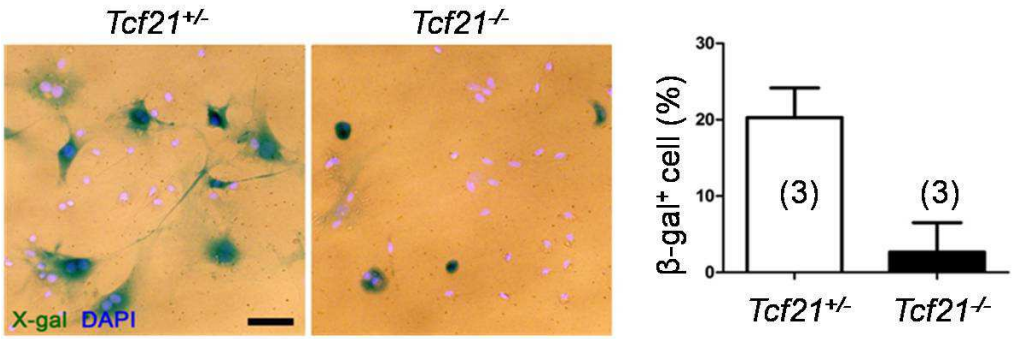


Figure 2-13. Cardiac fibroblasts cultures from *Tcf21*-null hearts

β-galactosidase-stained primary cardiac fibroblast cultures from control and *Tcf21*-null hearts. Nuclei are counterstained with DAPI. β-galactosidase$^{+}$ cells were counted and normalized with DAPI$^{+}$ cells. *n* values are indicated in parentheses.

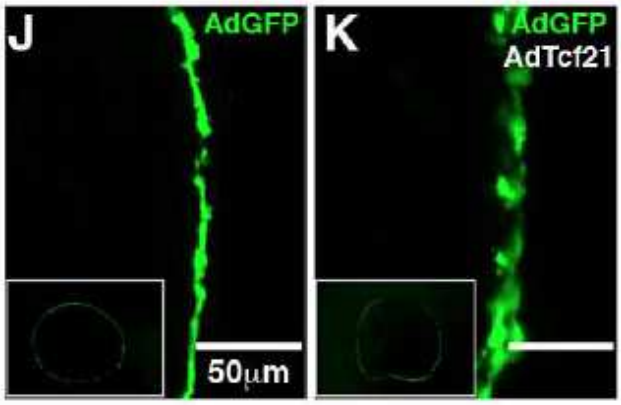


Figure 2-14. Ex vivo migration by Tcf21 overexpression

E12.5 wild-type hearts were transduced *ex vivo* with AdGFP in (J) the absence or (K) presence of AdTcf21. Scale bars represent indicated magnifications.

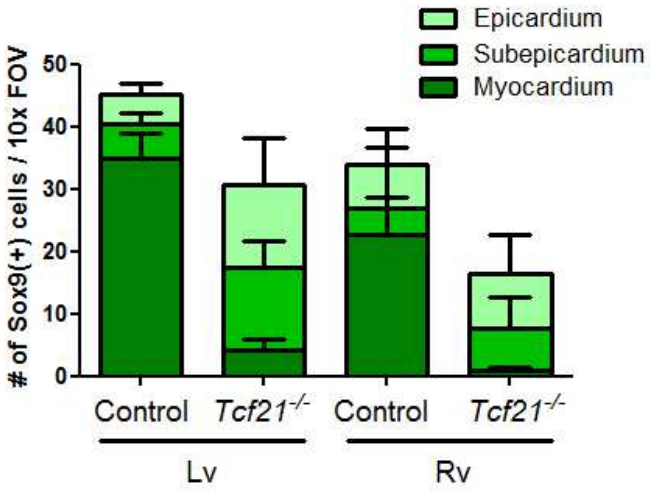


Figure 2-15. Sox9 expression in *Tcf21*-null hearts at E14.5

Sox9-expressing cells were detected and quantified by immunohistochemistry in control and *Tcf21*-null hearts at E14.5. Numbers of $Sox9^{+}$ cells in each compartments were counted both in left (Lv) and right ventricles (Rv) from the images of three nonconsecutive sections ($n$=4). Subepicardium was defined as the two- to three-cell-depth layer underneath epicardium.

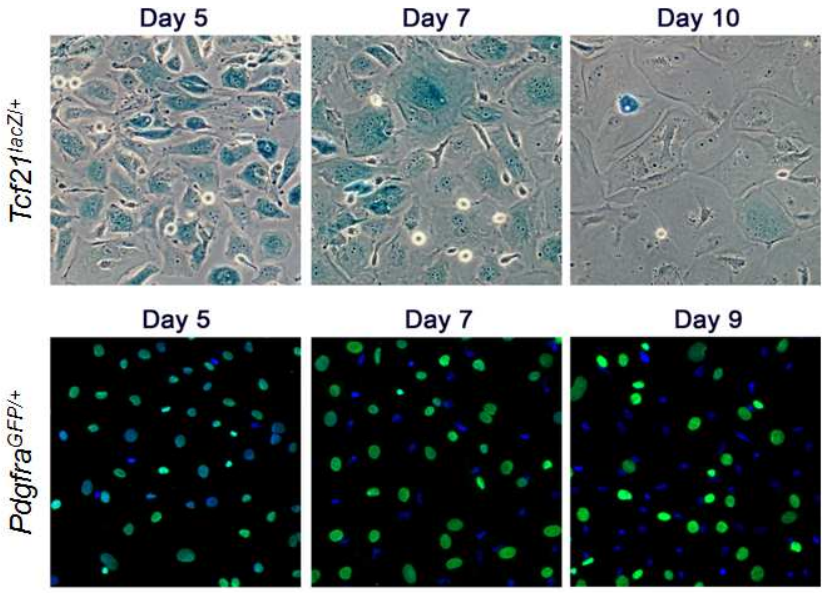


Figure 2-16. Epicardial reporter genes expression in primary epicardial cultures

Embryonic hearts of indicated genotypes were isolated at E12.5 and cultured for designated time. Heart explants were removed from the culture at day 3. Promoter activity of reporter genes, *lacZ* or *GFP* was detected by the staining for β-galactosidase activity or by antibody staining against GFP, respectively.

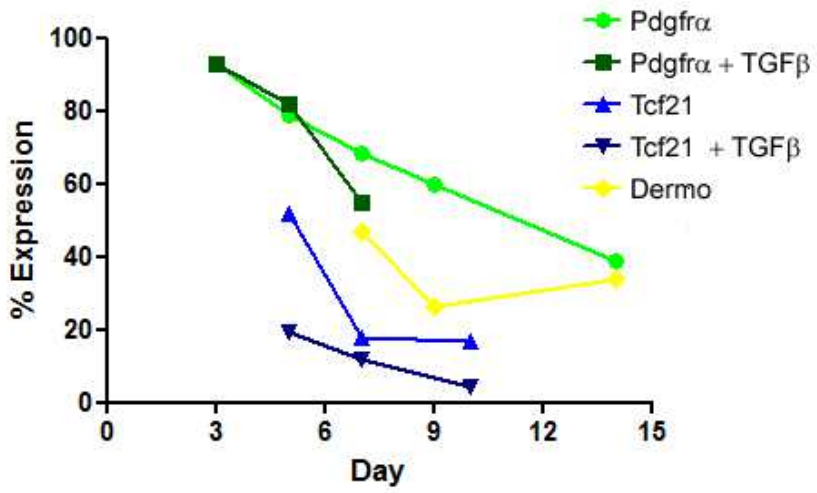


Figure 2-17 Dynamic expression of epicardial genes in primary epicardial cultures

Expression of *Pdgfra, Tcf21, Dermo* (*Twist2*) was traced in primary epicardial cultures for 14 days with or without the presence of TGFβ1. The promoter activity of *Pdgfra* and *Tcf21* were detected by reporter gene expressing, GFP and lacZ respectively, and $Dermo^{Cre}$ was traced by detecting YFP expression. Percent expression of the genes was calculated from the three images and normalized to total number of $DAPI^{+}$ nuclei.

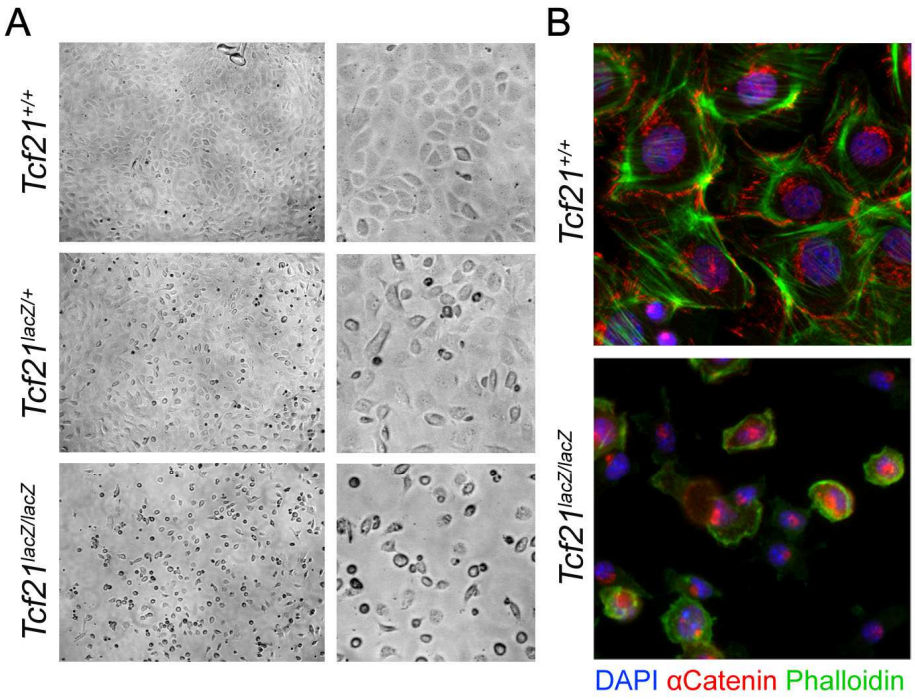
A
Tcf21+/+
Tcf21lacZ/+
Tcf21lacZ/lacZ
B
Tcf21+/+
Tcf21lacZ/lacZ
DAPI αCatenin Phalloidin

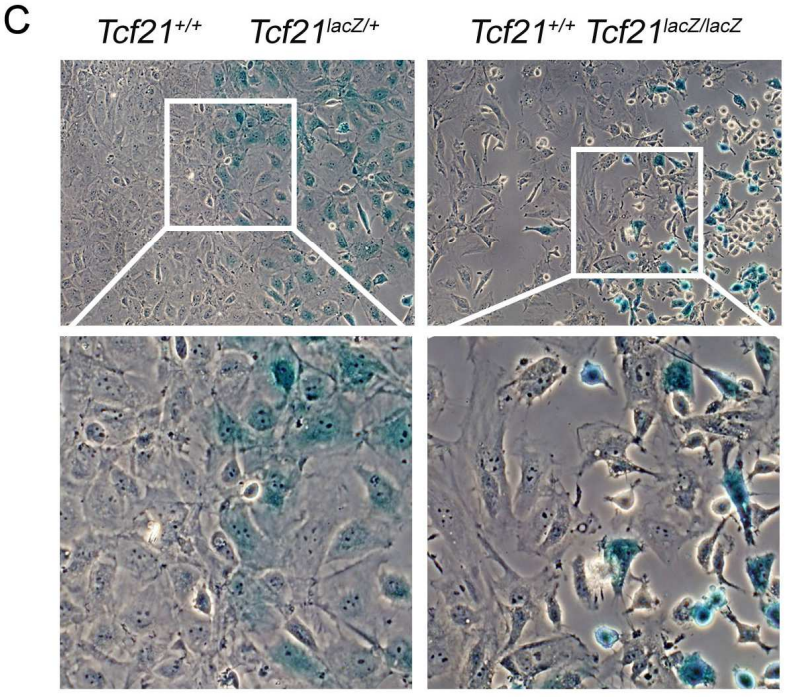
C
Tcf21+/+
Tcf21lacZ/+
Tcf21+/+
Tcf21lacZ/lacZ

Figure 2-18. Primary cultured epicardial cells from *Tcf21*-null hearts

(**A, B**) Embryonic hearts of indicated genotype were isolated and cultured for three days. After removing heart explants, primary epicardial cells were cultured for two more days before taking images or stained for (B) α-catenin and phalloidin. (**C**) Hearts from wild-type embryos were co-cultured with either *Tcf21*-heterozygote or mutant hearts. Cultures were stained for β-galactosidase activity to detect lacZ expression.

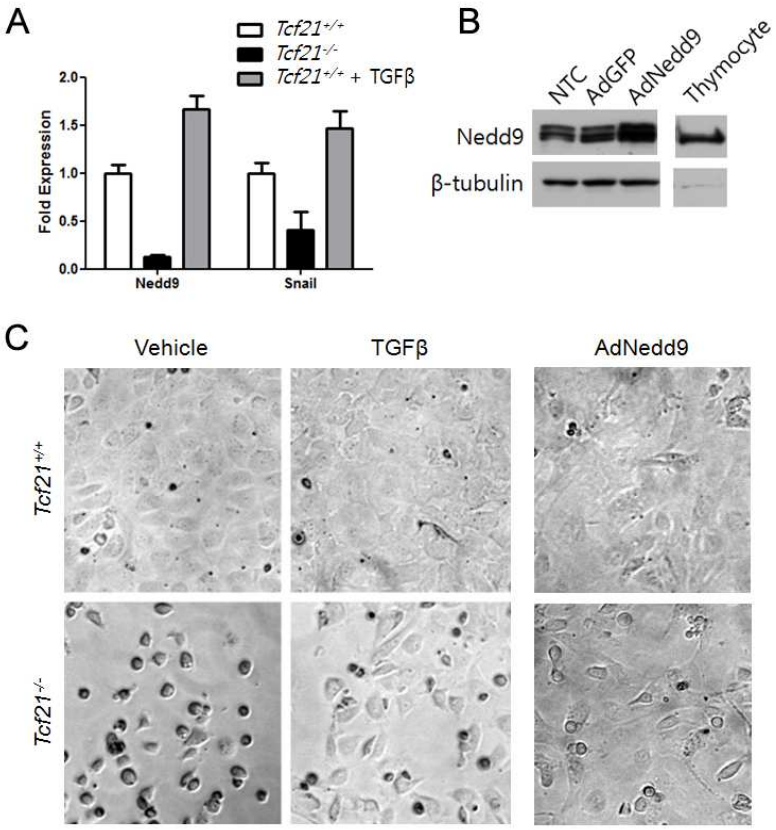


Figure 2-19. Nedd9 rescues defects of *Tcf21*-null primary epicardial cells

(**A**) The mRNA expression of *Nedd9* and *Snail* were measured in primary epicardial cultures with or without TGFβ1 by qRT-PCR. (**B**) Expression of Nedd9 was measured by immunoblotting in primary epicardial cultures or primary thymocyte cultures under the indicated conditions. NTC, non-transduced control. (**C**) Bright-field images of primary cultured epicardial cells after treatment of vehicle or TGFβ1, or after transduction with adenovirus expressing Nedd9.

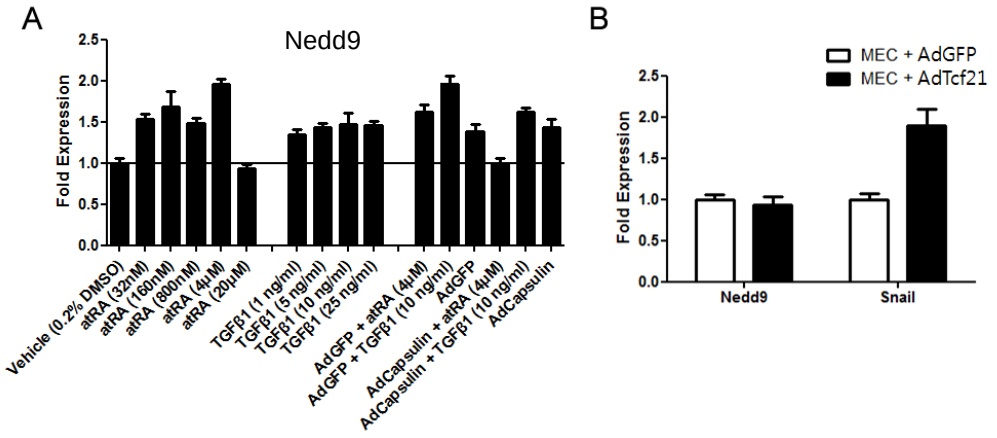


Figure 2-20. *Nedd9* and *Snail* expression

(**A**, **B**) The *Nedd9* and *Snail* expression were measured by qRT-PCR in MEC after the treatment of all trans retinoic acid (atRA) or TGFβ1, or after transduction with adenovirus expressing GFP, Nedd9 or Tcf21 (Capsulin).

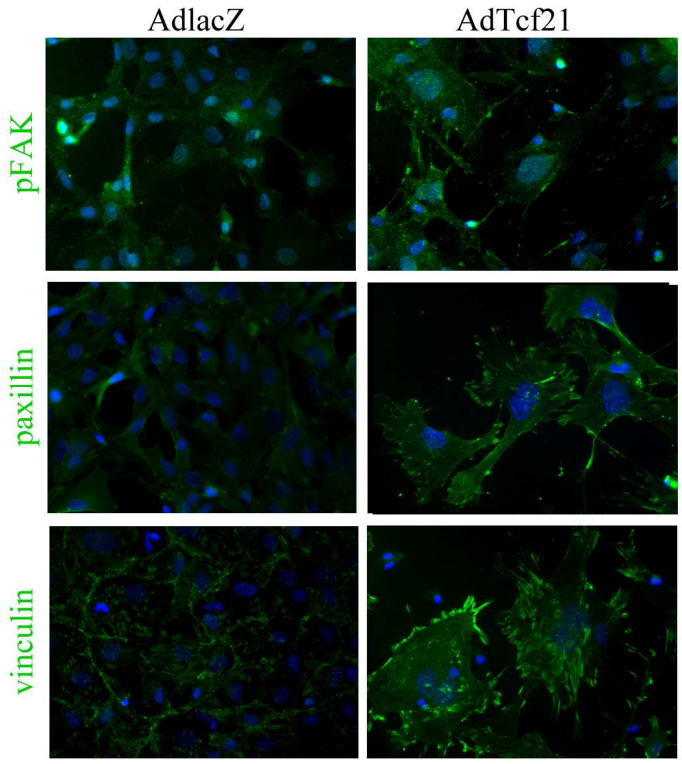


Figure 2-21. Focal adhesion formation by overexpression of Tcf21

Epicardial cultures were transduced with either AdlacZ or AdTcf21 for two days before stained for the phospho-focal adhesion kinase (pFAK), paxillin or vinculin. Nuclei were visualized by DAPI (blue).

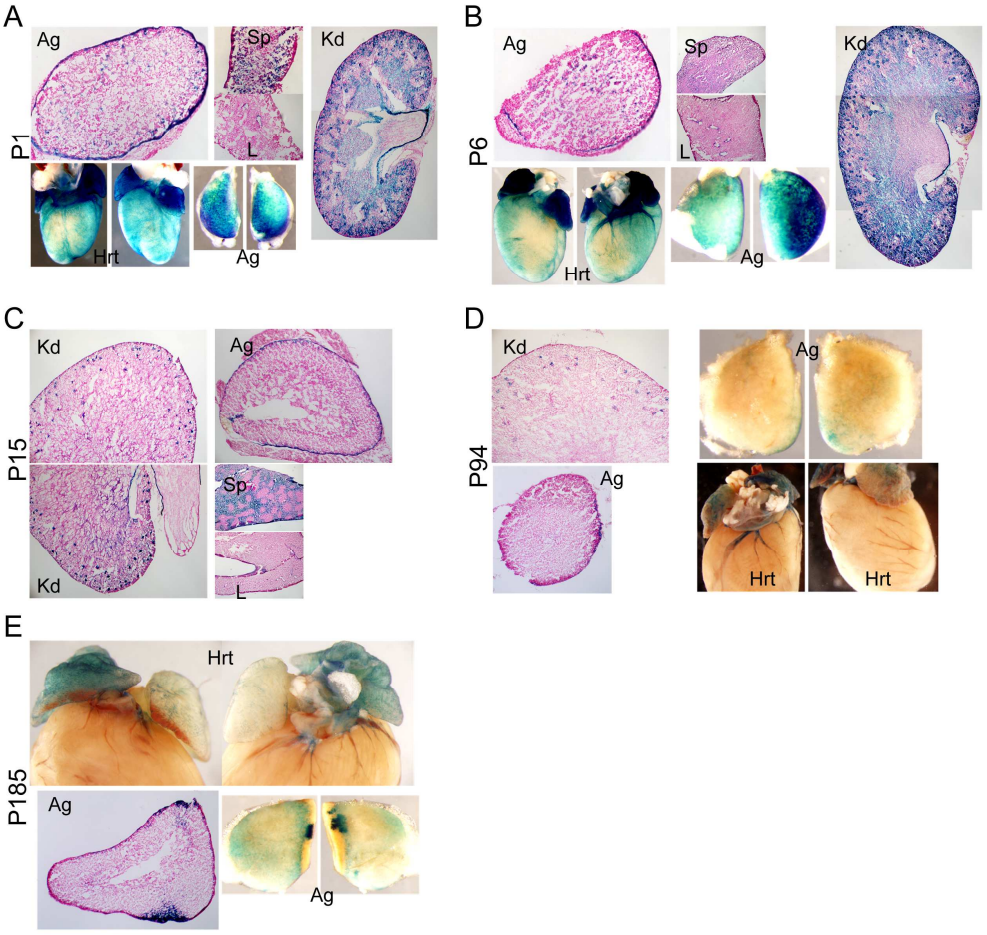


Figure 2-22. *Tcf21*-expressing cells in multiple organs

(**A-E**) Tcf21-expressing cells in heart (Hrt), kidney (Kd), adrenal gland (Ag), spleen (Sp) and liver (L) was detected in *Tcf21*$^{lacZ/+}$ mice at indicated age from P1 to P185. The promoter activity of *Tcf21* allele was visualized by detecting β-galactosidase activity. Note that the whole-mount images in B, D and E only have the staining close to surface due to the limited penetration of a fixative and staining solution.

Table 2-1. Down-regulated genes in *Tcf21*-null epicardial cultures[5].

| Genes | Fold changes | Genes | Fold changes |
|---|---|---|---|
| Slc38a5 | 11.95 | 8430408G22Rik | 1.75 |
| Mfap4 | 5.17 | Ltbp4 | 1.75 |
| Col1a1 | 3.38 | 1500015O10Rik | 1.73 |
| Pde1a | 3.20 | Snai1 | 1.73 |
| Rgs5 | 3.11 | Ptgds | 1.71 |
| Col3a1 | 3.08 | Srpx | 1.64 |
| Zbtb8 | 2.93 | Ly6a | 1.63 |
| Kcne1l | 2.87 | Reln | 1.62 |
| Nedd9 | 2.83 | Moxd1 | 1.61 |
| Dcn | 2.77 | Nrarp | 1.60 |
| Serping1 | 2.68 | Prrx1 | 1.60 |
| Ptn | 2.56 | Bcat1 | 1.60 |
| Olfml1 | 2.39 | Mrvi1 | 1.59 |
| Dpep1 | 2.33 | Mgll | 1.58 |
| Sphk1 | 2.23 | Gucy1a3 | 1.58 |
| Sox9 | 2.12 | Meox2 | 1.57 |
| Amhr2 | 2.05 | Notch3 | 1.57 |
| Spon2 | 2.05 | Lum | 1.57 |
| Pdgfra | 2.02 | Pdgfrb | 1.56 |
| Sulf1 | 1.96 | Mmp16 | 1.55 |
| Cldn5 | 1.91 | Meox1 | 1.53 |
| Rgs4 | 1.90 | Sytl2 | 1.53 |
| Wdfy1 | 1.87 | Tnxb | 1.52 |
| Ckm | 1.78 | Lpar4 | 1.52 |
| Ddx3y | 1.77 | Tnc | 1.51 |

[5] The microarray experiments were performed by Christopher Smith and Banu Eskiocak.

## CHAPTER THREE

## NF1 FUNCTION IN EPICARDIUM AND EPCARDIAL-DERIVED CELLS DEVELOPMENT

Seung Tae Baek and Michelle D. Tallquist. Nf1 limits epicardial derivative expansion by regulating epithelial to mesenchymal transition and proliferation. *Development*. 2012 Jun;139(11):2040-2049.

### Summary

The epicardium is the primary source of coronary vascular smooth muscle cells (cVSMCs) and fibroblasts that reside in the compact myocardium. To form these epicardial-derived cells (EPDCs), the epicardium undergoes the process of epithelial to mesenchymal transition (EMT). Although several signaling pathways have been identified that disrupt EMT, no pathway has been reported that restricts this developmental process. Here, we identify neurofibromin 1 (Nf1) as a key mediator of epicardial EMT. To determine the function of Nf1 during epicardial EMT and the formation of epicardial derivatives, cardiac fibroblasts and cVSMCs, we generated mice with a tissue-specific deletion of Nf1 in the epicardium. We found that mutant epicardial cells transitioned more readily to mesenchymal cells in vitro and in vivo. The mesothelial epicardium lost epithelial gene expression and became more invasive. Using lineage tracing of EPDCs, we found that the process of EMT occurred earlier in Nf1 mutant hearts, with an increase in epicardial cells entering the compact myocardium. Moreover,

loss of Nf1 caused increased EPDC proliferation and resulted in more cardiac fibroblasts and cVSMCs. Finally, we were able to partially reverse the excessive EMT caused by loss of Nf1 by disrupting Pdgfrα expression in the epicardium. Conversely, Nf1 activation was able to inhibit PDGF-induced epicardial EMT. Our results demonstrate a regulatory role for Nf1 during epicardial EMT and provide insights into the susceptibility of patients with disrupted NF1 signaling to cardiovascular disease.

**Introduction**

The epicardium, the outer epithelial layer of the heart, is a cell population that undergoes epithelial to mesenchymal transition (EMT) during development (Lie-Venema et al., 2007). Around embryonic day (E) 13.5, a subset of epicardial cells lose their epithelial characteristics but gain mesenchymal properties to migrate into the heart to differentiate into coronary vascular smooth muscle cells (cVSMCs) and cardiac fibroblasts (Dettman et al., 1998; Manner et al., 2001; Mikawa and Gourdie, 1996). Several growth factors including transforming growth factor β (TGFβ) (Mercado-Pimentel and Runyan, 2007; Xu et al., 2009b) and fibroblast growth factor (FGF) (Pennisi and Mikawa, 2009) have been implicated in the EMT process of epicardial cells during heart development, but little is understood about signals that limit the EMT process. Identification of such pathways will provide insights into the complex regulation of EMT during heart development. Because many of these same signaling pathways have also been suggested to play a key role in cardiac fibrosis, it may also provide insights into pathological EMT.

Recent findings show that disruption of Ras-mitogen activated protein kinase (MAPK) signaling results in several syndromes exhibiting congenital heart defects including Costello (Aoki et al., 2005), LEOPARD (Kontaridis et al., 2006), cardio-facio-cutaneous (Niihori et al., 2006) and Noonan (Schubbert et al., 2006) syndromes. Loss of neurofibromin 1 (Nf1), a Ras-GTPase activating protein (GAP), leads to hyperactivation of Ras and its downstream components (Cichowski and Jacks, 2001; Martin et al., 1990; Xu et al., 1990). While mutations in *Nf1* are best known for causing neurofibromatosis type 1 tumors of the skin and nervous system (Lynch and Gutmann, 2002), patients with *Nf1* mutations also have an increased risk for cardiovascular disorders (Lin et al., 2000). Studies in mice have significantly advanced our understanding of Nf1 function during heart development. Inactivation of *Nf1* causes lethality at mid-gestation with severe heart defects including malformation of the outflow tract, a thinned myocardium, a ventricular septal defect (VSD), and enlarged endocardial cushions (Brannan et al., 1994; Jacks et al., 1994). Loss of *Nf1* in vascular smooth muscle cell (VSMC) leads to an abnormal proliferative injury response (Xu et al., 2007), and cardiomyocyte-specific inactivation of *Nf1* results in pathological hypertrophy and heart failure in adult mice (Xu et al., 2009a). *Nf1*-null endocardial cushion cells exhibit abnormal EMT (Lakkis and Epstein, 1998), and endothelial-specific deletion of *Nf1* recapitulates many of the cardiovascular defects of *Nf1*-null mouse suggesting an indispensable role of Nf1 in endothelial cells during EMT (Gitler and Epstein, 2003).

Therefore, we investigated the function of Nf1 in epicardial development using *Cre/loxP* technology to inactivate *Nf1* in the mouse epicardium. We found that loss of Nf1 results in increased EMT and epicardial derived cells (EPDC) proliferation, leading

to a substantial expansion of this cell population that includes cardiac fibroblasts and cVSMCs. Our data point to a regulatory role for Nf1 in the process of EMT and suggest the possibility that patients with disruption of Nf1 may be more prone to cardiac complications such as fibrosis and coronary artery disease.

**Materials and Methods**

*Mice*

Mice were maintained on a mixed C57/BL6 X 129SV background. Mice with *Gata5-Cre* transgene (Merki et al., 2005) or $Wt1^{GFPCre}$ allele (Zhou et al., 2008) were crossed with mice with *Nf1* floxed ($Nf1^{fl}$) allele (Zhu et al., 2001) to generate $Nf1^{fl/fl}$;$Gata5\text{-}Cre^{Tg}$ (designated as $Nf1^{G5KO}$) and $Nf1^{fl/fl}$;$Wt1^{GFPCre}$, respectively. Controls were *Cre* negative littermates ($Nf1^{fl/fl}$ or $Nf1^{fl/+}$) unless otherwise indicated. For epicardial tracing experiments, male $Nf1^{fl/+}$; $Wt1^{CreERT2/+}$ mice were crossed with $Nf1^{fl/fl}$ or $Nf1^{fl/+}$ female mice with $ROSA26R^{LacZ}$ (Soriano, 1999) or $ROSA26R^{tdTomato}$ (Madisen et al., 2010) reporter alleles to generate $Nf1^{fl/fl}$; $Wt1^{CreERT2/+}$ (designated as $Nf1^{WTiKO}$). $Wt1^{CreERT2}$ was induced by oral administration of tamoxifen (MP Biomedicals, 02156738) to pregnant females at indicated embryonic stages and induction efficiency was traced by $ROSA26R^{LacZ}$ (designated as $R26R^{LacZ}$) or $ROSA26R^{tdTomato}$ (designated as $R26R^{T}$) reporter gene expression. Tamoxifen was dissolved in sunflower seed oil (Sigma) at 20 mg/ml and administrated to the final concentration of 0.1 mg per gram body weight. Other strains in these experiments include $Pdgfra^{fl}$ (Tallquist et al., 2003) and $K\text{-}Ras(G12D)^{fl}$ mice (JAX stock number 008180) (Jackson et al., 2001). All animal protocols were approved by the

Institutional Animal Care and Use Committee of the University of Texas Southwestern Medical Center and conform to NIH guidelines for care and use of laboratory animals. *Nf1*$^{fl}$ (Zhu et al., 2001) and *Gata5-Cre*$^{Tg}$ (Merki et al., 2005) mice were kindly provided by Dr. Luis Parada (UTSW, TX, USA) and Dr. Pilar Ruiz-Lozano (Sanford-Burnham Institute, CA, USA), respectively. *Wt1*$^{GFPCre}$ and *Wt1*$^{CreERT2}$ (Zhou et al., 2008) mice were kindly provided by Dr. William Pu (Harvard, MA, USA) and *XLacZ4*$^{Tg}$ (Tidhar et al., 2001) mice were kindly provided by Dr. Moshe Shani (Volcani Center, Israel).

*Primary epicardial cultures*

In vitro culture of epicardial cells was described previously (Mellgren et al., 2008). Ventricles from embryonic hearts at E12.5 were isolated and cultured in 1:1 mix of DMEM and M199 with 15% FBS supplemented with glutamate, antibiotics, and basic fibroblast growth factor (2 ng/mL, Sigma). After three days, heart explants were removed and cells were cultured for two additional days in media with reduced serum (10%). Epicardial nature of the culture was confirmed by the reporter expression of epicardial genes; *Tcf21*$^{LacZ}$ (Lu et al., 1998) or *Pdgfra*$^{GFP}$ (Hamilton et al., 2003; Smith et al., 2011) (Figure 3-S4). Cre expressing adenovirus, kindly provided by Dr. Robert Gerard (UTSW, TX, USA), was added to the culture as indicated. For RNA extraction followed by qRT-PCR analysis, hearts were cultured on 24-well plates. Loss of *Nf1* in *Nf1*$^{G5KO}$ cultures was confirmed by qRT-PCR. For immunostaining, hearts were placed on glass cover slips coated with collagen type IV (5 μg/cm$^2$, R&D Systems). Collagen-coated cover slips were prepared according to the manufacturer's protocol. For in vitro differentiation assay, epicardial cells were cultured for total 6 days followed by immunostaining.

*Tissues, staining and immunostaining*

Tissues and embryos were fixed in 4% PFA overnight at 4ºC, washed in PBS, dehydrated and paraffin embedded. For histological analysis, tissues were sectioned to 8 μm, rehydrated and stained with hematoxylin and eosin (Sigma) as previously described (Mellgren et al., 2008). For immunostaining, antigens were retrieved in citrate buffer (pH 6.0) at 98ºC for 15 minutes with temperature-controlled microwave (BioGenex). For frozen embedding, hearts were fixed in 4% PFA for one hour at 4ºC then embedded in OCT. Hearts were sectioned 10 μm, permeabilized with 0.1% Triton/PBS (PBT), blocked with 5% serum/PBT and stained with phalloidin (1:200, Invitrogen, A12379) or antibodies against vimentin (1:500, Sigma, V6630), SM-MHC (1:250, Chemicon, MAB3572), phospho-histone H3 (1:200, Upstate, 06-570), collagen IV (1:250, Chemicon, AB748), β-catenin (1:500, BD Bioscience, 610153) and α-catenin (1:100, Abcam, AB51032). Immunostaining for Wt1 (1:50, DAKO, M3561) was done with Vectastain mouse ABC kit followed by detection by DAB (Vector Labs).

For the detection of β-galactosidase activity, hearts were fixed in 2% formaldehyde/0.2% glutaraldehyde in PBS for 15 minutes. Hearts were then washed with PBS and stained whole mount with X-gal substrate (5-bromo 4-chloro 3-indoxyl beta-D-galactopyranoside, Gold Biotechnology, X4281C) or frozen embedded and sectioned followed by staining as described previously .

*Whole mount confocal imaging*

For whole mount immunostaining, hearts were isolated and fixed in 4% PFA, then permeabilized with PBT for 30 minutes, blocked with CAS Block (Invitrogen,

008120) for 30 minutes, and immunostained for β-catenin (1:200, BD Bioscience, 610153). Z-stack images (9 consecutive images spanning 32 μm in depth, 4 μm each) were taken from similar regions of the left ventricle of embryonic hearts starting from the epicardial surface using a LSM510META (grant NIH 1-S10-RR019406-01) mounted on Axiovert 200M (Zeiss). 3D images were reconstituted using ImageJ software, and the total number of cells expressing $R26R^T$ within a 150 μm x 150 μm x 32 μm area were counted in the subepicardial space.

*Collagen gel invasion assay*

Collagen gel invasion assay was done as described elsewhere (Boyer et al., 1999; Potts et al., 1991) with modifications. Embryonic hearts at embryonic day (E) 12.5 were isolated, and ventricles were placed and cultured on 1.6% collagen (Roche) gels. Collagen gels were prepared according to the manufacturer's suggestion. After three days, heart explants were removed and cultured for three more days before fixing in 4% PFA for 10 minutes for analysis. To detect invasion, collagen gels were frozen embedded and sectioned followed by staining with DAPI (Roche) and phalloidin. Invasion was identified by the presence of epicardial cells underneath the collagen gel surface. For quantification, invading cells were identified using a fluorescent microscope (Zeiss Axiovert 200 with a Hamamatsu ORCA-ER camera) and invasion was calculated by imaging each culture from the center of the culture and drawing a line where cells had left the plane of the collagen gel (the invasion front). For quantification, the number of cells that had invaded the gel was divided by the total number of cells within the 20x field of view from three different images (Merki et al., 2005).

*Ex vivo migration assay*

Ex vivo migration assay was done as described previously (Mellgren et al., 2008). Embryonic hearts at E12.5 were isolated and incubated with adenovirus expressing GFP or Nf1 gap-related domain (Miller et al., 2010), kindly provided by Dr. Robert Gerard (UT Southwestern) and Dr. Nancy Ratner (Cincinnati Children's), respectively. PDGF-BB (R&D Systems), Imatinib mesylate (Sigma), AG1296 (Sigma) and U0126 (Sigma) were added to the cultures as indicated. After two days, hearts were fixed in 4% PFA and frozen-embedded, sectioned and stained for DAPI. For quantification, $GFP^+$ cells underneath the epicardium were counted in a 40x field of view from five nonconsecutive sections.

*Quantification and Statistical analysis*

For mesenchymal index, primary cultured epicardial cells were stained for α-catenin and phalloidin as described above, and cells exhibiting a mesenchymal morphology were identified by the loss of adherens junctions and cortical actin, and robust formation of actin stress fibers (Sridurongrit et al., 2008). Mesenchymal cells were counted and divided by the total number of cells in 40x field of view from three different regions of the cultures. β-galactosidase staining was quantified as previously described (Morgan et al., 2008). Epicardial differentiation of smooth muscle cells was quantified followed by immunostaining against SM-MHC. SM-MHC positive area was measured and divided by DAPI positive are in three 40x field of view images using ImageJ (NIH). All experiments used a minimum of two independent litters, and data were analyzed by a Student's *t*-test using Prism 5 (GraphPad Software).

*qRT-PCR*

For quantitative real-time PCR, primary epicardial cells were collected as described above. RNA isolation and cDNA synthesis were done as described previously with slight modifications (Mellgren et al., 2008). Briefly, primary epicardial cultures from three hearts of each genotype were combined followed by RNA isolation using Trizol (Invitrogen). cDNA was synthesized using Superscript III reverse transcriptase (Invitrogen). Gene transcription was analyzed using standard qRT-PCR with iTAQ Sybr Green master mix (Bio-Rad) and CFX96 instrument (Bio-Rad). Each sample was run in triplicate. Sequences of primers are summarized previously (Smith et al., 2011).

*In situ hybridization on tissue sections*

Section in situ hybridization was performed as described previously (Schaeren-Wiemers and Gerfin-Moser, 1993; Smith et al., 2011). Briefly, embryonic hearts were isolated, fixed in 4% PFA, frozen embedded and sectioned 16 μm. Sections were digested with proteinase K (15 μg/ml, Fisher Scientific, BP1700-100) followed by brief fixation with 4% PFA and acetylated with acetic anhydride before hybridizing with digoxigenin-labeled RNA probes for *Pdgfra* (Bostrom et al., 1996), *Col1a1*, *Col3a1* and *Nf1*. Sections were then immunostained for digoxigenin (1:2000, Roche, 11093274910) followed by development with BM purple (Roche, 11442074001). Plasmids for *Col1a1* and *Col3a1* probes were kindly provided by Benoit de Crombrugghe (MD Anderson). The plasmid for *Nf1* probe was prepared from a 338 bp 3' untranslated region fragment of the Nf1 gene corresponding to positions 9881-10,218 (GeneBank L10370.1).

## Results

*Epicardial inactivation of Nf1 results in aberrant epicardium development*

Loss of *Nf1* in cardiomyocytes or the endocardial cushions results in heart abnormalities (Gitler et al., 2003; Xu et al., 2009a), but no reports have addressed the disrupted epicardium observed in *Nf1* null hearts (Brannan et al., 1994). To determine if *Nf1* might have a primary role in epicardial development, we performed in situ hybridization for *Nf1* transcripts. *Nf1* expression was detected in the epicardium, endocardium, endocardial cushions and myocardium at E11.5, but by E12.5 myocardial expression was decreased (Figure 3-S1). Epicardial expression continued until E13.5, but by E14.5-E15.5, epicardial expression was limited to a few cells in the epicardium (Figure 3-1A, Figure 3-S1).

To investigate Nf1 function in epicardial development, we initially used two mouse lines with constitutive expression of Cre in the epicardium, the *Gata5-Cre*$^{Tg}$ (Merki et al., 2005) and the *Wt1*$^{GFPCre}$ (Zhou et al., 2008) mouse lines. We monitored loss of *Nf1* transcript by *Gata5-Cre*$^{Tg}$ driven recombination (referred to as *Nf1*$^{G5KO}$) and found little expression in the epicardium and endocardial cushions at E13.5 (Figure 3-1B). Using Wt1 protein expression to track the epicardium and undifferentiated EPDCs (Moore et al., 1999), we found that unlike control hearts where Wt1$^{+}$ cells were restricted to the epicardium at E12.5, in *Nf1*$^{G5KO}$ hearts, Wt1$^{+}$ cells were detected in not only the epicardium but also in the subepicardial zone (Figure 3-1C). To determine if these cells had adopted a mesenchymal phenotype, we stained for vimentin. Vimentin is a marker for mesenchymal cells and often indicates that a cell has undergone the process of EMT

(Perez-Pomares et al., 1997). At E12.5, control hearts had few vimentin$^{+}$ cells in the subepicardium (Figure 3-1D), but noticeably, in *Nf1*$^{G5KO}$ hearts, there were multiple patches of vimentin$^{+}$ cells in the subepicardium. These patches were often concomitant with a disrupted basement membrane (collagen IV) (Figure 3-1D). Similar patches of vimentin-positive cells were also found when *Nf1* expression was disrupted using a *Wt1*$^{CreGFP}$ allele for recombination (Figure 3-1D).

Based on ROSA26 reporter activity, both of these epicardial Cre lines recombine in a significant number of cardiomyocytes and in the endocardial cushions (Figure 3-S5). Therefore, we performed the remaining in vivo experiments employing an inducible, epicardial specific Cre mouse, *Wt1*$^{CreERT2}$ (Zhou et al., 2008). First, we confirmed the fidelity of recombination in this line to demonstrate epicardial specific Cre activity with tamoxifen induction at E10.5 and E12.5. Single administration of tamoxifen at E10.5 resulted in reporter gene (*R26R*$^{T}$) expression in approximately 95% of the epicardial cells after 24 hours (Figure 3-S6). Lineage tracing and in situ hybridization for *Nf1* demonstrated that in *Nf1* conditional embryos transcripts were reduced in the epicardium just 24 hours after induction (Figure 3-1B), that epicardial cells were exclusively tagged, and that lineage tagged cells migrated into the heart ventricles as expected (Figure 3-S2A). The only other lineage-tagged regions were the atrioventricular valves, where epicardial cell contribution has been previously reported (de Lange et al., 2004). By contrast, at these time points of induction no lineage-tagged cells were detected in the cardiomyocyte population nor in the semilunar valves (Figure 3-S2B,C).

To specifically examine Nf1's role in the epicardium, we generated *Nf1*$^{fl/fl}$; *Wt1*$^{CreERT2/+}$ mice (referred to as *Nf1*$^{WTiKO}$). We obtained the expected Mendelian ratios of

animals and detected no overt phenotype in *Nf1*$^{WTiKO}$ animals suggesting that epicardial inactivation of *Nf1* by *Wt1*$^{CreERT2}$ at E12.5 did not cause embryonic nor postnatal lethality. Gross morphology of heart valves as well as heart size in *Nf1*$^{WTiKO}$ mice was comparable to controls (Figure 3-S9). Because we observed vimentin$^{+}$ cells in the ventricles at time points earlier than expected (Figure 3-1D), we wanted to determine if premature EMT occurred upon loss of *Nf1*. Therefore, we traced migration of epicardial cells labeled at E10.5. These hearts revealed that a substantial number of epicardial cells were present immediately below the basement membrane in *Nf1*$^{WTiKO}$ hearts while tagged cells remained in the epicardium in controls (Figure 3-1E). These data suggested that in the absence of Nf1, epicardial cells migrate into the heart earlier than expected in all three genotypes examined (*Nf1*$^{G5KO}$, *Nf1*$^{fl/fl}$; *Wt1*$^{CreGFP/+}$ and *Nf1*$^{WTiKO}$).

*Loss of Nf1 results in spontaneous EMT of epicardial cells in vitro*

From the above data, we hypothesized that loss of Nf1 could result in accelerated EMT. First, we tested this possibility in vitro. We generated primary cultured epicardial cells from E12.5 hearts, which uniformly expressed epicardial genes, *Tcf21* and *Pdgfra* (Figure 3-S4). After 3 days of culture, without any exogenous stimulus, control epicardial cells remained a cobblestone monolayer, while *Nf1*$^{G5KO}$ epicardial cells exhibited a mesenchymal morphology (Figure 3-2A). We investigated two hallmarks of EMT, the loss of cell-cell contacts and formation of actin stress fibers, by localization of β-catenin and filamentous actin, respectively. Control epicardial cells maintained cell-cell contacts, had extensive cellular junctions, and exhibited cortical actin. However, *Nf1*$^{G5KO}$ epicardial cells formed extensive actin stress fibers and lost their junctions (Figure 3-2B). These

changes were inhibited by a Rho-associated protein kinase inhibitor, Y27632 (Uehata et al., 1997), suggesting that known EMT signaling pathways were occurring in the *Nf1* mutant cultures (Figure 3-S7). These results also demonstrated a cell autonomous role for Nf1 in regulating EMT.

Although morphology is commonly used as a readout for EMT, changes in gene expression from epithelial to mesenchymal can also be used to detect the transition. We measured the expression of epithelial markers, such as *Krt14* (Chamulitrat et al., 2003; Ke et al., 2008) and *Bves* (Wada et al., 2001), by qRT-PCR (Figure 3-2C). Consistent with a switch from epithelial to mesenchymal cell type, we found that epithelial gene expression was down regulated in $Nf1^{G5KO}$ cultures. By contrast, mesenchymal gene expression, *Col7a1* (Vindevoghel et al., 1998), *Mmp10* (Wilkins-Port and Higgins, 2007), *Sox9* (Cheung et al., 2005; Sakai et al., 2006), and *Opg* (Corallini et al., 2009; Sakata et al., 1999; Vidal et al., 1998), was up regulated (Figure 3-2C). We also observed an increased level of mesenchymal gene expression in heterozygous cultures.

One additional criterion for transition from an epithelial phenotype to a mesenchymal phenotype is invasion into a collagen gel (Thiery and Sleeman, 2006). In a collagen gel assay (Boyer et al., 1999; Potts et al., 1991), about 12% of control epicardial cells invaded the collagen gel along the edge of the culture (Figure 3-2D,F). In $Nf1^{G5KO}$ epicardial cultures, about 60% of the cells in the same perimeter of the epicardial culture had invaded into the collagen gel and formed actin stress fibers (Figure 3-2D,F).

When epicardial cells undergo EMT, they differentiate predominantly into two cell types, cVSMCs and cardiac fibroblasts (Mikawa and Gourdie, 1996; Vrancken Peeters et al., 1999). To determine if the increased EMT led to an increased number of

differentiated cells in vitro, we examined the expression of SM-MHC, a smooth muscle cell marker. Epicardial cultures from *Nf1*$^{G5KO}$ and to a lesser extent *Nf1* heterozygous hearts possessed an increased number of SM-MHC-expressing cells compared to control cultures (Figure 3-2E,G). In summary, *Nf1* mutant epicardial cells spontaneously lost epithelial characteristics and adopted a mesenchymal phenotype, including an increase in mesenchymal gene expression, invasiveness, and differentiation. It should be noted that loss of Nf1 resulted in EMT under basal culture conditions. Therefore, these cultured epicardial cells may be poised to undergo EMT, and signaling by Nf1 could be a key regulatory pathway inhibiting this process.

*Loss of Nf1 enhances EMT of epicardial cells in vivo*

To determine if the loss of Nf1 had a direct effect on EMT, we induced temporal deletions of *Nf1* between stages E10.5 and E12.5. These embryos, therefore, had wild-type expression of Nf1 until just before the stage of EMT. This tracing resulted in efficient R26R$^{T}$ reporter expression in a high percentage of the epicardium (Figure 3-3A). We then quantified the number of EPDC that had migrated into the heart ventricle using whole mount confocal microscopy at each time point. Figure 3-3 is representative of optical sections comparing control and *Nf1*$^{WTiKO}$ hearts (Figure 3-S3 for images at other time points). At E11.5, very few R26R$^{T}$-positive cells were detected in the control myocardial compartment (Figure 3-3A,B, Figure 3-S3). Tagged epicardial cells were observed in the ventricle at E12.5 and further increased at E13.5 suggesting that EMT began around E12.5 in control hearts (Figure 3-3B, Figure 3-S3). However, in *Nf1*$^{WTiKO}$ hearts, at each time point examined, a greater number of R26R$^{T}$-positive cells were

detected within the myocardial compartment (Figure 3-3B, Figure 3-S3). The existence of migrated mutant epicardial cells at E11.5 suggested that epicardial EMT occurs earlier in the mutant hearts, and the increase of migrated epicardial cells demonstrated that as in vitro, loss of Nf1 results in an increased number of cells undergoing the process of EMT. Because confocal imaging only allowed us to examine a small region and window of migrated epicardial cells, we also traced EPDC in heart sections using two different reporters. A similar increase in $R26R^{T}$- or $R26R^{lacZ}$-positive EPDC was detected at E13.5 and E14.5 upon loss of Nf1 at E12.5 in both the right and left ventricle (Figure 3-4A-D). To demonstrate that the increased EMT was a cell autonomous event, embryos was treated with a limiting tamoxifen dose, thereby creating hearts with a minor population of cells lacking Nf1. We compared control and $Nf1^{WTiKO}$ hearts with a similar number of tagged epicardial cells and found that the number of cells with Cre activity ($R26R^{T}$-positive cells) was increased in the ventricular regions of $Nf1^{WTiKO}$ hearts compared to controls (Figure 3-S10). These data further support that loss of Nf1 leads to a cell autonomous increase in epicardial EMT.

Recent data have suggested a potential role for Sox9 in epicardial EMT (Smith et al., 2011). Sox9 expression is significantly reduced in epicardial cells that fail to undergo EMT, suggesting that Sox9 expression correlates with epicardial EMT. In addition, Sox9 is involved in neural crest cell and endocardial cushion EMT (Akiyama et al., 2004; Sakai et al., 2006) and also has been shown to be a downstream mediator of Nf1-dependent metastasis (Powers et al., 2007). Thus, we examined Sox9 expression at E12.5 and E13.5. Hearts from $Nf1^{G5KO}$ mice possessed an increased number of $Sox9^{+}$ cells within the ventricular area at the time of EMT, E13.5, supporting our hypothesis that

epicardial EMT was enhanced upon loss of Nf1 (Figure 3-S11).

To determine how loss of Nf1 impacted the proliferation and survival of epicardial cells and EPDC at later stages of development, we inactivated Nf1 at E12.5 and quantified the number of proliferating cells (phospho-histone $H3^{+}$ cells) within the $R26R^{T}$-positive epicardial and EPDC population. At E13.5 we saw a modest increase in proliferation of *Nf1*-deficient epicardial cells (Figure 3-4E). At the same stage, a similar number of the EPDC in both control and mutant hearts were in mitosis (Figure 3-4E). However, we found at later stages, Nf1-deficient EPDC exhibited increased proliferation (Figure 3-4E). Because alterations in cell survival were reported in Nf1-deficient endocardial cushions (Lakkis and Epstein, 1998), we examined $Nf1^{WTiKO}$ and $Nf1^{G5KO}$ hearts for apoptosis using an antibody for cleaved-caspase 3 at various time points from E12.5 to P0 and observed no difference in apoptotic cell numbers in control and mutant hearts.

*Epicardial inactivation of Nf1 results in expansion of cardiac fibroblast and cVSMC in vi vo*

Because enhanced epicardial cell EMT and EPDC proliferation were observed, we reasoned that there might be an expansion of EPDC. As cardiac fibroblasts and cVSMC are the predominant populations of cells derived from the epicardium, we determined how loss of Nf1 impacted these cells. Using in situ hybridization for three genes that identify cardiac fibroblasts, *Col1a1*, *Col3a1* and *Pdgfra* (Smith et al., 2011), we found an increased number of cardiac fibroblasts in mutant hearts when compared to controls (Figure 3-5A,C). Similar expansion of *Col1a1*- or *Pdgfra*-expressing cells was

also detected in *Nf1*$^{G5KO}$ hearts (Figure 3-S12). Collagen I is also expressed by some VSMCs (Ponticos et al., 2004), therefore, it is likely that this particular probe overestimated the number of fibroblasts, but the data clearly demonstrated an obvious increase in non-vessel associated *Col1a1*-, as well as *Col3a1*- and *Pdgfra*-expressing cells. This increase in cell numbers was not restricted to the cardiac fibroblast lineage. We utilized the *XLacZ4*$^{Tg}$ mouse (Tidhar et al., 2001) that expresses a nuclear-localized β-galactosidase in VSMCs and efficiently tags cVSMCs (Mellgren et al., 2008). We found that loss of Nf1 also resulted in an expansion of the VSMC lineage of cells (Figure 3-5B). Not only were more cVSMCs detected at E17.5, but the increase also appeared to lead to an extended and a more highly branched cVSMC-coated network of coronary vasculature (Figure 3-5D).

*Nf1 regulation of Ras signaling plays a role in PDGF-induced epicardial EMT*

It is established that loss of Nf1 leads to prolonged activation of the Ras-MAPK pathway in cardiomyocytes and VSMC (Cichowski and Jacks, 2001; Xu et al., 2009a; Xu et al., 2007). To determine if activation of ERK1/2 is responsible for EMT in Nf1-deficient epicardial cells, we inhibited the MAP kinase pathway and measured EMT by ex vivo migration assay (Mellgren et al., 2008). The epicardium of E12.5 hearts was labeled by adenoviral GFP transduction, and migration of GFP-expressing epicardial cells into the myocardium was quantified. In control hearts, GFP$^{+}$ cells were restricted to the epicardium, however, *Nf1*$^{G5KO}$ hearts possessed an increased number of GFP$^{+}$ cells within the myocardium suggesting enhanced ability of *Nf1*-null epicardial cells to leave the epicardial layer (Figure 3-6A,B). The increased migration was abolished when hearts

were cultured in the presence of U0126, an inhibitor of both MEK1 and MEK2 (Figure 3-6A,B). These data suggest that activation of ERK is responsible for EMT in Nf1-deficient epicardial cells.

Loss of Nf1 alone does not lead to extended activation of Ras. Upstream signals are required to initiate Ras signaling, then in the absence of Nf1, Ras remains in its active state (McCormick, 1995). We have recently reported that PDGF receptor signaling is an essential component of epicardial EMT. Pdgfrα and Pdgfrβ are expressed in the epicardium and inactivation of these receptors in epicardial cells disrupts the process of EMT (Mellgren et al., 2008; Smith et al., 2011). To determine if PDGF signaling could be one pathway upstream of Ras-Nf1 signaling, we inhibited PDGF receptor tyrosine kinase activity in $Nf1^{G5KO}$ epicardial cells. Imatinib mesylate, a potent inhibitor of both Pdgfrα and Pdgfrβ, inhibited the EMT phenotype caused by loss of Nf1 in the epicardial culture EMT assay (Figure 3-S8) and in the ex vivo migration of epicardial cells (Figure 3-6A,B). Similar results were observed using AG1296, another inhibitor of the PDGF receptors.

Next, we tested if Nf1 Ras-GAP activity could negatively regulate PDGF-induced EMT in the ex vivo migration assay. Stimulation with PDGF-BB induced epicardial cell migration into the myocardium, however, adenoviral transduction of the Nf1 GAP-related domain (Nf1-GRD) (Hiatt et al., 2001; Miller et al., 2010) significantly reduced PDGF-BB-induced EMT (Figure 3-6C,D). Conversely, we determined if activation of Ras induced epicardial EMT using epicardial cultures from *K-Ras(G12D)*$^{fl/+}$ embryos. This transgene expresses a Cre-inducible oncogenic form of K-Ras (Jackson et al., 2001). While control cultures had intact cellular junctions with cortical actin, when *K-Ras(G12D)* expression was induced, the epicardial cultures formed actin stress fibers and

lost cellular junctions similar to *Nf1*$^{fl/fl}$ cultures (Figure 3-6E). Similarly, *K-Ras*$^{fl/+}$*;Wt1*$^{CreERT2/+}$ hearts had an increased number of Wt1$^{+}$ cells in the myocardial compartment. This suggests that activation of Ras also results in increased epicardial EMT in vivo (Figure 3-6F,G).

Finally, we determined if loss of *Pdgfra* signaling could partially rescue the excess EMT observed in the *Nf1*$^{WTiKO}$ heart. As loss of Pdgfrα specifically affects only cardiac fibroblast progenitor EMT (Smith et al., 2011), we predicted that loss of Pdgfrα in an *Nf1*$^{WTiKO}$ mutant background would lead to a reduction in EPDC entering the epicardium compared to an *Nf1*$^{WTiKO}$ mutant that possessed Pdgfrα signaling. Consistent with our previous data, *Nf1*$^{WTiKO}$ hearts had more Wt1$^{+}$ cells present within the myocardium compared to wild-type controls, however, simultaneous inactivation of both *Pdgfra* and *Nf1* resulted in a significant reduction of migrated Wt1$^{+}$ cells (Figure 3-6F,G). One reason that we may only observe a partial rescue of the *Nf1*$^{WTiKO}$ EMT phenotype could be the presence of VSMC progenitors which still express Pdgfrβ (Mellgren et al., 2008; Smith et al., 2011) and should continue to have excess Ras signaling due to loss of Nf1. Consistent with the data above, detection of cardiac fibroblasts in these animal suggest that the expansion of cardiac fibroblasts by the loss of Nf1 was partially rescued by further loss of Pdgfra. In conclusion, our results show that Nf1 is a key regulator of epicardial EMT and that this increased EMT as well as an increased rate of proliferation results in expansion of cardiac fibroblasts and VSMC.

**Discussion**

EMT is an essential process that plays a significant role in embryogenesis during gastrulation, heart development, and neural crest cell formation (Thiery et al., 2009). There is now very compelling evidence that EMT is an essential component of tumor metastasis (Thiery et al., 2009; Yang and Weinberg, 2008). Because the best-known activity for Nf1 is its GAP activity, it is assumed that loss of Nf1 leads to abnormal signaling of Ras. A further link with EMT can then be drawn because Ras signaling can induce EMT. One mechanism is by cooperating with TGFβ to promote Snail transcriptional activity (Horiguchi et al., 2009; Janda et al., 2002). Another is by activating MAPK and Rac, potentially leading to disruption of epithelial junctions (Edme et al., 2002). In fact, many of the EMT-inducing abilities of epidermal growth factor and hepatocyte growth factor have been directly linked to Ras activity (Boyer et al., 1997; Herrera, 1998). Here, we provide evidence that loss of *Nf1* increases EMT in mouse epicardial cells, suggesting a possible 'regulatory role' for Nf1 in Ras-driven EMT.

Interestingly, loss of Nf1 does not lead to persistent EMT. Instead, the EMT we observed is only amplified by occurring earlier and more robustly, as might be expected by its signaling role downstream of Ras. Nf1 does not initiate signaling (McCormick, 1995). Other factors must be upstream to activate the Ras-MAPK pathway. Epicardial EMT is distinct from neural crest cell EMT in that only a subset of cells become mesenchymal, suggesting that the inductive signal is regionally localized and controlled temporally, thus providing an explanation for why epicardial EMT in the absence of Nf1 is still partially restricted. Indeed, we have shown that by inhibiting one of these potential

upstream growth factor pathways, PDGF (Mellgren et al., 2008; Smith et al., 2011), we can block the effects of loss of Nf1. Interestingly, increased neointima formation in *Nf1* heterozygote mice can also be mitigated by Imatinib treatment suggesting a possible role for PDGF signaling on exaggerated vascular injury response by the loss of *Nf1* (Lasater et al., 2008). Because inhibition of MAPK also blunted the effect of loss of Nf1 on EMT, it likely that Nf1 attenuates these inductive signals only in the epicardial cells that have been stimulated to undergo the process of EMT.

Cardiovascular disease is a frequent cause of death in persons with neurofibromatosis 1 who are less than 30 years old (Rasmussen et al., 2001). While some of this lethality is attributed to congenital abnormalities (Friedman et al., 2002; Lin et al., 2000), our findings also point to the possibility that an increase in the proliferation of epicardial-derived noncardiomyocyte lineages may also contribute to some of the heart abnormalities. As was the case with EMT, loss of Nf1 did not lead to excessive overgrowth of these cells under normal circumstances. It is likely that local environmental cues ultimately determine the differentiation and survival of EPDC. For example, endothelial cells, which secrete PDGF ligands, are important regulators of cVSMC migration and proliferation (Tomanek, 2005). Similarly, local limitations of growth factor production by these cells might account for the lack of excessive cVSMC proliferation. Therefore, loss of Nf1 results in a controlled expansion of EPDC rather than massive hyperplasia. This phenomenon would be reminiscent of what occurs with Nf1-mediated tumorigenicity, where disruptions in the microenvironment are necessary for tumor progression (Zhu et al., 2002). Nonetheless, because loss of Nf1 is often linked to increased proliferation (Lynch and Gutmann, 2002), during a pathological response to

heart injury, Nf1-deficient cells may respond more robustly by enhanced proliferation and fibrotic activity. Most Nf1 patients would be haploinsufficient in somatic cells, but our data and others suggest that even cells with reduced Nf1 protein may have elevated levels of GTP-bound Ras thus leading to increased signaling and downstream cellular events (Atit et al., 1999; Ingram et al., 2000). In summary, we demonstrate that epicardial loss of *Nf1* results in early and increased EMT which leads to the expansion of cardiac fibroblasts and cVSMC. We were able to mitigate the increased EMT by altering PDGF signaling which has recently been implicated in epicardial EMT (Smith et al., 2011). Our work indicates that EPDC, along with endocardial-derived valve cells, and cardiomyocytes, are sensitive to perturbations in Nf1 activity. Further investigations will be required to determine what the long-term outcomes of this EPDC expansion means to physiology of the heart under pathological and non-pathological conditions.

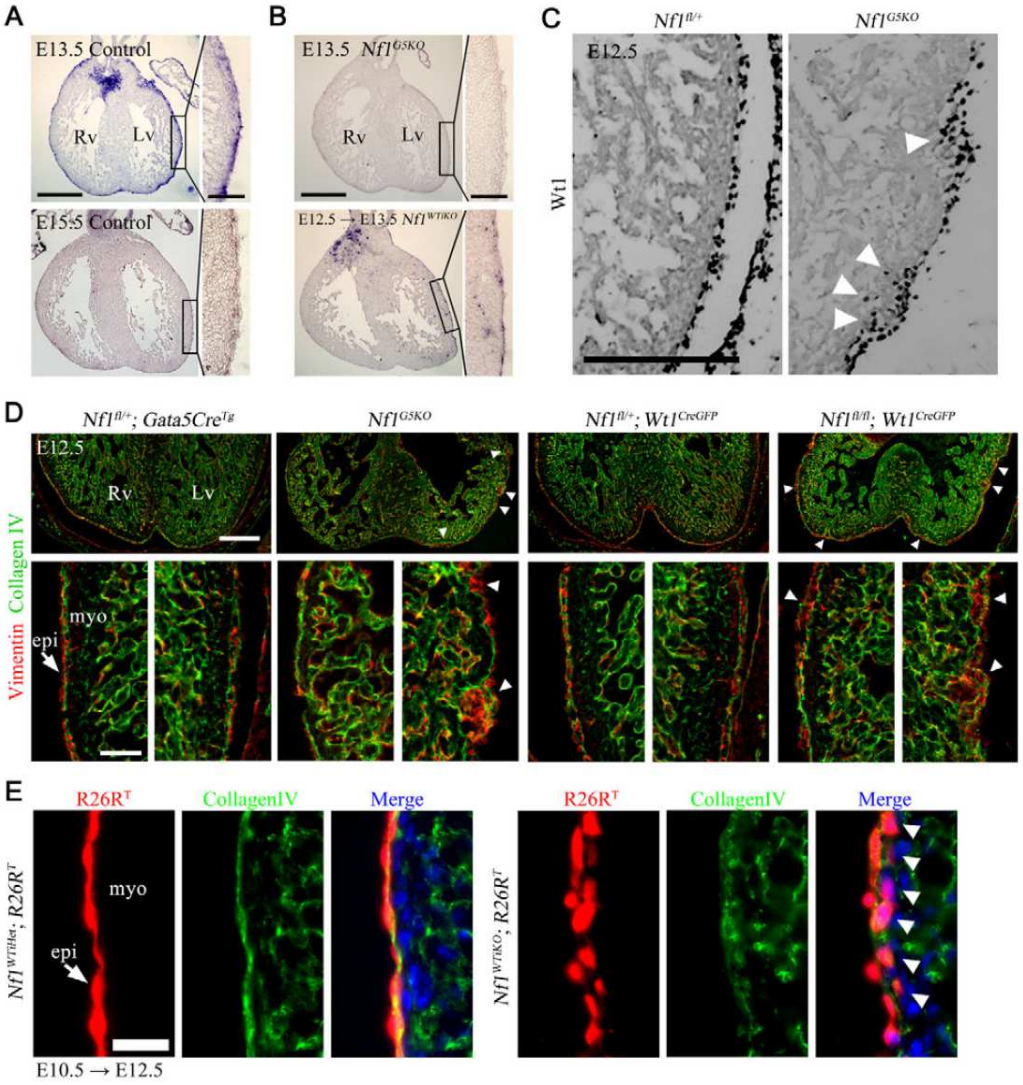


Figure 3-1. Disruption of epicardial development by loss of Nf1 in epicardium

(**A,B**) *Nf1* mRNA expression was detected by in situ hybridization in heart sections of the indicated genotype. *Nf1*$^{WTiKO}$ mouse embryos were maternally induced with tamoxifen for Cre activity at E12.5 for 24 hours before processing (E12.5 → E13.5). The boxed regions are shown at higher magnification in the insets. (**C**) Immunohistochemistry (IHC) for the

epicardial marker Wt1. Arrowheads indicate increased invasion of $Wt1^{+}$ cells. (**D**) IHC for vimentin and collagen IV in embryonic hearts of the indicated genotype. Arrowheads indicate expansion of epicardial cells into the subepicardium. Bottom panels are higher magnifications of left and right ventricle. Arrow indicates epicardium. (**E**) $R26R^{T}$ fluorescence in heart sections of the indicated genotype. Oral tamoxifen administration is indicated by the stage of administration followed by the stage of isolation (E10.5 → E12.5). Arrows indicate epicardium. Arrowheads indicate migrated epicardial cells (below the basement membrane, collagen IV). Rv, right ventricle; Lv, left ventricle; epi, epicardium; myo, myocardium. Scale bars: 500 μm in A,B; 100 μm in A,B insets; 200 μm in C,D top; 50 μm in D bottom; 25 μm in E.

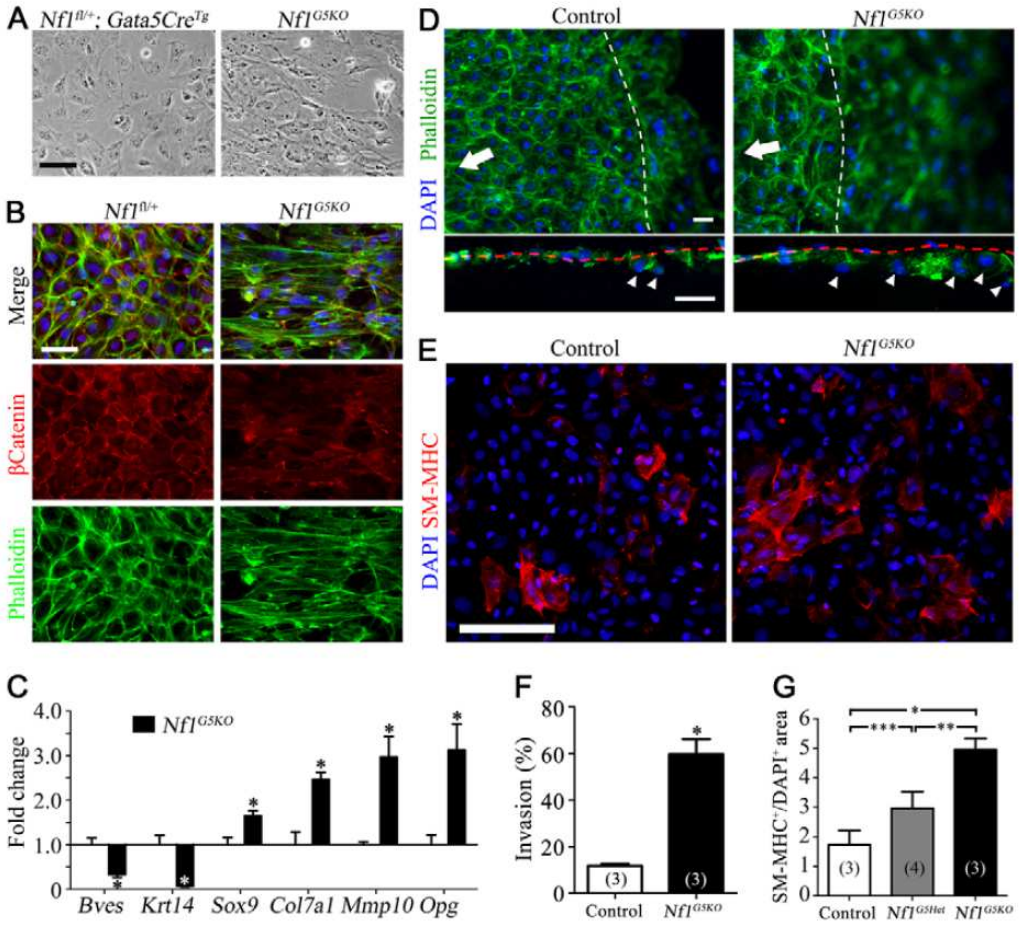


Figure 3-2. Loss of Nf1 in epicardial cells results in a phenotypic change to mesenchymal cells in vitro

(**A,B**) Seventy-two hour primary cultured epicardial cells from E12.5 mouse hearts. (A) Brightfield images. (B) Cultures stained for adherens junctions (β-catenin) and actin stress fibers (phalloidin). Nuclei were detected with DAPI. (**C**) mRNA expression of epithelial (*Bves*, *Krt14*) and mesenchymal (*Sox9*, *Col7a1*, *Mmp10*, *Opg*) genes. qRT-PCR was used to quantify gene expression in primary epicardial cell cultures. Data were

compared with control cultures represented by a baseline of 1.0. For each gene, at least five independent experiments were quantified in triplicate. Values are mean ± s.d. *$P$<0.0001. (**D**) Embryonic hearts of the indicated genotype were cultured on collagen gels to measure invasion. Actin stress fibers were stained with phalloidin and nuclei were detected with DAPI. Arrows indicate the center of the heart explants and white dashed lines delineate the invasion front. Invasion of epicardial cells was detected by fluorescence microscopy after sectioning (bottom). Red dashed lines indicate the collagen gel surface and arrowheads indicate invading cells. (**E**) Differentiation of epicardial cells into smooth muscle cells was detected by IHC for SM-MHC. Actin and nuclei were visualized with phalloidin and DAPI, respectively. (**F**) Quantification of invasion of epicardial cells into the collagen gel. Values are mean ± s.d. *$P$<0.0001. (**G**) Quantification of VSMC differentiation. The SM-MHC fluorescent area was normalized to the nuclear area. Data are mean ± s.d. $n$ values are indicated in parentheses. *$P$<0.001; **$P$<0.005; ***$P$<0.05. Scale bars: 50 μm in A,B,D; 100 μm in E.

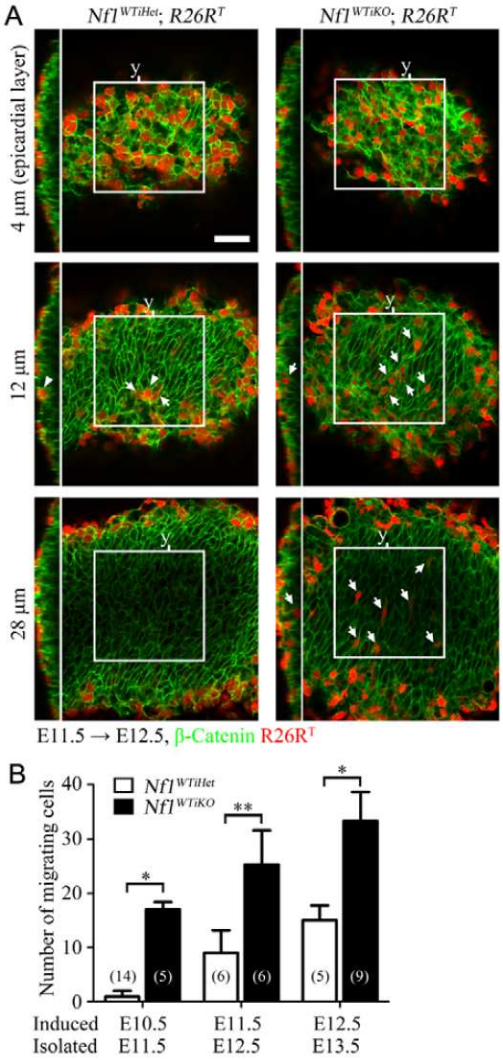


Figure 3-3. Early and increased EMT in vivo upon the loss of Nf1 in epicardial cells

(**A**) Representative whole-mount confocal optical sections of the indicated genotype. Induction by tamoxifen was at E11.5, hearts were isolated at E12.5 and whole-mount-stained for β-catenin to distinguish individual cells. *z*-stack images were taken from the epicardium (defined as 0 µm) using a confocal microscope. Nine consecutive images of 4

μm optical thickness spanning a total of 32 μm were taken in similar regions of the heart left ventricle. Examples at 4, 12 and 28 μm depth are shown. Boxed regions indicate the area used for quantification (150 μm X 150 μm). An orthogonal view of the indicated y-axis (y) of each *z*-stacked image is shown to the left. Arrows indicate examples of migrated cells in the heart ventricular region. Arrowheads indicate cells in the epicardium. See Figure 3-S3 for examples of the full panel of images at each tracing time point. Scale bar: 50 μm. (**B**) Quantification of $R26R^{T}$-positive cells in the myocardial region of hearts at the indicated tracing time points. The number of $R26R^{T}$-positive cells in the left ventricular region of the myocardial area (150 μm X 150 μm X 32 μm) was counted using ImageJ. Data are mean ± s.d. *n* values are indicated in parentheses. **P*<0.0001; ***P*<0.0005.

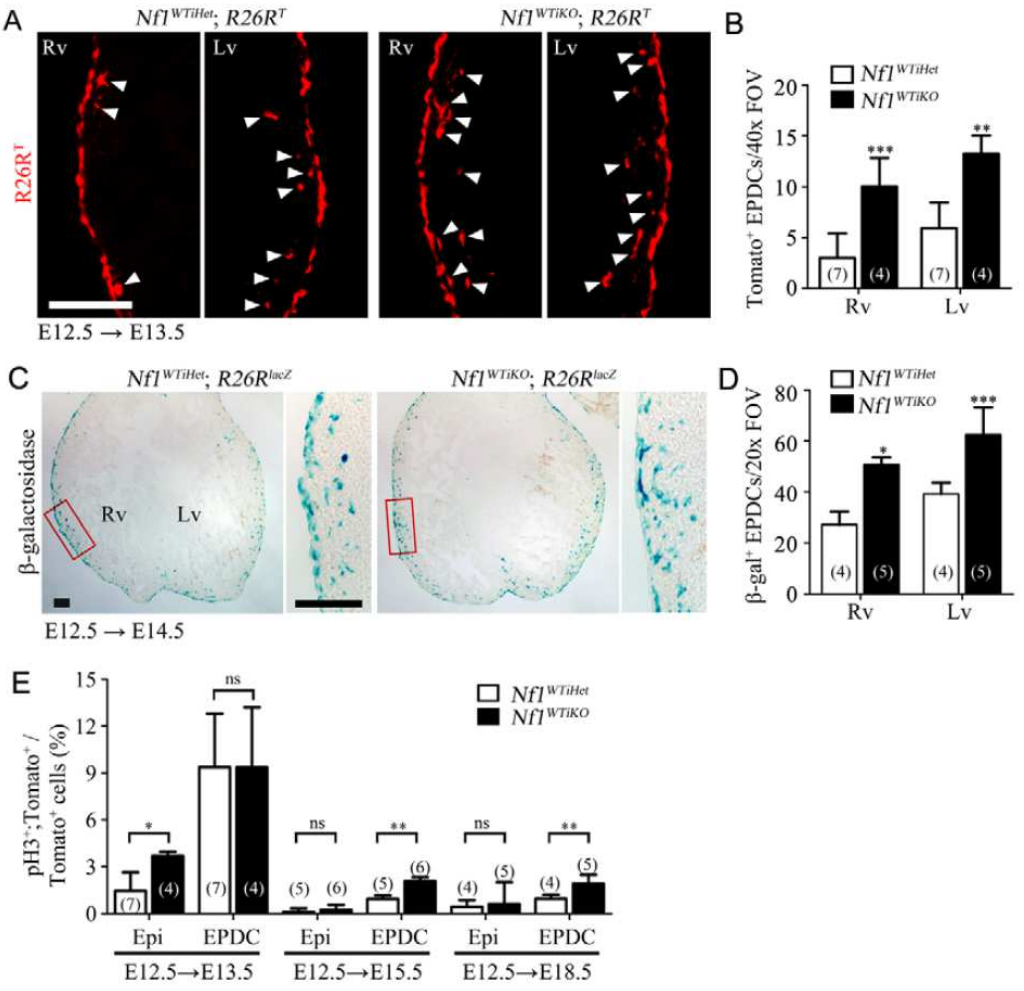


Figure 3-4. Migration and proliferation of EPDCs after inactivation of *Nf1* in vivo

(**A,C**) R26R$^{T}$ (A) and R26R$^{lacZ}$ (C) epicardial lineage tracing was used to identify migrated epicardial cells in hearts of the indicated genotype. Induction with tamoxifen was at E12.5, and heart sections were imaged for R26R$^{T}$ fluorescence at E13.5 (A) or stained for β-galactosidase activity at E14.5 (C). In C, the boxed regions are shown at higher magnification in the insets. Arrowheads in A designate EPDCs expressing R26R$^{T}$.

Scale bars: 100 μm. (**B,D**) Quantification of migrated $R26R^{T}$-positive or $R26R^{lacZ}$-positive EPDCs in A and C, respectively. Images were taken from similar regions of heart in both left and right ventricles with a 40X or 20X field of view and counted for $R26R^{T}$-positive or $R26R^{lacZ}$-positive cells within the myocardial ventricular wall. Data are mean ± s.d. *n* values are indicated in parentheses. **P*<0.0001; ***P*<0.001; ****P*<0.005. (**E**) Quantification of Wt1 lineage-tagged cellular proliferation. Embryos were maternally induced with tamoxifen at E12.5. Heart sections were immunostained for phospho-histone H3 (pH3) to detect mitotic cells. The $pH3^{+}$ $Tomato^{+}$ cells were counted in epicardial or myocardial regions and normalized to the total number of $Tomato^{+}$ cells in epicardium (Epi) or myocardial ventricular wall (EPDC). Nuclei were visualized with DAPI for quantification and images were taken from similar regions of heart in both left and right ventricles with a 20X field of view. *n* values are indicated in parentheses. **P*<0.01; ***P*<0.05; ns, no significant difference. Rv, right ventricle; Lv, left ventricle; FOV, field of view.

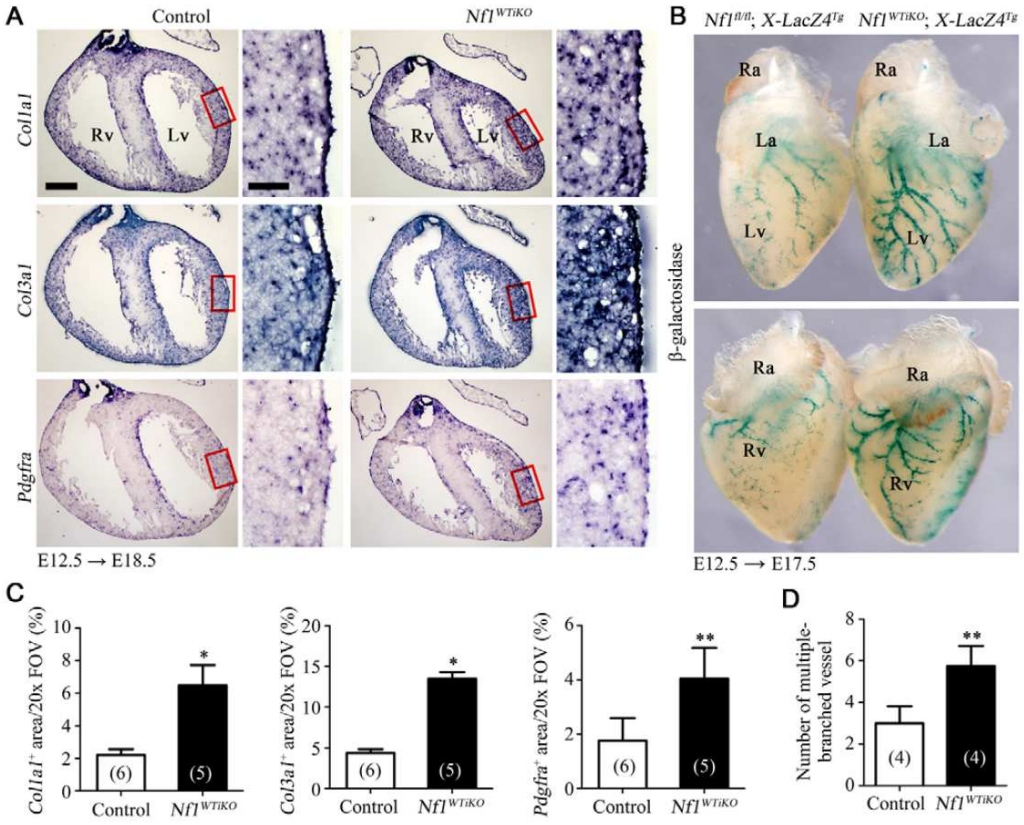


Figure 3-5. Expansion of EPDCs upon loss of Nf1 in the epicardium

(**A**) In situ hybridization at E18.5 for cardiac fibroblast marker genes (*Col1a1*, *Col3a1* and *Pdgfra*). Mouse embryos were induced with tamoxifen at E12.5 and hearts were isolated at E18.5. The boxed regions are shown at higher magnification in the insets. Scale bars: 500 μm; 100 μm in insets. (**B**) Whole-mount β-galactosidase staining (blue) of *XLacZ4* hearts for detection of VSMCs. Tamoxifen was administrated maternally at E12.5 before heart isolation at E17.5. (**C**) Quantification of the area positive for *Col1a1*, *Col3a1* or *Pdgfra* in A from 20X field-of-view images taken in similar regions of the left

ventricle. (**D**) Quantification of multi-branched (three or more) SMC-coated vessels in B. Data are mean ± s.d. *n* values are indicated in parentheses. **P*<0.001; ***P*<0.005. Ra, right atrium; La, left atrium; Rv, right ventricle; Lv, left ventricle; FOV, field of view.

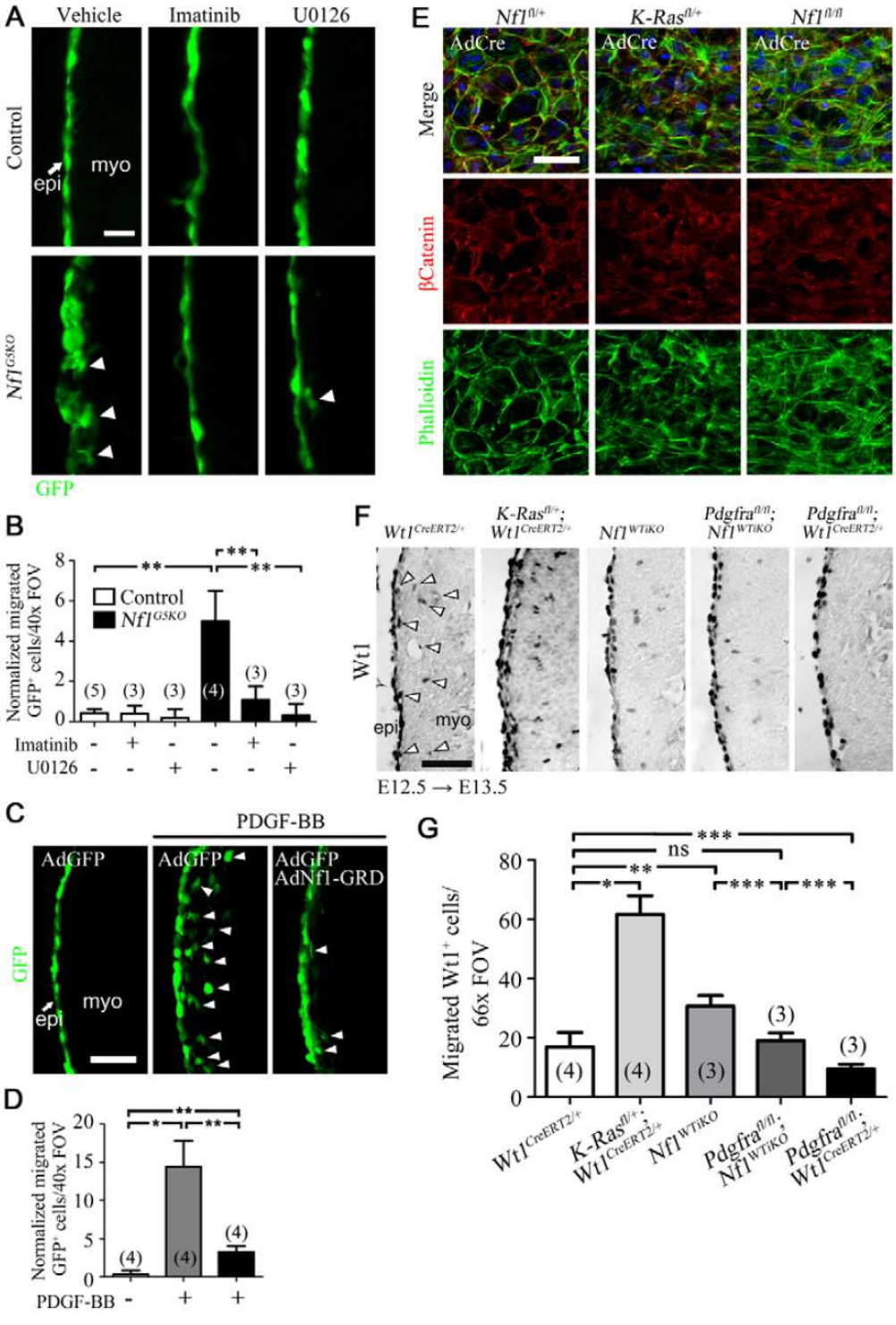
A
Vehicle
Imatinib
U0126
Control
Nf1G5KO
epi
myo
GFP
B
Normalized migrated GFP+ cells/40x FOV
Control
Nf1G5KO
Imatinib
U0126
C
PDGF-BB
AdGFP
AdNf1-GRD
D
PDGF-BB
E
Nf1fl/+
K-Rasfl/+
Nf1fl/fl
AdCre
Merge
βCatenin
Phalloidin
F
Wt1CreERT2/+
K-Ras fl/+; Wt1CreERT2/+
Nf1WTiKO
Pdgfrafl/fl; Nf1WTiKO
Pdgfrafl/fl; Wt1CreERT2/+
Wt1
E12.5 → E13.5
G
Migrated Wt1+ cells/ 66x FOV
ns

Figure 3-6. Regulation of epicardial EMT by Nf1.

(**A,C**) Representative GFP fluorescence images of the ex vivo migration assay. E12.5 mouse hearts were cultured and epicardial cells were labeled by adenoviral GFP transduction. Arrowheads indicate epicardial cell migration. Arrow indicates epicardium (epi); myo, myocardium. (A) Hearts were treated with 2 μM imatinib mesylate (a potent inhibitor of both Pdgfrα and Pdgfrβ) or U0126 (an inhibitor of both Mek1 and Mek2) where indicated. Hearts were cultured for 2 days before analyzing migration by GFP fluorescence. (C) Hearts were cultured in the presence or absence of Nf1 GAP-related domain (Nf1-GRD) adenovirus. After 18 hours, recombinant PDGF-BB was added to a final concentration of 20 ng/ml. Hearts were then cultured for 2 more days before analyzing migration by GFP fluorescence. (**B,D**) Quantification of migration in A and C, respectively. Migrated $GFP^+$ cells were quantified and normalized by multiplying by adenoviral transduction efficiency ($GFP^+$ cells in epicardium/total number of epicardial cells in a 40X field of view). Data are mean ± s.d. *n* values are indicated in parentheses. **P*<0.0005; ***P*<0.001. (**E**) Representative fluorescent images of primary epicardial cell cultures. E12.5 hearts of the indicated genotype were isolated and cultured on collagen-coated coverslips for 3 days. Heart explants were then removed and adenovirus for Cre expression (AdCre) added to the cultures. After 2 days, cells were fixed and stained with phalloidin and anti-β-catenin antibody to visualize actin stress fibers and cellular junctions, respectively. Nuclei were detected with DAPI. (**F**) IHC for Wt1 in left ventricle of the indicated genotype. Images were taken in a 66X field of view and $Wt1^+$ cells in the subepicardium and ventricle were quantified. Arrowheads illustrate cells that would be quantified. Cropped images of quantified regions are shown. Induction by tamoxifen was

at E12.5 and hearts were isolated after 24 hours. (**G**) Quantification of $Wt1^+$ cells in F. $Wt1^+$ cells in the myocardial compartment of the left ventricle were counted in 66X field-of-view images. Data are mean ± s.d. *n* values are indicated in parentheses. **P*<0.0001; ***P*<0.001; ****P*<0.05; ns, no significant difference. FOV, field of view. Scale bars: 200 μm in A; 50 μm in C,E,F.


Figure 3-S1. Nf1 expression in embryonic mouse heart

*Nf1* mRNA expression was detected in heart sections at the indicated stages by in situ hybridization. The boxed regions are shown at higher magnification in the insets. Scale bars: 1 mm; 100 μm in inset.

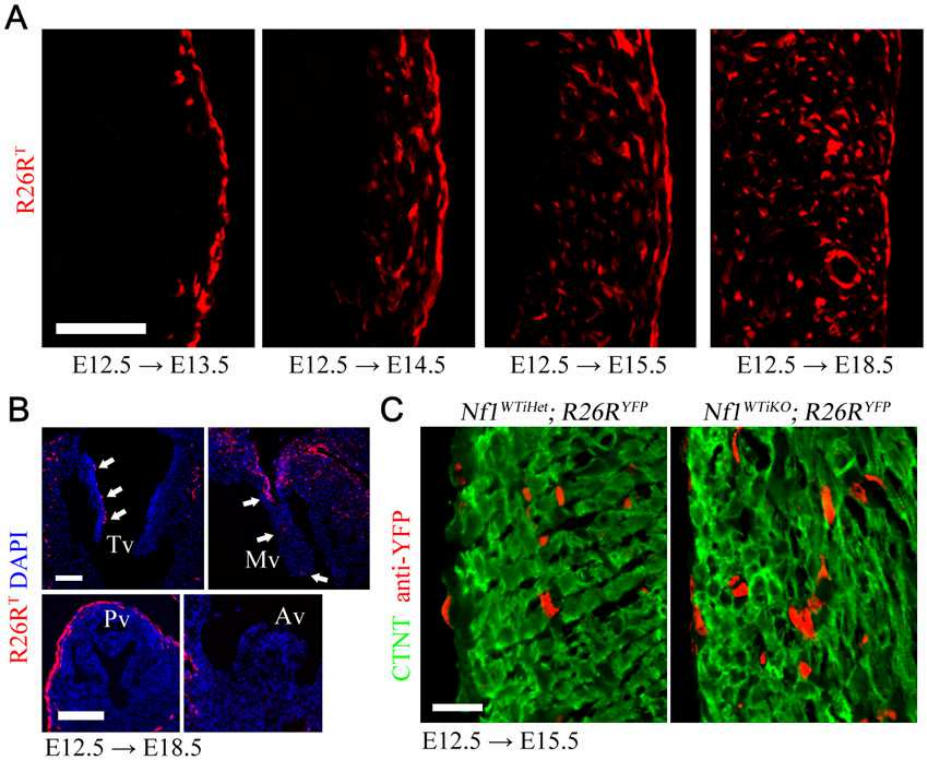


Figure 3-S2. Epicardial cell tracing by *Wt1*$^{CreERT2}$

(**A**) R26R$^{T}$ fluorescence images at indicated stages after *Wt1*$^{CreERT2}$ induction by tamoxifen. (**B**) R26R$^{T}$ fluorescence images at E18.5. Nuclei were detected with DAPI. Arrows indicate the R26R$^{T}$-positive cells in heart valves. Tv; tricuspid valve, Mv; mitral valve, Pv; pulmonary valve, Av; aortic valve. (**C**) Immunostained images for cardiac troponin T (CTNT) and YFP in the indicated genotypes at E15.5. Oral administration of tamoxifen to pregnant females occurred at E12.5. Scale bars: 200 μm in A; 100 μm in B; 20 μm in C.

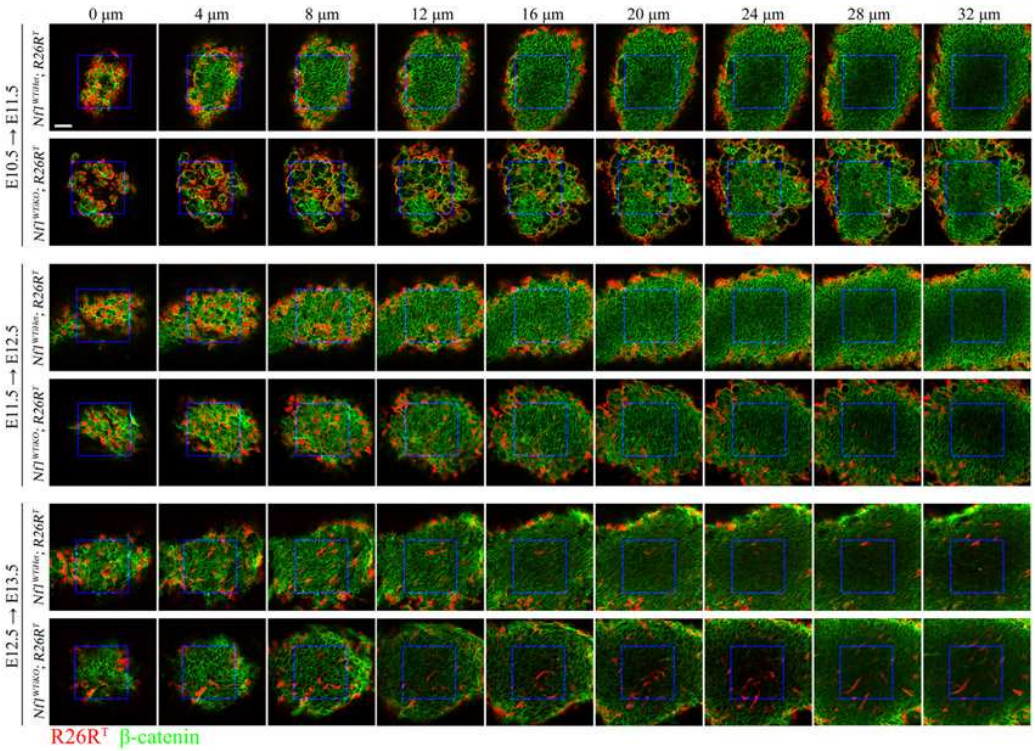


Figure 3-S3. Early and increased epicardial migration in *Nf1*$^{WTiKO}$ hearts

Representative whole-mount *z*-stack images of indicated genotypes. *Wt1*$^{CreERT2}$ was induced by tamoxifen at E10.5, E11.5 or E12.5 and hearts isolated after 24 hours. Hearts were whole-mount-stained for β-catenin to distinguish individual cells. *z*-stack images were taken starting at epicardial cells (designated as 0 µm) using a confocal microscope (total of nine images of 4 µm optical thickness spanning 32 µm depth) in similar regions of the left ventricle. The orthogonal view was used to determine if the same cell appeared in more than two consecutive images, and it was only counted once in this circumstance. Boxed areas indicate regions used for quantification (150 µm × 150 µm) starting at the 4 µm image. Scale bar: 50 µm.

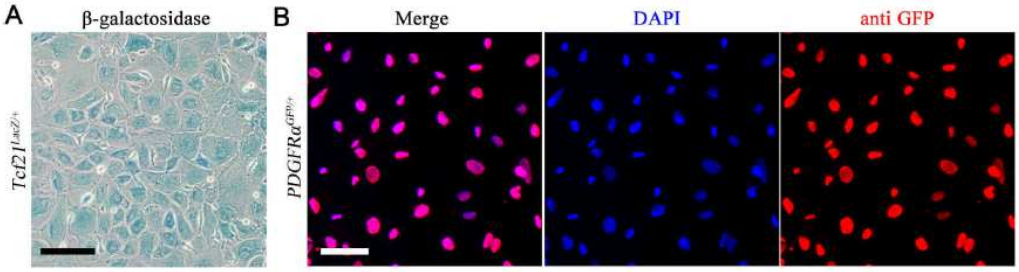


Figure 3-S4. Epicardial genes expression of primary epicardial cultures.

(**A, B**) Embryonic hearts of indicated genotypes were isolated at E12.5 and cultured for 3 days as described in Material and Methods. Identification of epicardial gene expression was detected by (A) staining for β-galactosidase activity for *Tcf21*$^{lacZ}$ or (B) immunostaining against GFP for *Pdgfra*$^{GFP}$. Nuclear was visualized by DAPI. Scale bars, 100 μm.

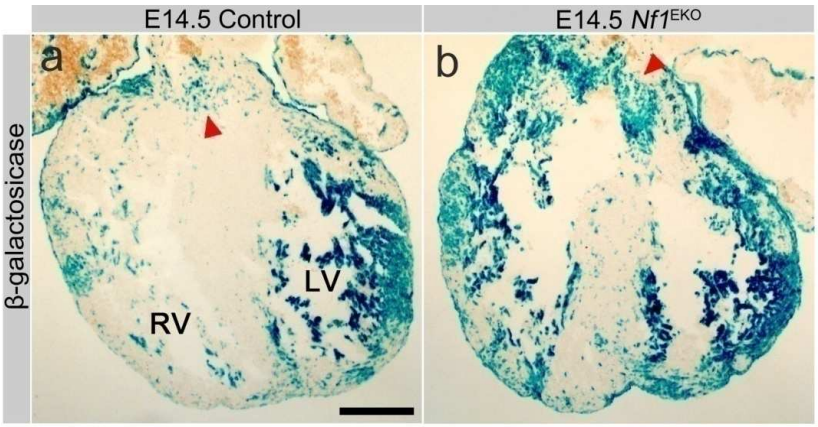


Figure 3-S5. The *Gata5Cre*$^{Tg}$ activity in *Nf1*$^{G5KO}$ hearts.

The *Gata5Cre*$^{Tg}$ activity in the hearts of indicated genotype at E14.5 was visualized by detecting β-galactosidase activity. Arrow heads indicate endocardial cusion regions. Rv, right ventricle; Lv, left ventricle.

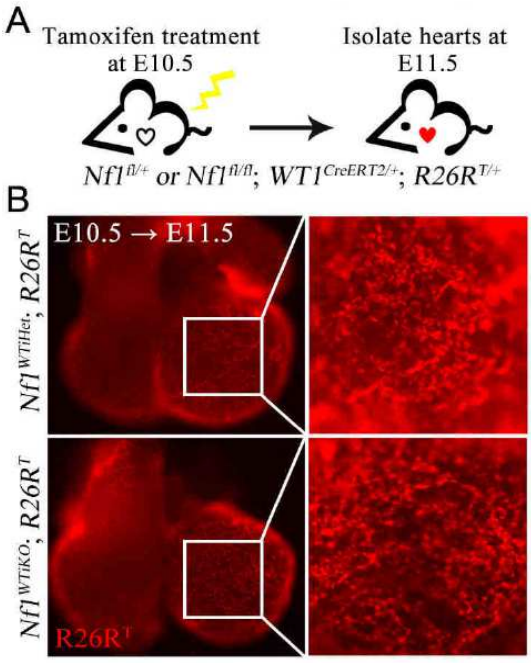


Figure 3-S6. Epicardial expression of R26R$^{T}$ reporter.

(**A**) Schematic representation of temporal restriction of Cre labeling with *Wt1*$^{CreERT2}$ by tamoxifen (**B**) Ventral view of hearts of the indicated genotypes: *Nf1*$^{WTiHet}$ (*Nf1*$^{fl/+}$; *Wt1*$^{CreERT2/+}$), *Nf1*$^{WTiKO}$ (*Nf1*$^{fl/fl}$; *Wt1*$^{CreERT2/+}$). Pregnant females were induced with tamoxifen at E10.5, and embryonic hearts were isolated at E11.5 for R26R$^{T}$ fluorescence imaging. Higher magnification of boxed regions is shown.

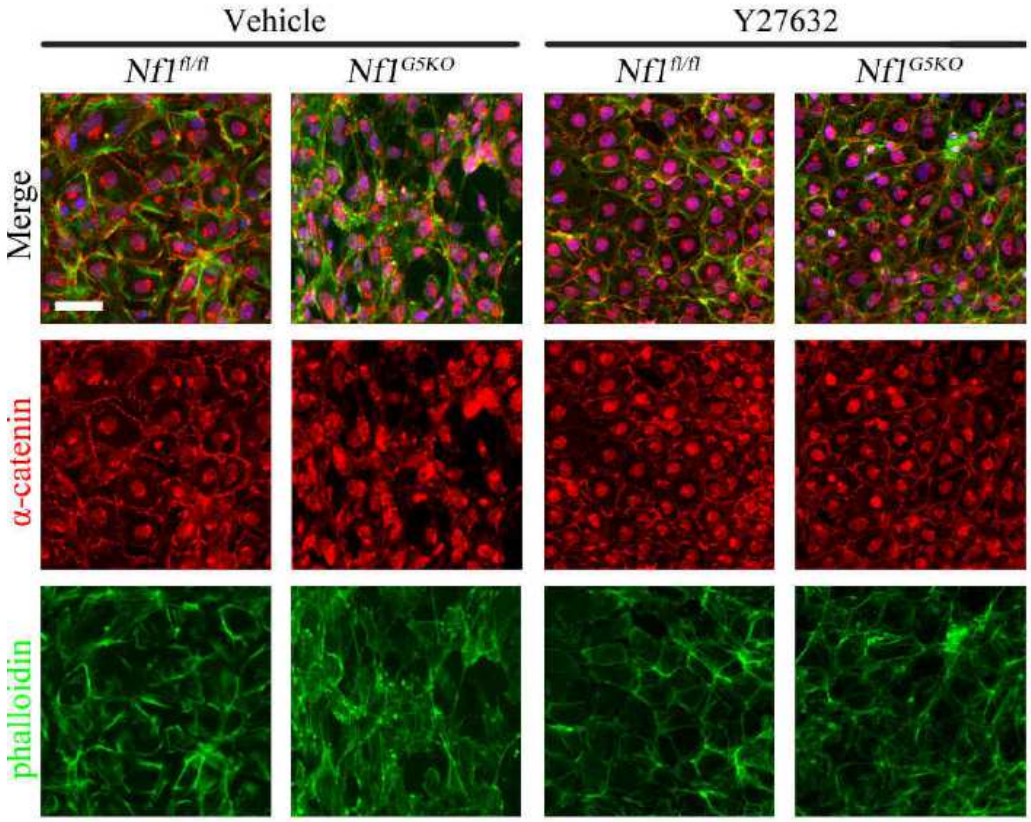


Figure 3-S7. Inhibition of EMT phenotypes by Y27632 in *Nf1* mutant epicardial cultures

Fluorescence images of primary epicardial cultures of indicated genotype. Hearts were isolated and placed in for 3 days with or without the presence of Y27632 (10 μg/ml, Rho-associated protein kinase inhibitor). Cultures were then fixed and stained for actin stress fiber (phalloidin) and adherens junctions (α-catenin). Nuclei were detected with DAPI. Scale bar, 50 μm.

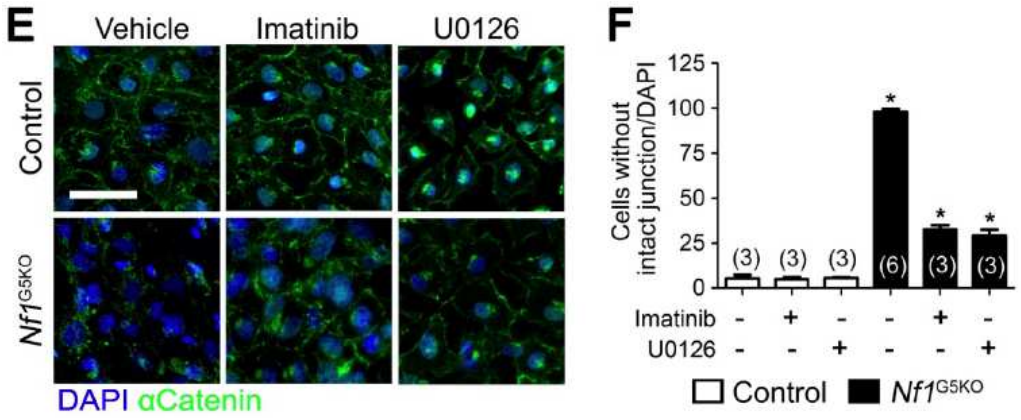


Figure 3-S8. Regulation of EMT mediated by PDGFR signaling in *Nf1* null epicardium

**E,** Primary epicardial cell cultures in the presence or absence of indicated inhibitors were immunostained for α-catenin to visualize cellular junctions. Nuclei were detected with DAPI. **F**, Epicardial cells with disrupted cellular junction were counted and normalized to the number of $DAPI^{+}$ nuclei. Scale bar, 50 μm. *n* values are indicated in parentheses. **P*<0.0001, ***P*<0.005, ****P*<0.01.

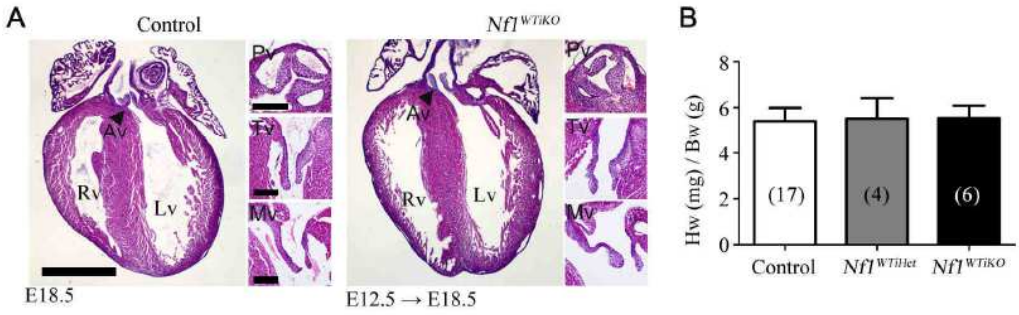


Figure 3-S9. Normal development of heart valves in *Nf1*$^{WTiKO}$

(**A**) Hematoxylin and eosin stained images of heart sections at E18.5. Arrow heads indicate aortic valves (Av). Scale bar, 1 mm. Pulmonary valve (Pv), tricuspid valve (Tv) and mitral valve (Mv) are shown. Rv, right ventricle; Lv, left ventricle. Scale bars, 200 μm. (**B**) Heart to body weight of 1 month old mice of indicated genotype. Tamoxifen was administrated maternally at E12.5 for cre activity. Data are represented as mean ± sd. *n* values are indicated in parentheses.

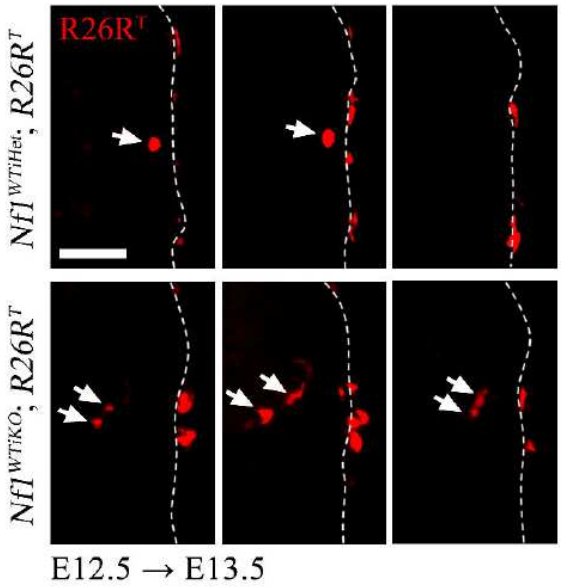


Figure 3-S10. R26R$^{T}$ epicardial lineage tracing with low-dose tamoxifen induction

Embryos were induced at E12.5 with low-dose tamoxifen (2.5 μg per gram-body-weight), and hearts were isolated and sectioned to 10 μm after 24 hours at E13.5. Three consecutive sections are shown. Arrows indicate R26R$^{T}$-positive cells in myocardial compartment. Dotted lines separate the epicardium from the subepicardium. Scale bars, 50 μm.

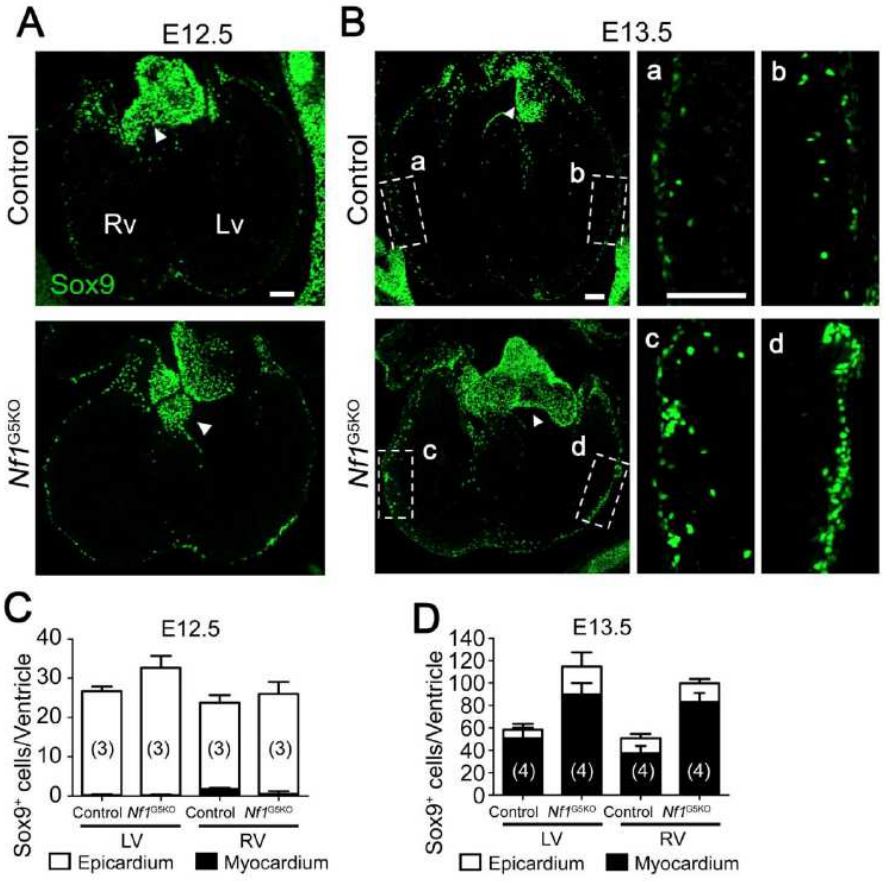


Figure 3-S11. Sox9 expression in *Nf1*$^{G5KO}$ hearts

**A**, **B**, Representative images of heart sections at (A) E12.5 and (B) E13.5 immunostained for Sox9. Sox9 expression was detected in the epicardium and beneath the epicardial layer as well as in the endocardial cushions (arrowheads). Boxed regions (a-d) are shown under higher magnification. Scale bars, 100 μm. **C**, **D**, Quantification of Sox9$^{+}$ cells in epicardium and myocardial ventricular wall at (C) E12.5 and (D) E13.5. Values are shown as means ± sd. *n* values are indicated in parentheses.

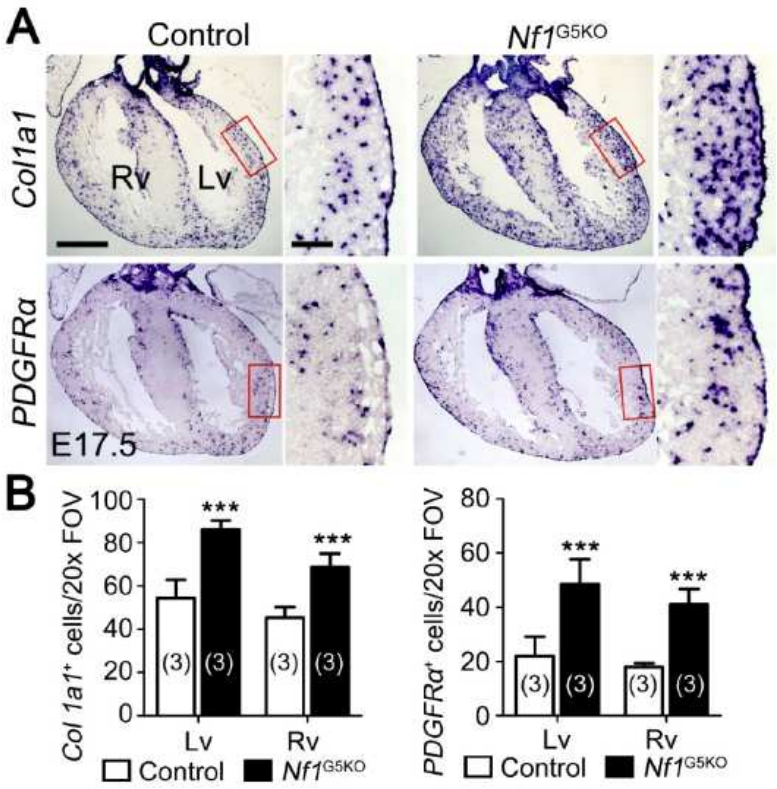


Figure 3-S12. Expansion of cardiac fibroblast markers in *Nf1*$^{G5KO}$ hearts

**A**, In situ hybridization at E17.5 for *Col1a1* and *Pdgfra*. Scale bar, 500 μm. Right panels show higher magnifications of boxed regions. Scale bar, 100 μm. B. Quantification of *Col1a1*- or *Pdgfra*-expressing cells in 20X field of view (FOV). Scale bar, 50 μm. *n* values are indicated in parentheses. ***$P$<0.01.

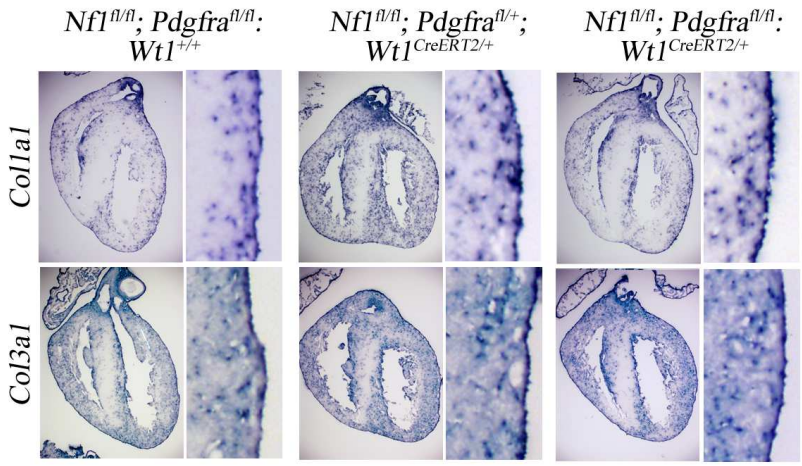


Figure 3-S13. Partial loss of cardiac fibroblast-expansion in *Nf1*$^{WTiKO}$ hearts by inactivation of *Pdgfra*

Pregnant females were induced with tamoxifen at E12.5 and embryonic hearts were isolated at E18.5. Cardiac fibroblasts were detected by in situ hybridization of *Col1a1* and *Col3a1*.

Table 3-1. Recovery of *Nf1*; *Gata5Cre*$^{Tg}$ embryos and offspring

| Age | N | Isolated | Expected |
|---|---|---|---|
| E12.5 | 613 | 156 | 153 |
| E13.5 | 121 | 25 | 30 |
| E14.5 | 53 | 10 | 13 |
| E15.5 | 85 | 24 | 21 |
| E16.5 - E18.5 | 130 | 30 | 33 |
| P0 | 26 | 6‡ | 7 |

‡ pups were born but expired within 12 hours

## CHAPTER FOUR

# NF1 AND CARDIAC FIBROBLASTS FUNCTION IN ADULT HEARTS

### Introduction

Cardiac hypertrophy is an adaptive process that occurs in response to pathological and physiological stress. However, sustained overload can cause hypertrophic cardiomyopathy that predisposes patients to develop heart failure. During cardiac hypertrophy, cardiomyocytes undergo complex structural remodeling including enlargement of individual cells and rearrangement of muscle fibers. Numerous reports have shown the role of non-muscle cells in both cardiac hypertrophy and heart failure. Cardiac fibroblasts have a pivotal function in the adaptive response of hearts to pressure overload. Collagen-rich ECM is derived from cardiac fibroblasts and its excessive accumulation correlates with impaired heart function and cardiac failure. Cardiac fibroblasts interact with cardiomyocytes and affect their function (Takeda et al., 2010; Teekakirikul et al., 2010). Upon stress, they produce growth factors, such as periostin, endothelin-1 and cardiotrophin-1, which have been shown to induce hypertrophic responses (Harada et al., 1997; Kuwahara et al., 1999; Oka et al., 2007). Cardiac fibroblasts also affect proliferation of cardiomyocytes in developing hearts (Ieda et al., 2009). However, the role of cardiac fibroblasts during adaptive responses remains unclear.

This chapter summarizes pilot studies on 1) the physiological role of EPDCs during cardiac hypertrophy; 2) the function of Nf1 and Pdgfrα in EPDCs, particularly in cardiac fibroblasts. It is worth noting that 1) some results are preliminary and would need

further validation with more of animals and repeats. 2) the genetic backgrounds of the animals are different and have not been back-crossed enough generation to rule out any effects of strain differences. However, results described in this chapter will provide essential data to optimize the mouse models to investigate the role of Nf1 during cardiac hypertrophy response specifically in cardiac fibroblast. *Nf1*$^{WTiKO}$ mouse model was initially tested to study the role of EPDCs in response to pressure overload or isoproterenol treatment. A mouse model with cardiac fibroblast-specific inactivation of *Nf1* was generated using the *Tcf21*$^{iCre}$ allele. Finally, mouse models to study specific functions of *Nf1* in cardiac fibroblast have been generated and evaluated.

**Material and Methods**

*Mice*

Mice were maintained on a mixed C57/Bl6 X 129SV background. The strains used in the experiment includes *PDGFRα*$^{fl}$ (Tallquist et al., 2003), *PDGFRβ*$^{fl}$ (Richarte et al., 2007; Schmahl et al., 2008), *Tcf21*$^{iCre}$ (Acharya et al., 2011), *Nf1* floxed (*Nf1*$^{fl}$) (Zhu et al., 2001), *Wt1*$^{CreERT2}$ (Zhou et al., 2008) and *Gata5Cre*$^{Tg/0}$ (Merki et al., 2005). Reporter strains used in the study include: *ROSA26R*$^{lacZ}$ (Soriano, 1999) or *ROSA26R*$^{tdTomato}$ (Madisen et al., 2010). All animal protocols and experiments were approved by the UTSW IACUC and conformed to National Institutes of Health guidelines for care and use of laboratory animals. All procedures described in this study were approved by the Institutional Animal Care and Use Committees of UT Southwestern Medical Center and conformed to NIH guidelines for care and use of laboratory animals.

*Tamoxifen induction*

Mice were induced embryonically by oral administration of tamoxifen (MP Biomedicals, 02156738) to pregnant females at indicated embryonic stages. For postnatal induction, intragastric injection was used for the mice at P7 or earlier or oral gavage for older mice. Tamoxifen was dissolved in sunflower seed oil (Sigma) at 20 mg/ml and administrated to the final concentration of 0.1 mg per gram body weight.

*Mouse models of cardiac hypertrophy*

Cardiac pressure overload model induced by TAB was performed as described previously (Rockman et al., 1991). After anesthetized by intraperitoneal injection of avertin, mice underwent either a sham operation or were subjected to TAC. Isoproterenol (25 mg/kg/day) or saline were administered using osmotic minipumps (Alzet) implanted subcutaneously. Mice were sacrificed after three weeks after TAB or 2 weeks after isoproterenol administration.

*Histological analysis*

Hearts were isolated in the Krebs buffer (118 mM NaCl, 4.7 mM KCl, 2.5 mM $CaCl_2$, 1.2 mM $KH_2PO_4$, 1.2 mM $MgSO_4$, 25 mM $NaHCO_3$ and 11 mM Glucose) and fixed in 4% PFA or 10% buffered formalin for 2 days at 4ºC and paraffin embedded. For histological analysis, tissues were sectioned to 8 μm, rehydrated and stained with hematoxylin and eosin (Sigma), masson's trichrome or picrosirius red.

For the measurement of cardiomyocyte cross-sectional area, heart sections were deparaffinized and incubated with fluorescence-conjugated wheat germ agglutinin

(Sigma). Mean cardiomyocyte cross-sectional area was determined using ImageJ.

*BrdU incorporation assay*

BrdU (Sigma) was injected into the peritoneum 3 days before harvesting hearts. Hearts were processed for paraffin embedding. Antigens were retrieved in citrate buffer (pH 6.0) at 98ºC for 15 minutes with temperature-controlled microwave (BioGenex). BrdU-positive nuclei were visualized by andibody staining followed by DAB (Vector Labs).

**Results and Discussion**

*Altered cardiac stress response in $Nf1^{WTiKO}$ mice*

In the previous chapter, we have shown that loss of Nf1 in the epicardium during heart development leads to an expansion of EPDCs in $Nf1^{WTiKO}$ mice. To investigate how the expansion of EPDCs affected postnatal heart function, we examined the hearts from $Nf1^{WTiKO}$ mice postnatally. As shown in Figure 4-1, the size of the hearts of $Nf1^{WTiKO}$ animals was comparable to that of controls and no significant difference was found in the amount of EMC by Masson trichrome staining. Furthermore, no sign of cardiomyocytes hypertrophy was detected in $Nf1^{WTiKO}$ animals. These results suggest that the physiology of the heart was maintained even with excess EPDCs during development.

Under stress conditions, such as cardiac injury or hypertension, hearts undergo a series of homeostatic responses to adapt to the stress. To understand the physiological role of EPDCs during stress conditions, two cardiac stress models were utilized to induce

cardiac hypertrophy: thoracic aortic banding (TAB) or β-adrenergic agonist isoproterenol treatment. TAB operation increases pressure in the proximal aorta and commonly used to induce cardiac hypertrophy (Errami et al., 2008; Frey et al., 2004; Hill et al., 2000). Isoproterenol-induced cardiac hypertrophy is well-characterized model of cardiac hypertrophy associated with fibrosis and myocardial ischaemia (Brodde, 1988; Szabo et al., 1975; Taylor and Tang, 1984).

First, we examined hearts after three weeks of TAB. As shown in Figure 4-1, hearts of $Nf1^{WTiKO}$ mice show stress responses to a greater extent than control mice. No differences were observed in heart size, ECM deposition and cardiomyocyte hypertrophy between control and $Nf1^{WTiKO}$ hearts under sham conditions. However, under the TAB condition, hearts from $Nf1^{WTiKO}$ animals were enlarged with increased ECM deposition and the cellular size of cardiomyocytes was also increased, suggesting that $Nf1^{WTiKO}$ hearts were more responsive to induction of cardiomyocyte hypertrophy.

Next, we examined cardiac hypertrophic response after treatment with isoproterenol for two weeks. Saline treated $Nf1^{WTiKO}$ hearts were similar to controls in heart size, ECM deposition, proliferation rate, and cardiomyocyte hypertrophy (Figure 4-2, Figure 4-3 and Table 4-1). Control mice responded to isoproterenol as reported previously, with a significant increase in heart size, more ECM deposition, and increased proliferation. Cardiomyocyte hypertrophy was also significantly increased compared to saline treated controls. However, no significant differences in heart size, ECM deposition and cardiomyocyte hypertrophy were found in $Nf1^{WTiKO}$ hearts treated with isoproterenol compared to saline treated group. These results suggest that isoproterenol-induced cardiac hypertrophy response is abolished in $Nf1^{WTiKO}$ animals. Interestingly, in $Nf1^{WTiKO}$ hearts,

increased proliferation was observed in hearts treated with isoproterenol (Figure 4-3).

*Altered cardiac stress response in PDGFR$^{EKO}$ mice*

Previously, our lab reported that loss of *Pdgfra* or *Pdgfrb* in epicardium results in specific loss of cardiac fibroblasts or cVSMCs, respectively. To understand how the loss of EPDCs affects heart function during cardiac hypertrophic response, we investigated the *Pdgfra; Pdgfrb; Gata5Cre$^{Tg/0}$* (*PDGFR$^{EKO}$*) mouse model after the treatment of saline or isoproterenol for two weeks (Figure 4-4, Table 4-1). As reported previously, no significant difference in heart size and function was detected when treated with saline. Treatment of isoproterenol induced cardiac hypertrophy in control mice as described in the previous section. However, when treated with isoproterenol, *PDGFR$^{EKO}$* mice have multiple fibrotic lesions in the hearts and also show ECM deposition to a greater extent than control mice. These results are in sharp contrast to the TAB treated mice described by Christopher Smith (unpublished data) where *PDGFR$^{EKO}$* mice had less fibrotic response compared to control when operated for TAB. These results can be explained by two possibilities. First, cardiac fibroblasts are heterogeneous and have multiple origins other than epicardium. Robust fibrotic response might be explained by different responsiveness of each cardiac fibroblast subpopulations. The non-resident cardiac fibroblasts may contribute to the fibrotic response in *PDGFR$^{EKO}$* hearts. Second, non-fibroblast populations within hearts might be responsible for matrix deposition in *PDGFR$^{EKO}$* hearts. Further studies are needed to investigate the heterogeneity of cardiac fibroblasts and contribution of resident cardiac fibroblasts during cardiac stresses responses. Interestingly, expansion of Tcf21-lineage tagged cells was noticed in TAB-

operated hearts (Caroline Sung, unpublished) suggesting that epicardially-derived cardiac fibroblasts do expand in response to injury. It will be interesting to test whether similar expansion can be observed after isoproterenol treatment.

*Mouse models to study the function of Nf1 in cardiac fibroblasts*

Altered responses to cardiac stress in $Nf1^{WTiKO}$ mouse can be attributed to either the expansion of EPDCs or loss of *Nf1* in EPDCs. Embryonic phenotypes of *Nf1*-loss can be ruled out by inactivating *Nf1* durring adult stage. To inactivate Nf1 in the adult, Cre was activated by oral administration of tamoxifen (20 mg/kg/day) in two month old control and $Nf1^{WTiKO}$ mice for five consecutive days. After 4 months, hearts were examined for the cells expressing $R26R^{T}$ reporter gene. As shown in Figure 4-5, $Wt1^{CreERT}$-lineage-tagged cells were detected predominantly in the epicardium and also within the myocardial region. As reported previously, $Wt1^{CreERT}$-lineage-tagged cells were also detected in most of the glomeruli suggesting that the tamoxifen induction was highly efficient. We then examined the heart size and ECM deposition of adult-induced $Nf1^{WTiKO}$ mouse model. As shown in Figure 4-6 and Table 4-1, no significant difference was detected in heart size between control and adult-induced $Nf1^{WTiKO}$ mice. MTC and picrosirius red staining also showed similar levels of collagen deposition. These results suggest that the loss of *Nf1* in the Wt1-lineage cells of heart in the adult did not result in any detectable differences. However, we observed differences in the numbers and the types of tagged cells between embryonic induction and adult induction. Embryonic induction mostly tagged epicardial cells and EPDCs. However, endothelial cells seem also tagged by adult induction.

The *Nf1*$^{WTiKO}$ mouse model that was described in previous sections has expansion in both cardiac fibroblast and VSMC. To test the second scenario and understand the specific role of cardiac fibroblasts during cardiac hypertrophic response, *Tcf21*$^{iCre}$ allele was utilized to generate *Nf1*$^{fl/fl}$; *Tcf21*$^{iCre}$ mice. By postnatal administration of tamoxifen, *Nf1* was specifically inactivated in the cardiac fibroblast population but not during embryonic development. The Cre was activated by oral administration of tamoxifen (0.2 mg/kg/day) in two month old control and *Nf1*$^{fl/fl}$; *Tcf21*$^{iCre/+}$ mice for five consecutive days. Heart function was measured by echocardiogram after four weeks later. Hearts were then isolated to measure the total amount of collagen by hydroxyproline assay. No significant difference in fractional shortening and hydroxyproline was found between controls and *Nf1*$^{fl/fl}$; *Tcf21*$^{iCre/+}$ mice (Figure 4-7). However, we need to verify the level of *Nf1* deletion in cardiac fibroblasts before drawing any definite conclusions. The results above may indicate a major role of EPDCs in the cardiac stress response.

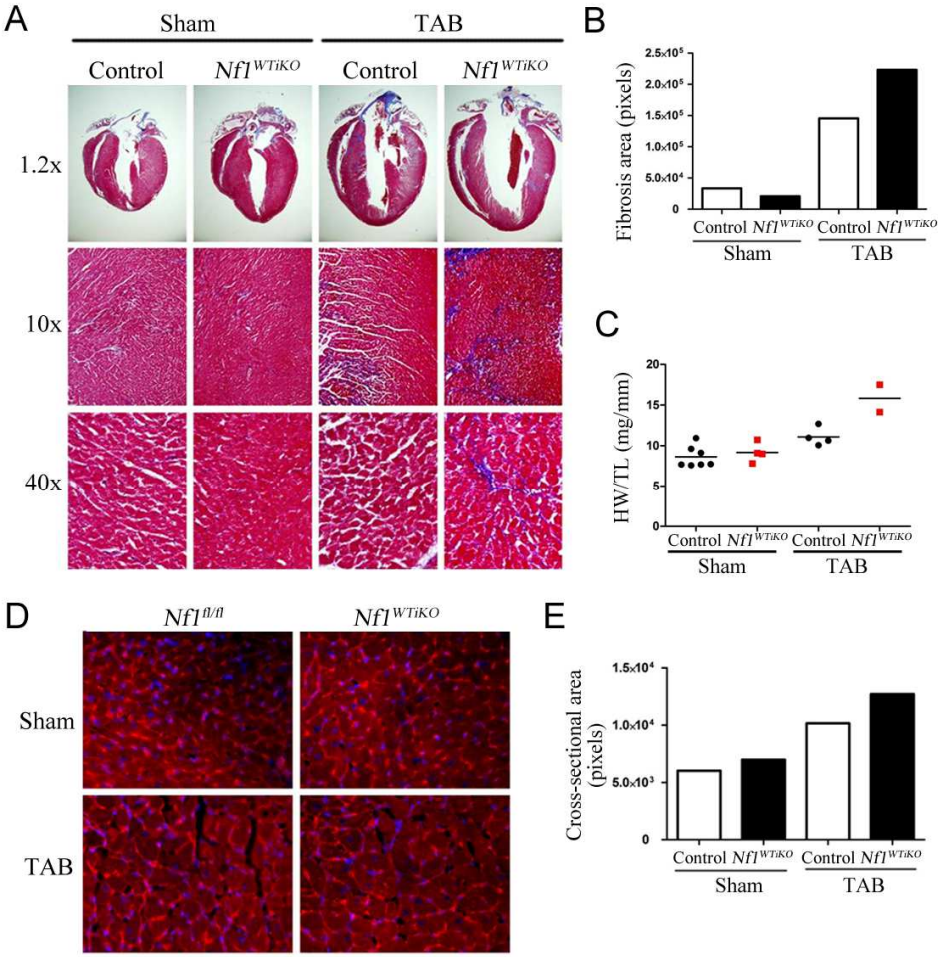


Figure 4-1. Cardiac stress response induced by pressure overload

Control and *Nf1*$^{WTiKO}$ mice are subjected to sham or TAB operation followed by isolation of hearts after 21 days. (**A**) Representative images of Masson trichrome-stained heart sections from mice with indicated genotypes. High-magnification images are also shown. (**B**) Quantification of fibrosis area in (A). Images of similar region in heart left ventricle were taken and ECM-stained area (blue staining) were quantified by normalized with

total tissue area using ImageJ software. (**C**) Heart weight (HW) to tibia length (TL) (mg/mm). (**D**) Representative cross-sectional images of heart left ventricles. Cell membrane was visualized by incubating tissue sections with fluorescence-labeled WGA. Nuclei were visualized by DAPI. (**E**) Mean cross-sectional area in (D).

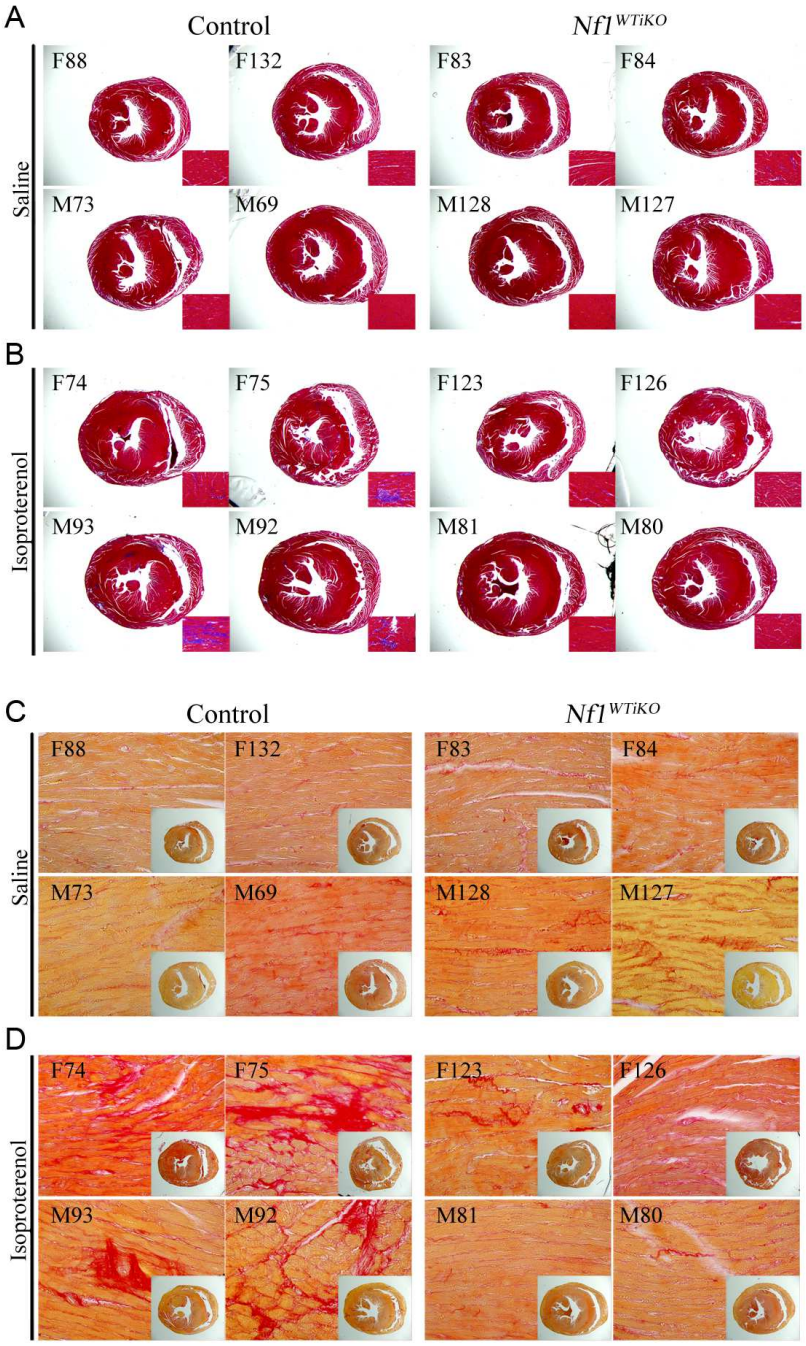
A
Control
Nf1 WTiKO
Saline
F88
F132
F83
F84
M73
M69
M128
M127
B
Isoproterenol
F74
F75
F123
F126
M93
M92
M81
M80
C
Control
Nf1 WTiKO
Saline
F88
F132
F83
F84
M73
M69
M128
M127
D
Isoproterenol
F74
F75
F123
F126
M93
M92
M81
M80

Figure 4-2. Attenuated fibrotic response in *Nf1*$^{WTiKO}$ mice

Control and *Nf1*$^{WTiKO}$ mice are subjected to treat saline or isoproterenol for 14 days. (**A**, **B**) Representative images of Masson trichrome-stained heart sections from mice with indicated genotypes. High-magnification images are shown as insets. (**C**, **D**) Representative picrosirius red-stained sections. Low-magnification images are shown as insets. Identification numbers for individual mice are shown on the images. See Table 4-1.

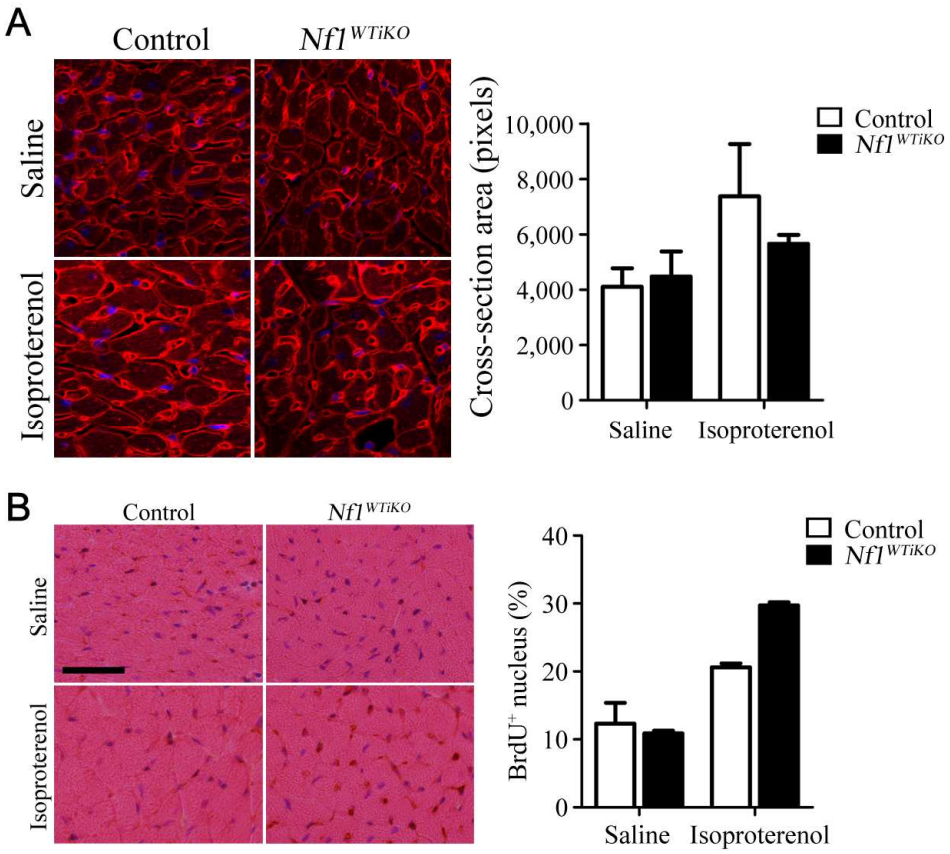


Figure 4-3. Cardiomyocyte hypertrophy and proliferation after treatment of isoproterenol (**A**) Confocal fluorescence images of heart sections from saline or isoproterenol treated mice of indicated genotypes. Sections were stained for membrane (wheat germ agglutinin) and nuclei (DAPI). Mean cross-sectional area was determined for each condition. 100 to 200 cells were counted from the three non-consecutive images (*n*=4). (**B**) Tissue sections were stained for BrdU using anti-BrdU antibody and counter stained with H&E. Mean BrdU incorporation was calculated by normalizing $BrdU^+$ nuclei over total number of nuclei among non-cardiomyocyte population.

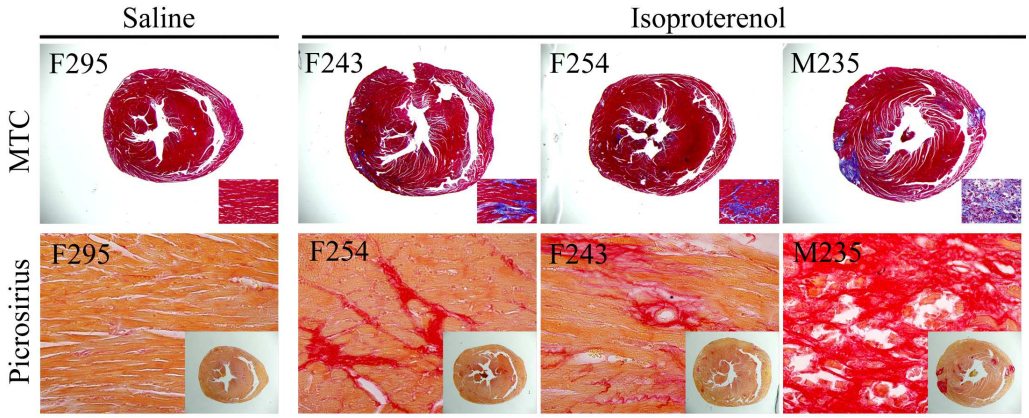


Figure 4-4. Fibrotic response of *PDGFR*$^{EKO}$ hearts after treatment of isoproterenol

Control and *PDGFR*$^{EKO}$ mice are subjected to treat saline or isoproterenol for 14 days. Representative images of Masson trichrome- (MTC) or picrosirius red-stained heart sections were shown. High- or low-magnification images are shown as insets. Identification numbers for individual mice are shown on the images.

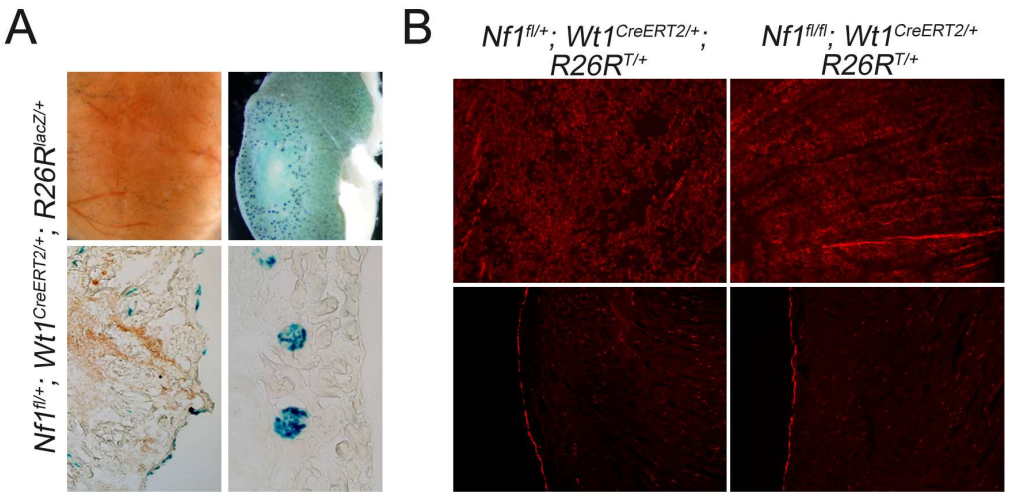


Figure 4-5. Postnatal tracing of *Wt1*$^{CreERT2}$

(**A**) Mice were induced with tamoxifen for 4 days and hearts and kidney were isolated three weeks later followed by staining for β-galactosidase activity. Whole-mount (upper panels) or sectioned (lower panels) images are shown. (**B**) Mice of indicated genotypes were induced with tamoxifen for 5 days and hearts were isolated 4 months later followed by fluorescence imaging for R26R$^{T}$ expression. Whole-mount (upper panels) or sectioned (lower panels) images are shown.

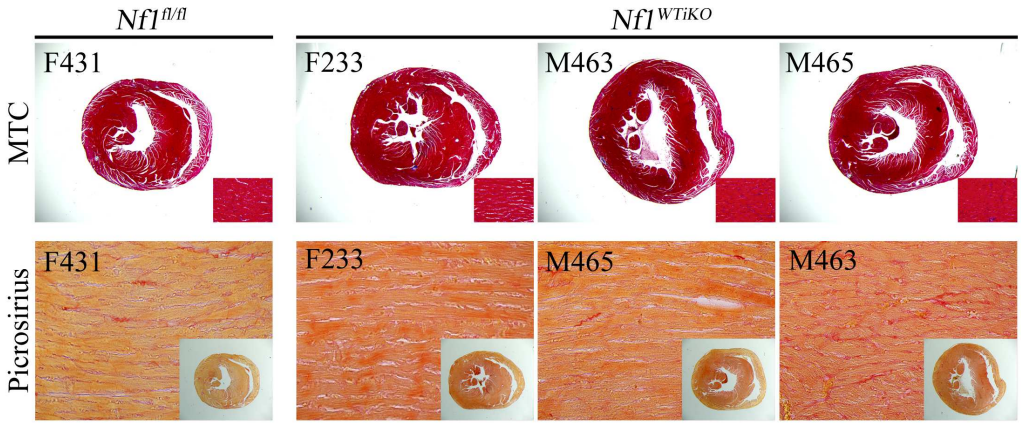


Figure 4-6. No sign of fibrotic response of postnatally-induced *Nf1*$^{WTiKO}$ mous heart

Control and *Nf1*$^{WTiKO}$ mice are treated with tamoxifen for 5 days. After 4 months, hearts were isolated, sectioned and stained with picrosirius red. Low-magnification images are shown as insets.

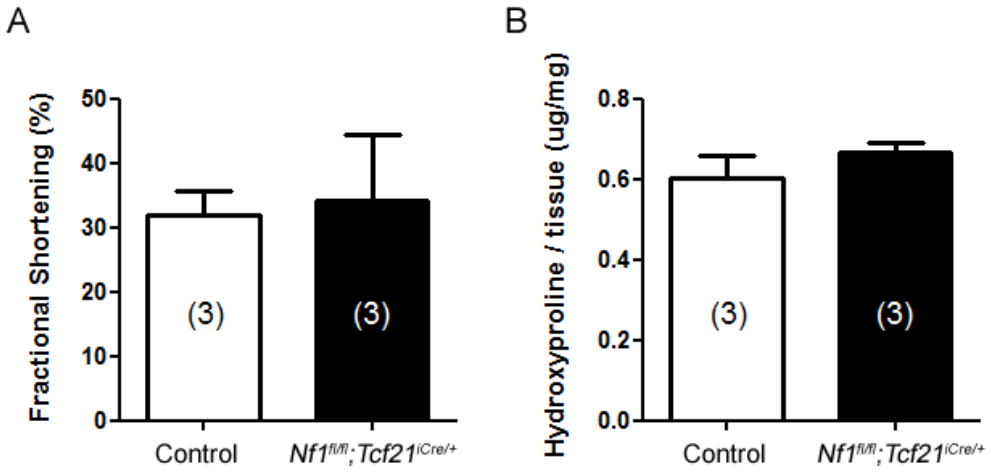


Figure 4-7. No difference in heart function and collagen of *Nf1*$^{fl/fl}$;*Tcf21*$^{iCre/+}$ hearts

Two month-old mice were induced with tamoxifen (20mg/g-body-weight) for five consecutive days. After four weeks, mice were subjected to echocardiogram to measure (A) fractional shortening followed by (B) hydroxylproline measurment. The amount of hydroxylproline was normalized to tissue weight (μg/mg). *n* values are indicated in parentheses.

Table 4-1. Heart size of *Nf1*$^{WTiKO}$ or *PDGFR*$^{EKO}$ mice

| Figure | Sex | # | Genotype | Tamoxifen | Treatment | BW (g) | HW (mg) | TL (mm) | HW/BW | HW/TL |
|---|---|---|---|---|---|---|---|---|---|---|
| Figure 4-2 | F | 123 | *Nf1*$^{fl/fl}$ *Wt1*$^{CreERT2/+}$ | E12.5 | Isoproterenol | **24.4** | **142.3** | 17.1 | 5.83 | 8.32 |
| | F | 126 | *Nf1*$^{fl/fl}$ *Wt1*$^{CreERT2/+}$ | | Isoproterenol | **23.2** | **137.5** | 17.0 | 5.93 | 8.09 |
| | M | 80 | *Nf1*$^{fl/fl}$ *Wt1*$^{CreERT2/+}$ | | Isoproterenol | **33.5** | **162.4** | 17.3 | 4.85 | 9.39 |
| | M | 81 | *Nf1*$^{fl/fl}$ *Wt1*$^{CreERT2/+}$ | | Isoproterenol | **31.9** | **167.4** | 17.5 | 5.24 | 9.57 |
| | M | 128 | *Nf1*$^{fl/fl}$ *Wt1*$^{CreERT2/+}$ | | Saline | **29.4** | **147.4** | 17.0 | 5.01 | 8.67 |
| | M | 127 | *Nf1*$^{fl/fl}$ *Wt1*$^{CreERT2/+}$ | | Saline | **29.4** | **136.9** | 17.2 | 4.66 | 7.96 |
| | F | 84 | *Nf1*$^{fl/fl}$ *Wt1*$^{CreERT2/+}$ | | Saline | **22.6** | **130.0** | 17.1 | 5.75 | 7.60 |
| | F | 83 | *Nf1*$^{fl/fl}$ *Wt1*$^{CreERT2/+}$ | | Saline | **22.5** | **112.5** | 17.2 | 5.00 | 6.54 |
| | F | 74 | *Nf1*$^{fl/fl}$ *Wt1*$^{+/+}$ | | Isoproterenol | **28.5** | **172.0** | 17.6 | 6.04 | 9.77 |
| | F | 75 | *Nf1*$^{fl/fl}$ *Wt1*$^{+/+}$ | | Isoproterenol | **26.1** | **158.2** | 17.5 | 6.07 | 9.04 |
| | M | 92 | *Nf1*$^{fl/fl}$ *Wt1*$^{+/+}$ | | Isoproterenol | **33.9** | **181.6** | 17.8 | 5.36 | 10.20 |
| | M | 93 | *Nf1*$^{fl/fl}$ *Wt1*$^{+/+}$ | | Isoproterenol | **32.4** | **171.6** | 17.3 | 5.29 | 9.92 |
| | F | 88 | *Nf1*$^{fl/fl}$ *Wt1*$^{+/+}$ | | Saline | **25.0** | **113.7** | 17.0 | 4.55 | 6.69 |
| | F | 132 | *Nf1*$^{fl/fl}$ *Wt1*$^{+/+}$ | | Saline | **22.6** | **108.3** | 17.5 | 4.79 | 6.19 |
| | M | 73 | *Nf1*$^{fl/fl}$ *Wt1*$^{+/+}$ | | Saline | **32.4** | **164.2** | 17.4 | 5.07 | 9.44 |
| | M | 69 | *Nf1*$^{fl/fl}$ *Wt1*$^{+/+}$ | | Saline | **30.4** | **157.9** | 17.3 | 5.19 | 9.13 |
| Figure 4-4 | M | 235 | *Pdgfra*$^{fl/fl}$ *Pdgfrb*$^{fl/fl}$ *Gata5Cre*$^{Tg}$ | - | Isoproterenol | **29.2** | **220.8** | 17.0 | 7.55 | 12.99 |
| | F | 243 | *Pdgfra*$^{fl/fl}$ *Pdgfrb*$^{fl/fl}$ *Gata5Cre*$^{Tg}$ | | Isoproterenol | **28.7** | **164.1** | 17.6 | 5.71 | 9.32 |
| | F | 254 | *Pdgfra*$^{fl/fl}$ *Pdgfrb*$^{fl/fl}$ *Gata5Cre*$^{Tg}$ | | Isoproterenol | **25.7** | **150.9** | 17.6 | 5.88 | 8.57 |
| | F | 295 | *Pdgfra*$^{fl/fl}$ | | Saline | **24.0** | **116.3** | 17.5 | 4.85 | 6.65 |
| Figure 4-6 | F | 431 | *Nf1*$^{fl/fl}$ *Wt1*$^{+/+}$ | Postnatal | - | **22.1** | **123.3** | 17.8 | 5.58 | 6.93 |
| | M | 463 | *Nf1*$^{fl/fl}$ *Wt1*$^{CreERT2/+}$ | | - | **24.5** | **160.2** | 18.0 | 6.54 | 8.90 |
| | F | 465 | *Nf1*$^{fl/fl}$ *Wt1*$^{CreERT2/+}$ | | - | **20.1** | 116.6 | 17.7 | 5.80 | 6.59 |
| | F | 233 | *Nf1*$^{fl/fl}$ *Wt1*$^{CreERT2/+}$ | | - | **21.3** | **116.6** | 17.2 | 5.47 | 6.78 |

BW, body weight; HW, heart weight; TL, tibia length.

# CHAPTER FIVE

# DISCUSSION

## EMT and epicardial fate specification

Clonal analysis of individual epicardial cells (Caroline Sung, unpublished) suggests that Tcf21-expressing epicardial cells are initially multipotent contributing initially to both cVSMCs and cardiac fibroblasts. However, Tcf21 becomes restricted to the cardiac fibroblast lineage at later developmental stages suggesting that fate specification in Tcf21 expressing cells occurs prior to or at the time of EMT. In the absence of Tcf21, cardiac fibroblast progenitors fail to undergo EMT resulting in a significant loss of cardiac fibroblasts suggesting a lineage-specific function for Tcf21 in epicardial development. It is interesting to note that Tcf21 expression is also enriched in adult cardiac fibroblast population suggesting its possible function in cardiac fibroblast homeostasis. Due to postnatal lethality of *Tcf21*-null animals, a conditional approach is suggested to study its' role in the adult hearts.

## *Tcf21* and *Pdgfra* in cardiac fibroblast development

A striking similar role for Pdgfrα function during epicardial EMT and cardiac fibroblast development has been reported in the paper Smith et al., 2011. Although some evidence such as reduction of Pdgfrα expressing cells in *Tcf21*-null heart support genetic interaction between *Tcf21* and *Pdgfra*, it is still not clear whether one regulates the other. Reduction of Pdgfrα-expressing cells in *Tcf21*-null hearts might be simply explained by loss of cardiac fibroblast population in the Tcf21 mutant mice. Again, a *Tcf21* conditional

mouse would be useful to address this question in vivo.

Although many studies report their function in synthesizing ECM and wound healing, fewer focus on their developmental program and cellular origin, especially for the cardiac fibroblasts. One of the difficulties is the absence of well-defined markers. The body of work described in the Chapter 2 established reproducible methods for the detection of embryonic and postnatal cardiac fibroblasts, and also revealed the utility of *Tcf21*$^{iCre}$ and *Pdgfra* as a tool and a marker gene for its detection. Specific and reproducible methods for the cardiac fibroblast detection will allow us to mine new genes that are involved in the developmental process, and also make it possible to study its function during the pathological process of heart disease.

**_Nf1_ in epicardial EMT**

In the paper Baek and Tallquist, 2012, we have reported that loss of *Nf1* in epicardial cells results in earlier and increased EMT that leads to expansion of cardiac fibroblasts and cVSMCs. Although the long-term effect of Nf1-loss and EPDC expansion during normal physiology has not been addressed in detail, no significant difference in heart function was detected in *Nf1*$^{WTiKO}$ mice. This can be, in part, explained by the molecular function of Nf1, as a negative regulator of Ras. Simple assumption is that the absence of Nf1 might have no effect unless the Ras is activated. Thus, *Nf1*$^{WTiKO}$ hearts will more likely respond differently under conditions where Ras is activated. Interestingly, EPDC-expansion by the loss of Nf1 also did not affect heart size and function.

It has not been addressed whether *Nf1* mutant epicardial cells undergo EMT even after the normal window of EMT, in part, due to the limitations of the current reagents. It

will be interesting to test wheter In the absence of *Nf1*, the process of EMT occurred earlier with an increase in epicardial cells entering the compact myocardium. *Wt1*$^{CreERT2}$ is expressed in both epicardial cells and a subpopulation of undifferentiated EPDCs. Thus, it is impossible to distinguish the cells that migrate before tamoxifen induction and expressing *Wt1* from the cells that had newly migrated that had lost Nf1. An inducible Cre that is only expressed in epicardial cells even after E15.5 will allow us to address the question properly. For this purpose, the generation of a *TrkB-CreERT2*$^{Tg}$ mouse line, where TrkB is only expressed in the epicardium was attempted, however, no founders showed consistent and efficient labeling of epicardium.

In summary, the work presented here reveals key mediators of epicardial EMT, *Nf1, Pdgfra* and *Tcf21*, and their functions in EPDCs formation especially in cardiac fibroblasts. Assuming the significance of cardiac fibroblasts during heart pathogenesis, a better understanding of its developmental process of would certainly contribute to the improvement of therapies of injured hearts and its potential utility for cardiac regeneration.

## BIBLIOGRAPHY

**Acharya, A., Baek, S. T., Banfi, S., Eskiocak, B. and Tallquist, M. D.** (2011). Efficient inducible Cre-mediated recombination in Tcf21 cell lineages in the heart and kidney. *Genesis*.

**Acharya, A., Baek, S. T., Huang, G., Eskiocak, B., Goetsch, S., Sung, C. Y., Banfi, S., Sauer, M. F., Olsen, G. S., Duffield, J. S. et al.** (2012). The bHLH transcription factor Tcf21 is required for lineage-specific EMT of cardiac fibroblast progenitors. *Development* **139**, 2139-49.

**Acloque, H., Adams, M. S., Fishwick, K., Bronner-Fraser, M. and Nieto, M. A.** (2009). Epithelial-mesenchymal transitions: the importance of changing cell state in development and disease. *J Clin Invest* **119**, 1438-49.

**Ahmed, S., Liu, C. C. and Nawshad, A.** (2007). Mechanisms of palatal epithelial seam disintegration by transforming growth factor (TGF) beta3. *Dev Biol* **309**, 193-207.

**Akiyama, H., Chaboissier, M. C., Behringer, R. R., Rowitch, D. H., Schedl, A., Epstein, J. A. and de Crombrugghe, B.** (2004). Essential role of Sox9 in the pathway that controls formation of cardiac valves and septa. *Proc Natl Acad Sci U S A* **101**, 6502-7.

**Aoki, Y., Niihori, T., Kawame, H., Kurosawa, K., Ohashi, H., Tanaka, Y., Filocamo, M., Kato, K., Suzuki, Y., Kure, S. et al.** (2005). Germline mutations in HRAS proto-oncogene cause Costello syndrome. *Nat Genet* **37**, 1038-40.

**Aquino, J. B., Lallemend, F., Marmigere, F., Adameyko, II, Golemis, E. A. and Ernfors, P.** (2009). The retinoic acid inducible Cas-family signaling protein Nedd9 regulates neural crest cell migration by modulating adhesion and actin dynamics. *Neuroscience* **162**, 1106-19.

**Atit, R. P., Crowe, M. J., Greenhalgh, D. G., Wenstrup, R. J. and Ratner, N.** (1999). The Nf1 tumor suppressor regulates mouse skin wound healing, fibroblast proliferation, and collagen deposited by fibroblasts. *J Invest Dermatol* **112**, 835-42.

**Austin, A. F., Compton, L. A., Love, J. D., Brown, C. B. and Barnett, J. V.** (2008). Primary and immortalized mouse epicardial cells undergo differentiation in response to TGFbeta. *Dev Dyn* **237**, 366-76.

**Boot, M. J., Gittenberger-De Groot, A. C., Van Iperen, L., Hierck, B. P. and Poelmann, R. E.** (2003). Spatiotemporally separated cardiac neural crest subpopulations that target the outflow tract septum and pharyngeal arch arteries. *Anat Rec A Discov Mol Cell Evol Biol* **275**, 1009-18.

**Bostrom, H., Willetts, K., Pekny, M., Leveen, P., Lindahl, P., Hedstrand, H., Pekna, M., Hellstrom, M., Gebre-Medhin, S., Schalling, M. et al.** (1996). PDGF-A signaling is a critical event in lung alveolar myofibroblast development and alveogenesis. *Cell* **85**, 863-73.

**Boyer, A. S., Ayerinskas, II, Vincent, E. B., McKinney, L. A., Weeks, D. L. and Runyan, R. B.** (1999). TGFbeta2 and TGFbeta3 have separate and sequential activities during epithelial-mesenchymal cell transformation in the embryonic heart. *Dev Biol* **208**, 530-45.

**Boyer, B., Roche, S., Denoyelle, M. and Thiery, J. P.** (1997). Src and Ras are involved in separate pathways in epithelial cell scattering. *EMBO J* **16**, 5904-13.

**Brannan, C. I., Perkins, A. S., Vogel, K. S., Ratner, N., Nordlund, M. L., Reid, S. W., Buchberg, A. M., Jenkins, N. A., Parada, L. F. and Copeland, N. G.** (1994). Targeted disruption of the neurofibromatosis type-1 gene leads to developmental abnormalities in heart and various neural crest-derived tissues. *Genes Dev* **8**, 1019-29.

**Brodde, O. E.** (1988). The functional importance of beta 1 and beta 2 adrenoceptors in the human heart. *Am J Cardiol* **62**, 24C-29C.

**Brown, R. D., Ambler, S. K., Mitchell, M. D. and Long, C. S.** (2005). The cardiac fibroblast: therapeutic target in myocardial remodeling and failure. *Annu Rev Pharmacol Toxicol* **45**, 657-87.

**Cai, C. L., Martin, J. C., Sun, Y., Cui, L., Wang, L., Ouyang, K., Yang, L., Bu, L., Liang, X., Zhang, X. et al.** (2008). A myocardial lineage derives from Tbx18 epicardial cells. *Nature* **454**, 104-8.

**Carver, E. A., Jiang, R., Lan, Y., Oram, K. F. and Gridley, T.** (2001). The mouse snail gene encodes a key regulator of the epithelial-mesenchymal transition. *Mol Cell Biol* **21**, 8184-8.

**Chamulitrat, W., Schmidt, R., Chunglok, W., Kohl, A. and Tomakidi, P.** (2003). Epithelium and fibroblast-like phenotypes derived from HPV16 E6/E7-immortalized human gingival keratinocytes following chronic ethanol treatment. *Eur J Cell Biol* **82**, 313-22.

**Cheung, M., Chaboissier, M. C., Mynett, A., Hirst, E., Schedl, A. and Briscoe, J.** (2005). The transcriptional control of trunk neural crest induction, survival, and delamination. *Dev Cell* **8**, 179-92.

**Christoffels, V. M., Grieskamp, T., Norden, J., Mommersteeg, M. T., Rudat, C. and Kispert, A.** (2009). Tbx18 and the fate of epicardial progenitors. *Nature* **458**, E8-9; discussion E9-10.

**Cichowski, K. and Jacks, T.** (2001). NF1 tumor suppressor gene function: narrowing the GAP. *Cell* **104**, 593-604.

**Corallini, F., Gonelli, A., D'Aurizio, F., di Iasio, M. G. and Vaccarezza, M.** (2009). Mesenchymal stem cells-derived vascular smooth muscle cells release abundant levels of osteoprotegerin. *Eur J Histochem* **53**, 19-24.

**Cui, S., Ross, A., Stallings, N., Parker, K. L., Capel, B. and Quaggin, S. E.** (2004). Disrupted gonadogenesis and male-to-female sex reversal in Pod1 knockout mice. *Development* **131**, 4095-105.

**Cui, S., Schwartz, L. and Quaggin, S. E.** (2003). Pod1 is required in stromal cells for glomerulogenesis. *Dev Dyn* **226**, 512-22.

**de Lange, F. J., Moorman, A. F., Anderson, R. H., Manner, J., Soufan, A. T., de Gier-de Vries, C., Schneider, M. D., Webb, S., van den Hoff, M. J. and Christoffels, V. M.** (2004). Lineage and morphogenetic analysis of the cardiac valves. *Circ Res* **95**, 645-54.

**del Monte, G., Casanova, J. C., Guadix, J. A., MacGrogan, D., Burch, J. B., Perez-Pomares, J. M. and de la Pompa, J. L.** (2011). Differential Notch signaling in

the epicardium is required for cardiac inflow development and coronary vessel morphogenesis. *Circ Res* **108**, 824-36.

**Dettman, R. W., Denetclaw, W., Jr., Ordahl, C. P. and Bristow, J.** (1998). Common epicardial origin of coronary vascular smooth muscle, perivascular fibroblasts, and intermyocardial fibroblasts in the avian heart. *Dev Biol* **193**, 169-81.

**Dettman, R. W., Pae, S. H., Morabito, C. and Bristow, J.** (2003). Inhibition of alpha4-integrin stimulates epicardial-mesenchymal transformation and alters migration and cell fate of epicardially derived mesenchyme. *Dev Biol* **257**, 315-28.

**Di Meglio, F., Castaldo, C., Nurzynska, D., Romano, V., Miraglia, R., Bancone, C., Langella, G., Vosa, C. and Montagnani, S.** Epithelial-mesenchymal transition of epicardial mesothelium is a source of cardiac CD117-positive stem cells in adult human heart. *J Mol Cell Cardiol* **49**, 719-27.

**Dokic, D. and Dettman, R. W.** (2006). VCAM-1 inhibits TGFbeta stimulated epithelial-mesenchymal transformation by modulating Rho activity and stabilizing intercellular adhesion in epicardial mesothelial cells. *Dev Biol* **299**, 489-504.

**Edme, N., Downward, J., Thiery, J. P. and Boyer, B.** (2002). Ras induces NBT-II epithelial cell scattering through the coordinate activities of Rac and MAPK pathways. *J Cell Sci* **115**, 2591-601.

**Eralp, I., Lie-Venema, H., DeRuiter, M. C., van den Akker, N. M., Bogers, A. J., Mentink, M. M., Poelmann, R. E. and Gittenberger-de Groot, A. C.** (2005). Coronary artery and orifice development is associated with proper timing of epicardial outgrowth and correlated Fas-ligand-associated apoptosis patterns. *Circ Res* **96**, 526-34.

**Errami, M., Galindo, C. L., Tassa, A. T., Dimaio, J. M., Hill, J. A. and Garner, H. R.** (2008). Doxycycline attenuates isoproterenol- and transverse aortic banding-induced cardiac hypertrophy in mice. *J Pharmacol Exp Ther* **324**, 1196-203.

**Fischer, A. N., Fuchs, E., Mikula, M., Huber, H., Beug, H. and Mikulits, W.** (2007). PDGF essentially links TGF-beta signaling to nuclear beta-catenin accumulation in hepatocellular carcinoma progression. *Oncogene* **26**, 3395-405.

**Frey, N., Katus, H. A., Olson, E. N. and Hill, J. A.** (2004). Hypertrophy of the heart: a new therapeutic target? *Circulation* **109**, 1580-9.

**Friedman, J. M., Arbiser, J., Epstein, J. A., Gutmann, D. H., Huot, S. J., Lin, A. E., McManus, B. and Korf, B. R.** (2002). Cardiovascular disease in neurofibromatosis 1: report of the NF1 Cardiovascular Task Force. *Genet Med* **4**, 105-11.

**Funato, N., Ohyama, K., Kuroda, T. and Nakamura, M.** (2003). Basic helix-loop-helix transcription factor epicardin/capsulin/Pod-1 suppresses differentiation by negative regulation of transcription. *J Biol Chem* **278**, 7486-93.

**Gitler, A. D. and Epstein, J. A.** (2003). Regulating heart development: the role of Nf1. *Cell Cycle* **2**, 96-8.

**Gitler, A. D., Zhu, Y., Ismat, F. A., Lu, M. M., Yamauchi, Y., Parada, L. F. and Epstein, J. A.** (2003). Nf1 has an essential role in endothelial cells. *Nat Genet* **33**, 75-9.

**Gittenberger-de Groot, A. C., Vrancken Peeters, M. P., Bergwerff, M., Mentink, M. M. and Poelmann, R. E.** (2000). Epicardial outgrowth inhibition leads to

compensatory mesothelial outflow tract collar and abnormal cardiac septation and coronary formation. *Circ Res* **87**, 969-71.

**Goldsmith, E. C., Hoffman, A., Morales, M. O., Potts, J. D., Price, R. L., McFadden, A., Rice, M. and Borg, T. K.** (2004). Organization of fibroblasts in the heart. *Dev Dyn* **230**, 787-94.

**Greenburg, G. and Hay, E. D.** (1982). Epithelia suspended in collagen gels can lose polarity and express characteristics of migrating mesenchymal cells. *J Cell Biol* **95**, 333-9.

**Greenburg, G. and Hay, E. D.** (1986). Cytodifferentiation and tissue phenotype change during transformation of embryonic lens epithelium to mesenchyme-like cells in vitro. *Dev Biol* **115**, 363-79.

**Grieskamp, T., Rudat, C., Ludtke, T. H., Norden, J. and Kispert, A.** (2011). Notch signaling regulates smooth muscle differentiation of epicardium-derived cells. *Circ Res* **108**, 813-23.

**Hamilton, T. G., Klinghoffer, R. A., Corrin, P. D. and Soriano, P.** (2003). Evolutionary divergence of platelet-derived growth factor alpha receptor signaling mechanisms. *Mol Cell Biol* **23**, 4013-25.

**Harada, M., Itoh, H., Nakagawa, O., Ogawa, Y., Miyamoto, Y., Kuwahara, K., Ogawa, E., Igaki, T., Yamashita, J., Masuda, I. et al.** (1997). Significance of ventricular myocytes and nonmyocytes interaction during cardiocyte hypertrophy: evidence for endothelin-1 as a paracrine hypertrophic factor from cardiac nonmyocytes. *Circulation* **96**, 3737-44.

**Herrera, R.** (1998). Modulation of hepatocyte growth factor-induced scattering of HT29 colon carcinoma cells. Involvement of the MAPK pathway. *J Cell Sci* **111 ( Pt 8)**, 1039-49.

**Hiatt, K. K., Ingram, D. A., Zhang, Y., Bollag, G. and Clapp, D. W.** (2001). Neurofibromin GTPase-activating protein-related domains restore normal growth in Nf1-/- cells. *J Biol Chem* **276**, 7240-5.

**Hill, J. A., Karimi, M., Kutschke, W., Davisson, R. L., Zimmerman, K., Wang, Z., Kerber, R. E. and Weiss, R. M.** (2000). Cardiac hypertrophy is not a required compensatory response to short-term pressure overload. *Circulation* **101**, 2863-9.

**Hong, C. Y., Gong, E. Y., Kim, K., Suh, J. H., Ko, H. M., Lee, H. J., Choi, H. S. and Lee, K.** (2005). Modulation of the expression and transactivation of androgen receptor by the basic helix-loop-helix transcription factor Pod-1 through recruitment of histone deacetylase 1. *Mol Endocrinol* **19**, 2245-57.

**Horiguchi, K., Shirakihara, T., Nakano, A., Imamura, T., Miyazono, K. and Saitoh, M.** (2009). Role of Ras signaling in the induction of snail by transforming growth factor-beta. *J Biol Chem* **284**, 245-53.

**Hudon-David, F., Bouzeghrane, F., Couture, P. and Thibault, G.** (2007). Thy-1 expression by cardiac fibroblasts: lack of association with myofibroblast contractile markers. *J Mol Cell Cardiol* **42**, 991-1000.

**Ieda, M., Tsuchihashi, T., Ivey, K. N., Ross, R. S., Hong, T. T., Shaw, R. M. and Srivastava, D.** (2009). Cardiac fibroblasts regulate myocardial proliferation through beta1 integrin signaling. *Dev Cell* **16**, 233-44.

**Ingram, D. A., Yang, F. C., Travers, J. B., Wenning, M. J., Hiatt, K., New, S., Hood, A., Shannon, K., Williams, D. A. and Clapp, D. W.** (2000). Genetic and biochemical evidence that haploinsufficiency of the Nf1 tumor suppressor gene modulates melanocyte and mast cell fates in vivo. *J Exp Med* **191**, 181-8.

**Jacks, T., Shih, T. S., Schmitt, E. M., Bronson, R. T., Bernards, A. and Weinberg, R. A.** (1994). Tumour predisposition in mice heterozygous for a targeted mutation in Nf1. *Nat Genet* **7**, 353-61.

**Jackson, E. L., Willis, N., Mercer, K., Bronson, R. T., Crowley, D., Montoya, R., Jacks, T. and Tuveson, D. A.** (2001). Analysis of lung tumor initiation and progression using conditional expression of oncogenic K-ras. *Genes Dev* **15**, 3243-8.

**Janda, E., Lehmann, K., Killisch, I., Jechlinger, M., Herzig, M., Downward, J., Beug, H. and Grunert, S.** (2002). Ras and TGF[beta] cooperatively regulate epithelial cell plasticity and metastasis: dissection of Ras signaling pathways. *J Cell Biol* **156**, 299-313.

**Jechlinger, M., Grunert, S., Tamir, I. H., Janda, E., Ludemann, S., Waerner, T., Seither, P., Weith, A., Beug, H. and Kraut, N.** (2003). Expression profiling of epithelial plasticity in tumor progression. *Oncogene* **22**, 7155-69.

**Katz, T. C., Singh, M. K., Degenhardt, K., Rivera-Feliciano, J., Johnson, R. L., Epstein, J. A. and Tabin, C. J.** Distinct compartments of the proepicardial organ give rise to coronary vascular endothelial cells. *Dev Cell* **22**, 639-50.

**Ke, X. S., Qu, Y., Goldfinger, N., Rostad, K., Hovland, R., Akslen, L. A., Rotter, V., Oyan, A. M. and Kalland, K. H.** (2008). Epithelial to mesenchymal transition of a primary prostate cell line with switches of cell adhesion modules but without malignant transformation. *PLoS One* **3**, e3368.

**Kikuchi, K., Holdway, J. E., Major, R. J., Blum, N., Dahn, R. D., Begemann, G. and Poss, K. D.** Retinoic acid production by endocardium and epicardium is an injury response essential for zebrafish heart regeneration. *Dev Cell* **20**, 397-404.

**Kikuchi, K., Holdway, J. E., Major, R. J., Blum, N., Dahn, R. D., Begemann, G. and Poss, K. D.** (2011). Retinoic acid production by endocardium and epicardium is an injury response essential for zebrafish heart regeneration. *Dev Cell* **20**, 397-404.

**Kivirikko, K. I., Myllyla, R. and Pihlajaniemi, T.** (1989). Protein hydroxylation: prolyl 4-hydroxylase, an enzyme with four cosubstrates and a multifunctional subunit. *Faseb J* **3**, 1609-17.

**Kokudo, T., Suzuki, Y., Yoshimatsu, Y., Yamazaki, T., Watabe, T. and Miyazono, K.** (2008). Snail is required for TGFbeta-induced endothelial-mesenchymal transition of embryonic stem cell-derived endothelial cells. *J Cell Sci* **121**, 3317-24.

**Komiyama, M., Ito, K. and Shimada, Y.** (1987). Origin and development of the epicardium in the mouse embryo. *Anat Embryol (Berl)* **176**, 183-9.

**Kontaridis, M. I., Swanson, K. D., David, F. S., Barford, D. and Neel, B. G.** (2006). PTPN11 (Shp2) mutations in LEOPARD syndrome have dominant negative, not activating, effects. *J Biol Chem* **281**, 6785-92.

**Kuwahara, K., Saito, Y., Harada, M., Ishikawa, M., Ogawa, E., Miyamoto, Y., Hamanaka, I., Kamitani, S., Kajiyama, N., Takahashi, N. et al.** (1999). Involvement of cardiotrophin-1 in cardiac myocyte-nonmyocyte interactions during hypertrophy of rat cardiac myocytes in vitro. *Circulation* **100**, 1116-24.

**Lakkis, M. M. and Epstein, J. A.** (1998). Neurofibromin modulation of ras activity is required for normal endocardial-mesenchymal transformation in the developing heart. *Development* **125**, 4359-67.

**Lasater, E. A., Bessler, W. K., Mead, L. E., Horn, W. E., Clapp, D. W., Conway, S. J., Ingram, D. A. and Li, F.** (2008). Nf1+/- mice have increased neointima formation via hyperactivation of a Gleevec sensitive molecular pathway. *Hum Mol Genet* **17**, 2336-44.

**Lepilina, A., Coon, A. N., Kikuchi, K., Holdway, J. E., Roberts, R. W., Burns, C. G. and Poss, K. D.** (2006). A dynamic epicardial injury response supports progenitor cell activity during zebrafish heart regeneration. *Cell* **127**, 607-19.

**Lie-Venema, H., Eralp, I., Maas, S., Gittenberger-De Groot, A. C., Poelmann, R. E. and DeRuiter, M. C.** (2005). Myocardial heterogeneity in permissiveness for epicardium-derived cells and endothelial precursor cells along the developing heart tube at the onset of coronary vascularization. *Anat Rec A Discov Mol Cell Evol Biol* **282**, 120-9.

**Lie-Venema, H., van den Akker, N. M., Bax, N. A., Winter, E. M., Maas, S., Kekarainen, T., Hoeben, R. C., deRuiter, M. C., Poelmann, R. E. and Gittenberger-de Groot, A. C.** (2007). Origin, fate, and function of epicardium-derived cells (EPDCs) in normal and abnormal cardiac development. *ScientificWorldJournal* **7**, 1777-98.

**Liem, K. F., Jr., Tremml, G., Roelink, H. and Jessell, T. M.** (1995). Dorsal differentiation of neural plate cells induced by BMP-mediated signals from epidermal ectoderm. *Cell* **82**, 969-79.

**Limana, F., Zacheo, A., Mocini, D., Mangoni, A., Borsellino, G., Diamantini, A., De Mori, R., Battistini, L., Vigna, E., Santini, M. et al.** (2007). Identification of myocardial and vascular precursor cells in human and mouse epicardium. *Circ Res* **101**, 1255-65.

**Lin, A. E., Birch, P. H., Korf, B. R., Tenconi, R., Niimura, M., Poyhonen, M., Armfield Uhas, K., Sigorini, M., Virdis, R., Romano, C. et al.** (2000). Cardiovascular malformations and other cardiovascular abnormalities in neurofibromatosis 1. *Am J Med Genet* **95**, 108-17.

**Lu, J., Chang, P., Richardson, J. A., Gan, L., Weiler, H. and Olson, E. N.** (2000). The basic helix-loop-helix transcription factor capsulin controls spleen organogenesis. *Proc Natl Acad Sci U S A* **97**, 9525-30.

**Lu, J., Landerholm, T. E., Wei, J. S., Dong, X. R., Wu, S. P., Liu, X., Nagata, K., Inagaki, M. and Majesky, M. W.** (2001). Coronary smooth muscle differentiation from proepicardial cells requires rhoA-mediated actin reorganization and p160 rho-kinase activity. *Dev Biol* **240**, 404-18.

**Lu, J., Richardson, J. A. and Olson, E. N.** (1998). Capsulin: a novel bHLH transcription factor expressed in epicardial progenitors and mesenchyme of visceral organs. *Mech Dev* **73**, 23-32.

**Lu, J. R., Bassel-Duby, R., Hawkins, A., Chang, P., Valdez, R., Wu, H., Gan, L., Shelton, J. M., Richardson, J. A. and Olson, E. N.** (2002). Control of facial muscle development by MyoR and capsulin. *Science* **298**, 2378-81.

**Lynch, T. M. and Gutmann, D. H.** (2002). Neurofibromatosis 1. *Neurol Clin* **20**, 841-65.

**Madisen, L., Zwingman, T. A., Sunkin, S. M., Oh, S. W., Zariwala, H. A., Gu, H., Ng, L. L., Palmiter, R. D., Hawrylycz, M. J., Jones, A. R. et al.** (2010). A robust and high-throughput Cre reporting and characterization system for the whole mouse brain. *Nat Neurosci* **13**, 133-40.

**Manner, J., Perez-Pomares, J. M., Macias, D. and Munoz-Chapuli, R.** (2001). The origin, formation and developmental significance of the epicardium: a review. *Cells Tissues Organs* **169**, 89-103.

**Martin, G. A., Viskochil, D., Bollag, G., McCabe, P. C., Crosier, W. J., Haubruck, H., Conroy, L., Clark, R., O'Connell, P., Cawthon, R. M. et al.** (1990). The GAP-related domain of the neurofibromatosis type 1 gene product interacts with ras p21. *Cell* **63**, 843-9.

**Martin, P.** (1997). Wound healing--aiming for perfect skin regeneration. *Science* **276**, 75-81.

**Martinez-Estrada, O. M., Lettice, L. A., Essafi, A., Guadix, J. A., Slight, J., Velecela, V., Hall, E., Reichmann, J., Devenney, P. S., Hohenstein, P. et al.** (2010). Wt1 is required for cardiovascular progenitor cell formation through transcriptional control of Snail and E-cadherin. *Nat Genet* **42**, 89-93.

**McCormick, F.** (1995). Ras signaling and NF1. *Curr Opin Genet Dev* **5**, 51-5.

**Mellgren, A. M., Smith, C. L., Olsen, G. S., Eskiocak, B., Zhou, B., Kazi, M. N., Ruiz, F. R., Pu, W. T. and Tallquist, M. D.** (2008). Platelet-derived growth factor receptor beta signaling is required for efficient epicardial cell migration and development of two distinct coronary vascular smooth muscle cell populations. *Circ Res* **103**, 1393-401.

**Mercado-Pimentel, M. E. and Runyan, R. B.** (2007). Multiple transforming growth factor-beta isoforms and receptors function during epithelial-mesenchymal cell transformation in the embryonic heart. *Cells Tissues Organs* **185**, 146-56.

**Merki, E., Zamora, M., Raya, A., Kawakami, Y., Wang, J., Zhang, X., Burch, J., Kubalak, S. W., Kaliman, P., Belmonte, J. C. et al.** (2005). Epicardial retinoid X receptor alpha is required for myocardial growth and coronary artery formation. *Proc Natl Acad Sci U S A* **102**, 18455-60.

**Mikawa, T. and Gourdie, R. G.** (1996). Pericardial mesoderm generates a population of coronary smooth muscle cells migrating into the heart along with ingrowth of the epicardial organ. *Dev Biol* **174**, 221-32.

**Miller, S. J., Lan, Z. D., Hardiman, A., Wu, J., Kordich, J. J., Patmore, D. M., Hegde, R. S., Cripe, T. P., Cancelas, J. A., Collins, M. H. et al.** (2010). Inhibition of Eyes Absent Homolog 4 expression induces malignant peripheral nerve sheath tumor necrosis. *Oncogene* **29**, 368-79.

**Moore, A. W., McInnes, L., Kreidberg, J., Hastie, N. D. and Schedl, A.** (1999). YAC complementation shows a requirement for Wt1 in the development of epicardium, adrenal gland and throughout nephrogenesis. *Development* **126**, 1845-57.

**Morgan, S. C., Lee, H. Y., Relaix, F., Sandell, L. L., Levorse, J. M. and Loeken, M. R.** (2008). Cardiac outflow tract septation failure in Pax3-deficient embryos is due to p53-dependent regulation of migrating cardiac neural crest. *Mech Dev* **125**, 757-67.

**Nag, A. C.** (1980). Study of non-muscle cells of the adult mammalian heart: a fine structural analysis and distribution. *Cytobios* **28**, 41-61.

**Nieto, M. A.** (2002). The snail superfamily of zinc-finger transcription factors. *Nat Rev Mol Cell Biol* **3**, 155-66.

**Niihori, T., Aoki, Y., Narumi, Y., Neri, G., Cave, H., Verloes, A., Okamoto, N., Hennekam, R. C., Gillessen-Kaesbach, G., Wieczorek, D. et al.** (2006). Germline KRAS and BRAF mutations in cardio-facio-cutaneous syndrome. *Nat Genet* **38**, 294-6.

**Norris, R. A., Borg, T. K., Butcher, J. T., Baudino, T. A., Banerjee, I. and Markwald, R. R.** (2008). Neonatal and adult cardiovascular pathophysiological remodeling and repair: developmental role of periostin. *Ann N Y Acad Sci* **1123**, 30-40.

**Oka, T., Xu, J., Kaiser, R. A., Melendez, J., Hambleton, M., Sargent, M. A., Lorts, A., Brunskill, E. W., Dorn, G. W., 2nd, Conway, S. J. et al.** (2007). Genetic manipulation of periostin expression reveals a role in cardiac hypertrophy and ventricular remodeling. *Circ Res* **101**, 313-21.

**Olivey, H. E., Compton, L. A. and Barnett, J. V.** (2004). Coronary vessel development: the epicardium delivers. *Trends Cardiovasc Med* **14**, 247-51.

**Olivotto, I., Cecchi, F., Poggesi, C. and Yacoub, M. H.** (2009). Developmental origins of hypertrophic cardiomyopathy phenotypes: a unifying hypothesis. *Nat Rev Cardiol* **6**, 317-21.

**Pardo, A. and Selman, M.** (2006). Matrix metalloproteases in aberrant fibrotic tissue remodeling. *Proc Am Thorac Soc* **3**, 383-8.

**Pennisi, D. J. and Mikawa, T.** (2009). FGFR-1 is required by epicardium-derived cells for myocardial invasion and correct coronary vascular lineage differentiation. *Dev Biol* **328**, 148-59.

**Perez-Pomares, J. M., Macias, D., Garcia-Garrido, L. and Munoz-Chapuli, R.** (1997). Contribution of the primitive epicardium to the subepicardial mesenchyme in hamster and chick embryos. *Dev Dyn* **210**, 96-105.

**Piette, D., Hendrickx, M., Willems, E., Kemp, C. R. and Leyns, L.** (2008). An optimized procedure for whole-mount in situ hybridization on mouse embryos and embryoid bodies. *Nat Protoc* **3**, 1194-201.

**Plotkin, M. and Mudunuri, V.** (2008). Pod1 induces myofibroblast differentiation in mesenchymal progenitor cells from mouse kidney. *J Cell Biochem* **103**, 675-90.

**Poelmann, R. E., Gittenberger-de Groot, A. C., Mentink, M. M., Bokenkamp, R. and Hogers, B.** (1993). Development of the cardiac coronary vascular endothelium, studied with antiendothelial antibodies, in chicken-quail chimeras. *Circ Res* **73**, 559-68.

**Ponticos, M., Partridge, T., Black, C. M., Abraham, D. J. and Bou-Gharios, G.** (2004). Regulation of collagen type I in vascular smooth muscle cells by competition between Nkx2.5 and deltaEF1/ZEB1. *Mol Cell Biol* **24**, 6151-61.

**Potts, J. D., Dagle, J. M., Walder, J. A., Weeks, D. L. and Runyan, R. B.** (1991). Epithelial-mesenchymal transformation of embryonic cardiac endothelial cells is inhibited by a modified antisense oligodeoxynucleotide to transforming growth factor beta 3. *Proc Natl Acad Sci U S A* **88**, 1516-20.

**Powers, J. F., Evinger, M. J., Zhi, J., Picard, K. L. and Tischler, A. S.** (2007). Pheochromocytomas in Nf1 knockout mice express a neural progenitor gene expression profile. *Neuroscience* **147**, 928-37.

**Quaggin, S. E., Schwartz, L., Cui, S., Igarashi, P., Deimling, J., Post, M. and Rossant, J.** (1999). The basic-helix-loop-helix protein pod1 is critically important for kidney and lung organogenesis. *Development* **126**, 5771-83.

**Rasmussen, S. A., Yang, Q. and Friedman, J. M.** (2001). Mortality in neurofibromatosis 1: an analysis using U.S. death certificates. *Am J Hum Genet* **68**, 1110-8.

**Red-Horse, K., Ueno, H., Weissman, I. L. and Krasnow, M. A.** Coronary arteries form by developmental reprogramming of venous cells. *Nature* **464**, 549-53.

**Rege, T. A. and Hagood, J. S.** (2006). Thy-1 as a regulator of cell-cell and cell-matrix interactions in axon regeneration, apoptosis, adhesion, migration, cancer, and fibrosis. *Faseb J* **20**, 1045-54.

**Richarte, A. M., Mead, H. B. and Tallquist, M. D.** (2007). Cooperation between the PDGF receptors in cardiac neural crest cell migration. *Dev Biol* **306**, 785-96.

**Rockman, H. A., Ross, R. S., Harris, A. N., Knowlton, K. U., Steinhelper, M. E., Field, L. J., Ross, J., Jr. and Chien, K. R.** (1991). Segregation of atrial-specific and inducible expression of an atrial natriuretic factor transgene in an in vivo murine model of cardiac hypertrophy. *Proc Natl Acad Sci U S A* **88**, 8277-81.

**Sakai, D., Suzuki, T., Osumi, N. and Wakamatsu, Y.** (2006). Cooperative action of Sox9, Snail2 and PKA signaling in early neural crest development. *Development* **133**, 1323-33.

**Sakata, M., Shiba, H., Komatsuzawa, H., Fujita, T., Ohta, K., Sugai, M., Suginaka, H. and Kurihara, H.** (1999). Expression of osteoprotegerin (osteoclastogenesis inhibitory factor) in cultures of human dental mesenchymal cells and epithelial cells. *J Bone Miner Res* **14**, 1486-92.

**Schaeren-Wiemers, N. and Gerfin-Moser, A.** (1993). A single protocol to detect transcripts of various types and expression levels in neural tissue and cultured cells: in situ hybridization using digoxigenin-labelled cRNA probes. *Histochemistry* **100**, 431-40.

**Schmahl, J., Rizzolo, K. and Soriano, P.** (2008). The PDGF signaling pathway controls multiple steroid-producing lineages. *Genes Dev* **22**, 3255-67.

**Schubbert, S., Zenker, M., Rowe, S. L., Boll, S., Klein, C., Bollag, G., van der Burgt, I., Musante, L., Kalscheuer, V., Wehner, L. E. et al.** (2006). Germline KRAS mutations cause Noonan syndrome. *Nat Genet* **38**, 331-6.

**Smith, C. L., Baek, S. T., Sung, C. Y. and Tallquist, M. D.** (2011). Epicardial-derived cell epithelial-to-mesenchymal transition and fate specification require PDGF receptor signaling. *Circ Res* **108**, e15-26.

**Smith, T. K. and Bader, D. M.** (2007). Signals from both sides: Control of cardiac development by the endocardium and epicardium. *Semin Cell Dev Biol* **18**, 84-9.

**Snider, P., Standley, K. N., Wang, J., Azhar, M., Doetschman, T. and Conway, S. J.** (2009). Origin of cardiac fibroblasts and the role of periostin. *Circ Res* **105**, 934-47.

**Soriano, P.** (1999). Generalized lacZ expression with the ROSA26 Cre reporter strain. *Nat Genet* **21**, 70-1.

**Souders, C. A., Bowers, S. L. and Baudino, T. A.** (2009). Cardiac fibroblast: the renaissance cell. *Circ Res* **105**, 1164-76.

**Sridurongrit, S., Larsson, J., Schwartz, R., Ruiz-Lozano, P. and Kaartinen, V.** (2008). Signaling via the Tgf-beta type I receptor Alk5 in heart development. *Dev Biol* **322**, 208-18.

**Srinivas, S., Watanabe, T., Lin, C. S., William, C. M., Tanabe, Y., Jessell, T. M. and Costantini, F.** (2001). Cre reporter strains produced by targeted insertion of EYFP and ECFP into the ROSA26 locus. *BMC Dev Biol* **1**, 4.

**Strutz, F., Okada, H., Lo, C. W., Danoff, T., Carone, R. L., Tomaszewski, J. E. and Neilson, E. G.** (1995). Identification and characterization of a fibroblast marker: FSP1. *J Cell Biol* **130**, 393-405.

**Szabo, J., Csaky, L. and Szegi, J.** (1975). Experimental cardiac hypertrophy induced by isoproterenol in the rat. *Acta Physiol Acad Sci Hung* **46**, 281-5.

**Takeda, N., Manabe, I., Uchino, Y., Eguchi, K., Matsumoto, S., Nishimura, S., Shindo, T., Sano, M., Otsu, K., Snider, P. et al.** (2010). Cardiac fibroblasts are essential for the adaptive response of the murine heart to pressure overload. *J Clin Invest* **120**, 254-65.

**Tallquist, M. D., French, W. J. and Soriano, P.** (2003). Additive effects of PDGF receptor beta signaling pathways in vascular smooth muscle cell development. *PLoS Biol* **1**, E52.

**Taylor, P. B. and Tang, Q.** (1984). Development of isoproterenol-induced cardiac hypertrophy. *Can J Physiol Pharmacol* **62**, 384-9.

**Teekakirikul, P., Eminaga, S., Toka, O., Alcalai, R., Wang, L., Wakimoto, H., Nayor, M., Konno, T., Gorham, J. M., Wolf, C. M. et al.** (2010). Cardiac fibrosis in mice with hypertrophic cardiomyopathy is mediated by non-myocyte proliferation and requires Tgf-beta. *J Clin Invest* **120**, 3520-9.

**Thiery, J. P., Acloque, H., Huang, R. Y. and Nieto, M. A.** (2009). Epithelial-mesenchymal transitions in development and disease. *Cell* **139**, 871-90.

**Thiery, J. P. and Sleeman, J. P.** (2006). Complex networks orchestrate epithelial-mesenchymal transitions. *Nat Rev Mol Cell Biol* **7**, 131-42.

**Tidhar, A., Reichenstein, M., Cohen, D., Faerman, A., Copeland, N. G., Gilbert, D. J., Jenkins, N. A. and Shani, M.** (2001). A novel transgenic marker for migrating limb muscle precursors and for vascular smooth muscle cells. *Dev Dyn* **220**, 60-73.

**Tomanek, R. J.** (2005). Formation of the coronary vasculature during development. *Angiogenesis* **8**, 273-84.

**Tomasek, J. J., Gabbiani, G., Hinz, B., Chaponnier, C. and Brown, R. A.** (2002). Myofibroblasts and mechano-regulation of connective tissue remodelling. *Nat Rev Mol Cell Biol* **3**, 349-63.

**Uehata, M., Ishizaki, T., Satoh, H., Ono, T., Kawahara, T., Morishita, T., Tamakawa, H., Yamagami, K., Inui, J., Maekawa, M. et al.** (1997). Calcium sensitization of smooth muscle mediated by a Rho-associated protein kinase in hypertension. *Nature* **389**, 990-4.

**Vallin, J., Thuret, R., Giacomello, E., Faraldo, M. M., Thiery, J. P. and Broders, F.** (2001). Cloning and characterization of three Xenopus slug promoters reveal direct regulation by Lef/beta-catenin signaling. *J Biol Chem* **276**, 30350-8.

**Van Den Akker, N. M., Lie-Venema, H., Maas, S., Eralp, I., DeRuiter, M. C., Poelmann, R. E. and Gittenberger-De Groot, A. C.** (2005). Platelet-derived growth factors in the developing avian heart and maturating coronary vasculature. *Dev Dyn* **233**, 1579-88.

**van Tuyn, J., Atsma, D. E., Winter, E. M., van der Velde-van Dijke, I., Pijnappels, D. A., Bax, N. A., Knaan-Shanzer, S., Gittenberger-de Groot, A. C., Poelmann, R. E., van der Laarse, A. et al.** (2007). Epicardial cells of human adults can undergo an epithelial-to-mesenchymal transition and obtain characteristics of smooth muscle cells in vitro. *Stem Cells* **25**, 271-8.

**van Tuyn, J., Knaan-Shanzer, S., van de Watering, M. J., de Graaf, M., van der Laarse, A., Schalij, M. J., van der Wall, E. E., de Vries, A. A. and Atsma, D. E.** (2005). Activation of cardiac and smooth muscle-specific genes in primary human cells after forced expression of human myocardin. *Cardiovasc Res* **67**, 245-55.

**Vidal, N. O., Brandstrom, H., Jonsson, K. B. and Ohlsson, C.** (1998). Osteoprotegerin mRNA is expressed in primary human osteoblast-like cells: down-regulation by glucocorticoids. *J Endocrinol* **159**, 191-5.

**Vindevoghel, L., Lechleider, R. J., Kon, A., de Caestecker, M. P., Uitto, J., Roberts, A. B. and Mauviel, A.** (1998). SMAD3/4-dependent transcriptional activation of the human type VII collagen gene (COL7A1) promoter by transforming growth factor beta. *Proc Natl Acad Sci U S A* **95**, 14769-74.

**von Scheven, G., Bothe, I., Ahmed, M. U., Alvares, L. E. and Dietrich, S.** (2006). Protein and genomic organisation of vertebrate MyoR and Capsulin genes and their expression during avian development. *Gene Expr Patterns* **6**, 383-93.

**Vrancken Peeters, M. P., Gittenberger-de Groot, A. C., Mentink, M. M. and Poelmann, R. E.** (1999). Smooth muscle cells and fibroblasts of the coronary arteries derive from epithelial-mesenchymal transformation of the epicardium. *Anat Embryol (Berl)* **199**, 367-78.

**Wada, A. M., Reese, D. E. and Bader, D. M.** (2001). Bves: prototype of a new class of cell adhesion molecules expressed during coronary artery development. *Development* **128**, 2085-93.

**Wilkins-Port, C. E. and Higgins, P. J.** (2007). Regulation of extracellular matrix remodeling following transforming growth factor-beta1/epidermal growth factor-stimulated epithelial-mesenchymal transition in human premalignant keratinocytes. *Cells Tissues Organs* **185**, 116-22.

**Winter, E. M. and Gittenberger-de Groot, A. C.** (2007). Epicardium-derived cells in cardiogenesis and cardiac regeneration. *Cell Mol Life Sci* **64**, 692-703.

**Winter, E. M., Grauss, R. W., Hogers, B., van Tuyn, J., van der Geest, R., Lie-Venema, H., Steijn, R. V., Maas, S., DeRuiter, M. C., deVries, A. A. et al.** (2007). Preservation of left ventricular function and attenuation of remodeling after transplantation of human epicardium-derived cells into the infarcted mouse heart. *Circulation* **116**, 917-27.

**Wynn, T. A.** (2004). Fibrotic disease and the T(H)1/T(H)2 paradigm. *Nat Rev Immunol* **4**, 583-94.

**Xu, G. F., O'Connell, P., Viskochil, D., Cawthon, R., Robertson, M., Culver, M., Dunn, D., Stevens, J., Gesteland, R., White, R. et al.** (1990). The neurofibromatosis type 1 gene encodes a protein related to GAP. *Cell* **62**, 599-608.

**Xu, J., Ismat, F. A., Wang, T., Lu, M. M., Antonucci, N. and Epstein, J. A.** (2009a). Cardiomyocyte-specific loss of neurofibromin promotes cardiac hypertrophy and dysfunction. *Circ Res* **105**, 304-11.

**Xu, J., Ismat, F. A., Wang, T., Yang, J. and Epstein, J. A.** (2007). NF1 regulates a Ras-dependent vascular smooth muscle proliferative injury response. *Circulation* **116**, 2148-56.

**Xu, J., Lamouille, S. and Derynck, R.** (2009b). TGF-beta-induced epithelial to mesenchymal transition. *Cell Res* **19**, 156-72.

**Yang, J. and Weinberg, R. A.** (2008). Epithelial-mesenchymal transition: at the crossroads of development and tumor metastasis. *Dev Cell* **14**, 818-29.

**Zak, R.** (1974). Development and proliferative capacity of cardiac muscle cells. *Circ Res* **35**, suppl II:17-26.

**Zamora, M., Manner, J. and Ruiz-Lozano, P.** (2007). Epicardium-derived progenitor cells require beta-catenin for coronary artery formation. *Proc Natl Acad Sci U S A* **104**, 18109-14.

**Zhang, Y., Riesterer, C., Ayrall, A. M., Sablitzky, F., Littlewood, T. D. and Reth, M.** (1996). Inducible site-directed recombination in mouse embryonic stem cells. *Nucleic Acids Res* **24**, 543-8.

**Zhou, B., Honor, L. B., He, H., Ma, Q., Oh, J. H., Butterfield, C., Lin, R. Z., Melero-Martin, J. M., Dolmatova, E., Duffy, H. S. et al.** Adult mouse epicardium modulates myocardial injury by secreting paracrine factors. *J Clin Invest* **121**, 1894-904.

**Zhou, B., Ma, Q., Rajagopal, S., Wu, S. M., Domian, I., Rivera-Feliciano, J., Jiang, D., von Gise, A., Ikeda, S., Chien, K. R. et al.** (2008). Epicardial progenitors contribute to the cardiomyocyte lineage in the developing heart. *Nature* **454**, 109-13.

**Zhu, Y., Ghosh, P., Charnay, P., Burns, D. K. and Parada, L. F.** (2002). Neurofibromas in NF1: Schwann cell origin and role of tumor environment. *Science* **296**, 920-2.

**Zhu, Y., Romero, M. I., Ghosh, P., Ye, Z., Charnay, P., Rushing, E. J., Marth, J. D. and Parada, L. F.** (2001). Ablation of NF1 function in neurons induces abnormal development of cerebral cortex and reactive gliosis in the brain. *Genes Dev* **15**, 859-76.